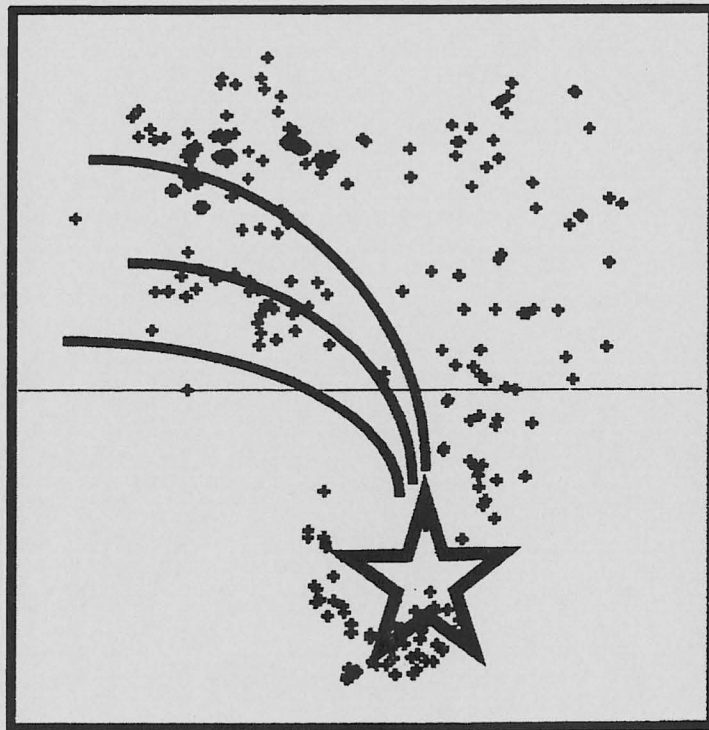
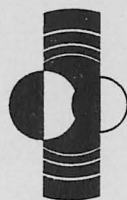


WORKSHOP ON
EXTRATERRESTRIAL MATERIALS
FROM COLD AND HOT DESERTS



July 6-8, 1999
Kwa-Maritane, Pilanesberg, South Africa

LPI Contribution No. 997



WORKSHOP ON
EXTRATERRESTRIAL MATERIALS
FROM COLD AND HOT DESERTS

July 6–8, 1999
Kwa-Maritane, Pilanesberg, South Africa

Edited by
Ludolf Schultz, Ian A. Franchi, Arch M. Reid, and Michael E. Zolensky

Sponsored by
Lunar and Planetary Institute
Max-Planck-Institut für Chemie
University of the Witwatersrand

Lunar and Planetary Institute 3600 Bay Area Boulevard Houston TX 77058-1113

LPI Contribution No. 997

Compiled in 2000 by
LUNAR AND PLANETARY INSTITUTE

The Institute is operated by the Universities Space Research Association under Contract No. NASW-4574 with the National Aeronautics and Space Administration.

Material in this volume may be copied without restraint for library, abstract service, education, or personal research purposes; however, republication of any paper or portion thereof requires the written permission of the authors as well as the appropriate acknowledgment of this publication.

This volume may be cited as

Schultz L.; Franchi I., Reid A., and Zolensky M., eds. (2000) *Workshop on Extraterrestrial Materials from Cold and Hot Deserts*. LPI Contribution No. 997, Lunar and Planetary Institute, Houston. 99 pp.

This volume is distributed by

ORDER DEPARTMENT
Lunar and Planetary Institute
3600 Bay Area Boulevard
Houston TX 77058-1113
Phone: 281-486-2172
Fax: 281-486-2186
E-mail: order@lpi.usra.edu

Mail order requestors will be invoiced for the cost of shipping and handling.

INTRODUCTION

Since 1969 expeditions from Japan, the United States, and European countries have recovered more than 20,000 meteorite specimens from remote ice fields of Antarctica. They represent approximately 4000–6000 distinct falls, more than all non-Antarctic meteorite falls and finds combined.

Recently many meteorite specimens of a new “population” have become available: meteorites from hot deserts. It turned out that suitable surfaces in hot deserts, like the Sahara in Africa, the Nullarbor Plain in Western and South Australia, or desert high plains of the U.S. (e.g., Roosevelt County, New Mexico), contain relatively high meteorite concentrations. For example, the 1985 Catalogue of Meteorites of the British Museum lists 20 meteorites from Algeria and Libya. Today, 1246 meteorites finds from these two countries have been published in MetBase 4.0.

Four workshops in 1982, 1985, 1988, and 1989 have discussed the connections between Antarctic glaciology and Antarctic meteorites, and the differences between Antarctic meteorites and modern falls. In 1995, a workshop addressed differences between meteorites from Antarctica, hot deserts, and modern falls, and the implications of possible different parent populations, infall rates, and weathering processes.

Since 1995 many more meteorites have been recovered from new areas of Antarctica and hot deserts around the world. Among these finds are several unusual and interesting specimens like lunar meteorites or SNCs of probable martian origin. The Annual Meeting of the Meteoritical Society took place in 1999 in Johannesburg, South Africa. As most of the recent desert finds originate from the Sahara, a special workshop was planned prior to this meeting in Africa. Topics discussed included micrometeorites, which have been collected in polar regions as well as directly in the upper atmosphere. The title “Workshop on Extraterrestrial Materials from Cold and Hot Deserts” was chosen and the following points were emphasized: (1) weathering processes, (2) terrestrial ages, (3) investigations of “unusual” meteorites, and (4) collection and curation.

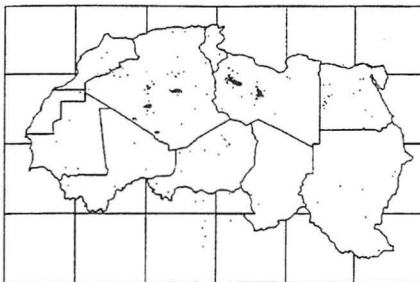


Fig. 1. Meteorite finds in the Sahara. Cluster in Algeria belongs to the Acfer and Tanesrouf finds, those in Libya to Hammadah al Hamra and Dar al Gani.



Fig. 2. Meteorite finds of the USA show a cluster in dry areas of Texas and New Mexico.

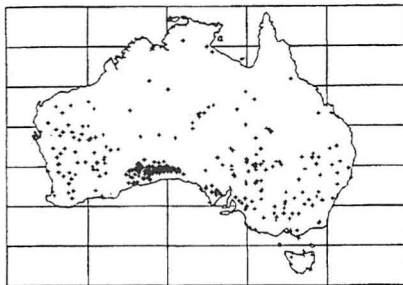


Fig. 3. Numerous meteorite finds show up at the Nullarbor desert in Australia.

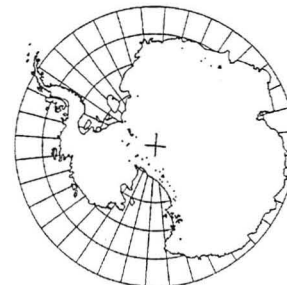


Fig. 4. The many Antarctic meteorites are found on Blue Icefields located along the Transantarctic Mountains and at the Yamato Mountains.

CONTENTS

| | |
|---|-----------|
| Program..... | ix |
| Summary of Previous Workshop..... | 1 |
| Workshop Summary | 3 |
| Collections, Collecting Areas, and Pairing Problems | 3 |
| Weathering Effects | 4 |
| Terrestrial Age Determinations | 5 |
| Interplanetary Dust Particles | 5 |
| Noble Gases and Cosmic-Ray Effects | 6 |
| Repositories of Desert Meteorites | 7 |
| Acknowledgments..... | 9 |
| Abstracts | 11 |
| The Natural Thermoluminescence Survey of Antarctic Meteorites: Ordinary Chondrites at the Grosvenor Mountains, MacAlpine Hills, Pecora Escarpment and Queen Alexandra Range, and New Data for Elephant Moraine Ice Fields <i>P. H. Benoit and D. W. G. Sears</i> | 11 |
| Meteorites from the Nullarbor, Australia: An Update <i>A. W. R. Bevan, P. A. Bland, and A. J. T. Jull.....</i> | 15 |
| Ice Flow as the Principal Sink for Antarctic Meteorites <i>P. A. Bland, A. J. T. Jull, A. W. R. Bevan, T. B. Smith, F. J. Berry, and C. T. Pillinger.....</i> | 17 |
| Pairing among EET87503 Group Howardites and Polymict Eucrites <i>P. C. Buchanan, D. J. Lindstrom, and D. W. Mittlefehldt.....</i> | 21 |
| Chemical Alteration of Hot Desert Meteorites: The Case of Shergottite Dar al Gani 476 <i>G. Crozaz and M. Wadhwa</i> | 25 |

| | |
|---|----|
| Chemical Compositions of Large Interplanetary Dust Particles from the Stratosphere and Small Antarctic Micrometeorites: Evidence for Element Loss and Addition in the Antarctic Micrometeorites <i>G. J. Flynn, S. R. Sutton, and W. Klöck</i> | 28 |
| The Influence of Terrestrial Weathering on Implanted Solar Gases in Lunar Meteorites <i>I. Franchi, A. B. Verchovsky, and C. T. Pillinger</i> | 33 |
| Meteorites from Cold and Hot Deserts: How Many, How Big, and What Sort <i>M. M. Grady</i> | 36 |
| Using ^{14}C and ^{14}C - ^{10}Be for Terrestrial Ages of Desert Meteorites <i>J. T. Jull, P. A. Bland, S. E. Klandrud, L. R. McHargue, A. W. R. Bevan, D. A. Kring, and F. Wlotzka</i> | 41 |
| The Gold Basin Strewn Field, Mojave Desert, and its Survival from the Late Pleistocene to the Present <i>D. A. Kring, A. J. T. Jull, and P. A. Bland</i> | 44 |
| Thermally Mobile Trace Elements in Carbonaceous Chondrites from Cold and Hot Deserts <i>M. E. Lipschutz</i> | 46 |
| Historical Notes on Three Exceptional Meteorites of Southern Africa: The Cape of Good Hope, Gibeon, and Hoba <i>U. B. Marvin</i> | 48 |
| Saharan Meteorites with Short or Complex Exposure Ages <i>S. Merchel, M. Altmair, T. Faestermann, U. Herpers, K. Knie, G. Korschinek, P. W. Kubik, S. Neumann, R. Michel, and M. Suter</i> | 53 |
| Cosmogenic and Trapped Gas Components in the Martian Meteorite Dar al Gani 476 from Hot Desert <i>S. V. S. Murty and R. K. Mohapatra</i> | 57 |
| Thermal Effects on Mineralogy, Noble Gas Composition, and Carbonaceous Material in CM Chondrites <i>T. Nakamura, T. Kitajima, and N. Takaoka</i> | 61 |
| Terrestrial Ages of Antarctic Meteorites — Up Date 1999 <i>K. Nishiizumi, M. W. Caffee, and K. C. Welten</i> | 64 |
| Type I Cosmic Spheres: Key to a Major but Poorly Sampled Asteroid Population? <i>L. E. Nyquist</i> | 65 |

| | |
|---|-----------|
| Do Weathering Effects Influence Cosmic Ray Exposure Ages of Enstatite Chondrites? <i>A. Patzer and L. Schultz</i> | 67 |
| Solar-Cosmic-Ray-Produced Nuclides in Extraterrestrial Matter <i>R. C. Reedy</i> | 69 |
| Noble Gases in 15 Meteorites from the Sahara: Eucrites, Ureilites, and Ordinary Chondrites <i>P. Scherer, M. Pättsch, and L. Schultz</i> | 72 |
| Deflation and Meteorite Exposure on Playa Lakes in the Southwestern United States: Unpaired Meteorites at Lucerne Dry Lake, California <i>R. S. Verish, A. E. Rubin, C. B. Moore, and R. A. Oriti</i> | 74 |
| Iron Meteorites from Antarctica: More Specimens, Still 40% Ungrouped <i>J. T. Wasson</i> | 76 |
| The Libyan Meteorite Population <i>D. Weber, J. Zipfel, and A. Bischoff</i> | 81 |
| Degree of Weathering of H-Chondrites from Frontier Mountain, Antarctica <i>K. C. Welten and K. Nishiizumi</i> | 83 |
| Cosmogenic Radionuclides in Hot Desert Chondrites with Low ¹⁴ C Activities: A Progress Report <i>K. C. Welten, K. Nishiizumi, and M. W. Caffee</i> | 88 |
| Noble Gases in Desert Meteorites: Howardites, Unequilibrated Chondrites, Regolith Breccias and an LL7 <i>R. Wieler, H. Baur, H. Busemann, V. S. Heber, and I. Leya</i> | 90 |
| Identical Origin for Halide and Sulfate Efflorescences on Meteorite Finds and Sulfate Veins in Orgueil <i>M. E. Zolensky</i> | 95 |
| List of Workshop Participants | 97 |

Program

Tuesday, July 6, 1999

Travel by bus from Johannesburg to Kwa Maritane Lodge at Pilanesberg
Registration

Wednesday, July 7, 1999

8.30–8.45 Welcome

8.45–9.20

HISTORICAL NOTE

Chair: L. Schultz

U. B. Marvin

Historical Notes on Three Exceptional Meteorites of Southern Africa: The Cape of Good Hope, Gibeon, and Hoba

COLLECTIONS, MECHANISMS, PAIRINGS

Chair: S. S. Russell

M. M. Grady

Meteorites from Cold and Hot Deserts: How Many, How Big, and What Sort

D. Weber, J. Zipfel, and A. Bischoff

The Libyan Meteorite Population

A. W. R. Bevan, P. A. Bland, and A. J. T. Jull

Meteorites from the Nullarbor, Australia: An Update

J. T. Wasson

Iron Meteorites from Antarctica: More Specimens, Still 40% Ungrouped

D. A. Kring, A. J. T. Jull, and P. A. Bland

The Gold Basin Strewn Field, Mojave Desert, and its Survival from the Late Pleistocene to the Present

P. C. Buchanan, D. J. Lindstrom, and D. W. Mittlefehldt

Pairing among EET87503 Group Howardites and Polymict Eucrites

P. A. Bland, A. J. T. Jull, A. W. R. Bevan, T. B. Smith, F. J. Berry, and C. T. Pillinger

Ice Flow as the Principal Sink for Antarctic Meteorites

R. S. Verish, A. E. Rubin, C. B. Moore, and R. A. Oriti (Poster)

Deflation and Meteorite Exposure on Playa Lakes in the Southwestern United States: Unpaired Meteorites at Lucerne Dry Lake, California

14.00–15.50

WEATHERING EFFECTS

Chair: I. A. Franchi

G. Crozaz, and M. Wadhwa

Chemical Alteration of Hot Desert Meteorites: The Case of Shergottite Dar al Gani 476

M. E. Lipschutz

Thermally Mobile Trace Elements in Carbonaceous Chondrites from Cold and Hot Deserts

T. Nakamura, T. Kitajima, and N. Takaoka

Thermal Effects on Mineralogy, Noble Gas Composition, and Carbonaceous Material in CM Chondrites

M. E. Zolensky

Identical Origin for Halide and Sulfate Efflorescences on Meteorite Finds and Sulfate Veins in Orgueil

K. C. Welten and K. Nishiizumi

Degree of Weathering of H-Chondrites from Frontier Mountain, Antarctica

16.10–17.50

**TERRESTRIAL AGES AND
INTERPLANETARY DUST PARTICLES**

Chair: M. E. Zolensky

J. T. Jull, P. A. Bland, S. E. Klandrud, L. R. McHargue, A. W. R. Bevan, D. A. Kring,
and F. Wlotzka

Using ^{14}C and ^{14}C - ^{10}Be for Terrestrial Ages of Desert Meteorites

K. Nishiizumi, M. W. Caffee, and K. C. Welten

Terrestrial Ages of Antarctic Meteorites — Up Date 1999

K. C. Welten, K. Nishiizumi, and M. W. Caffee

*Cosmogenic Radionuclides in Hot Desert Chondrites with Low ^{14}C Activities:
A Progress Report*

G. J. Flynn, S. R. Sutton, and W. Klöck

Chemical Compositions of Large Interplanetary Dust Particles from the Stratosphere and Small Antarctic Micrometeorites: Evidence for Element Loss and Addition in the Antarctic Micrometeorites

L. E. Nyquist

Type I Cosmic Spheres: Key to a Major but Poorly Sampled Asteroid Population?

Thursday, July 8, 1999

8.30–12.15

NOBLE GASES AND COSMIC-RAY EFFECTS

Chair: U. Herpers and R. Wieler

R. C. Reedy

Solar-Cosmic-Ray-Produced Nuclides in Extraterrestrial Matter

I. Franchi, A. B. Verchovsky, and C. T. Pillinger

The Influence of Terrestrial Weathering on Implanted Solar Gases in Lunar Meteorites

- S. V. S. Murty and R. K. Mohapatra
Cosmogenic and Trapped Gas Components in the Martian Meteorite Dar al Gani 476 from Hot Desert
- R. Wieler, H. Baur, H. Busemann, V. S. Heber, and I. Leya
Noble Gases in Desert Meteorites: Howardites, Unequilibrated Chondrites, Regolith Breccias and an LL7
- P. Scherer, M. Pätzsch, and L. Schultz
Noble Gases in 15 Meteorites from the Sahara: Eucrites, Ureilites, and Ordinary Chondrites
- P. H. Benoit and D. W.G.Sears
The Natural Thermoluminescence Survey of Antarctic Meteorites: Ordinary Chondrites at the Grosvenor Mountains, MacAlpine Hills, Pecora Escarpment and Queen Alexandra Range, and New Data for Elephant Moraine Ice Fields
- A. Patzer and L. Schultz
Do Weathering Effects Influence Cosmic Ray Exposure Ages of Enstatite Chondrites?
- S. Merchel, M. Altmaier, T. Faestermann, U. Herpers, K. Knie, G. Korschinek, P. W. Kubik, S. Neumann, R. Michel, and M. Suter
Saharan Meteorites with Short or Complex Exposure Ages

16:00

Departure to Johannesburg

SUMMARY OF PREVIOUS WORKSHOPS

Prior to the present workshop there have been five workshops specifically dealing with Antarctic meteorites and specimens found in hot desert areas. It is appropriate to briefly describe the previous meetings as background for this presentation.

The first workshop was held at the Lunar and Planetary Institute in Houston, April 19–21, 1982. The conveners were C. Bull (Ohio State University) and M. E. Lipschutz (Purdue University). The general theme of the meeting was the interface between Antarctic glaciology and meteorites found principally in blue ice areas. This first meeting was principally a learning effort for most attendees, and the report [1] reflected that fact. It is a compendium of information known at that time which stressed the need for studying blue ice areas as meteorite concentration regions and for utilizing the specimens as tracers of ice sheet movement.

The second workshop was held at the Max-Planck-Institut für Chemie in Mainz, Germany, July 10–12, 1985 [2]. The conveners were J. Annexstad (Houston), L. Schultz (Mainz), and H. Wänke (Mainz). This workshop was attended by 78 participants from 12 different countries. The purpose of this meeting was twofold: (1) to explore the possibility of general procedures for collection, curation, handling, and distribution of specimens worldwide; and (2) to discuss further the relationship between Antarctic meteorites and Antarctic glaciological processes. The workshop was held in Mainz just prior to the Meteoritical Society Meeting in Bordeaux.

The third workshop was entitled “Antarctic Meteorite Stranding Surfaces” and was held July 13–15, 1988, at the University of Pittsburgh. The conveners were W. Cassidy (Pittsburgh) and I. Whillans (Ohio State University). Twenty-four participants attended and 29 presentations were given with a primary focus on glaciological processes [3]. In general, the workshop participants urged the continued collection of meteorites from Antarctica and the glaciological investigation of stranding surfaces. The entire problem of meteorite transport and concentration is imperfectly understood and is a subject complicated by a number of interrelated factors. As noted by the editors: “The situation [meteorite recovery in Antarctica] appears to present a classic opportunity, in which one unexpected discovery, Antarctic meteorites, leads not only to fundamental insights in its own field but also opens exciting directions in another” [3].

The next workshop was held in Vienna, Austria, on July 27–28, 1989, prior to the Annual Meeting of the Meteoritical Society at the University of Vienna. Conveners were C. Koeberl (University of Vienna) and W. Cassidy (University of Pittsburgh). It was entitled “Differences Between Antarctic and Non-Antarctic Meteorites,” in

response to the large numbers of recovered specimens from Antarctica that appeared to differ from “modern falls.” The meeting was attended by 45 participants from 10 different countries and 25 papers were presented. Among the participants there seemed to be general agreement that there were measurable differences between Antarctic and non-Antarctic meteorite specimens. However, as pointed out by one summarizer, it was unclear whether the differences are due to terrestrial weathering or are of preterrestrial origin.

In the general workshop summary [4] it was noted that although differences had been recognized, there was no general agreement on causes among the workshop participants. The obvious differences are in type frequencies among rare or unique specimens, textures, terrestrial ages, and mass abundances. The real question was whether or not either population (Antarctic or non-Antarctic) is representative of an individual parent population. Even with the present data in hand, it seems that more specimens are needed to help complete the dataset. Although the Antarctic specimens do represent the best sample set presently available, the advent of new specimens from the dry desert areas of the world will add important new information.

The fifth workshop, entitled “Workshop on Meteorites from Cold and Hot Deserts,” was held in Nördlingen (Germany), July 20–22, 1994, just prior to the Meteoritical Society meeting in Prague. Conveners were L. Schultz (Mainz), J. O. Annexstad (Bemidji), and M. E. Zolensky (Houston). The meeting was attended by 59 participants from 11 countries and 32 papers were presented.

In this workshop possible differences between Antarctic meteorites, finds from hot deserts, and modern falls were again discussed as well as possible causes. During this workshop questions of curation and of coordination of future meteorite searches were explored.

REFERENCES

- [1] Bull C. and Lipschutz M., eds. (1982) *Workshop on Antarctic Glaciology and Meteorites*, LPI Tech. Rpt. 82-03, LPI, Houston. 57 pp. [2] Annexstad J. O., Schultz L., and Wänke H., eds. (1986) *Workshop on Antarctic Meteorites*, LPI Tech. Rpt. 86-01, LPI, Houston. 119 pp. [3] Cassidy W. A. and Whillans I. M., eds. (1990) *Workshop on Antarctic Meteorite Stranding Surfaces*, LPI Tech. Rpt. 90-03, LPI, Houston. 103 pp. [4] Koeberl C. and Cassidy W. A., eds. (1990) *Workshop on Differences Between Antarctic and Non-Antarctic Meteorites*, LPI Tech. Rpt. 90-01, LPI, Houston. 102 pp. [5] Schultz L., Annexstad J. O., and Zolensky M. E., eds. (1995) *Workshop on Meteorites from Cold and Hot Deserts*, LPI Tech. Rpt. 95-02, LPI, Houston. 83 pp.

WORKSHOP SUMMARY

COLLECTIONS, COLLECTING AREAS, AND PAIRING PROBLEMS

Meteoriticists, accustomed to working with the highly dispersed and not always readily available meteorites stored in museums and private collections, have yet to adjust completely to the flood, or more appropriately the shower, of new meteorite samples recovered from the Antarctic in recent years. These major discoveries from the Earth's cold deserts continue to accumulate and have now been supplemented by significant yields of meteorites from the hotter deserts of the world, particularly North Africa and Australia.

The magnitude of this new abundance is well revealed by the statistics presented by Monica Grady at the Workshop. The 5th Catalogue of Meteorites records, as of May 1999, some 22,152 meteorites with 17,474 Antarctic finds (no allowance made for possible pairings), 1508 Saharan meteorite samples (Algeria and Libya), and over 250 meteorites from the Nullarbor Region of Western and South Australia. Meteorite recovery in any area depends on abundance, a function of concentration mechanisms in the ice deserts, of preservation, as reflected in terrestrial age distributions among the samples, and of ease of recognition in visual surveys. The importance of the latter criterion is evident in Grady's observation if the lower mean size of samples recovered from the Antarctic. Grady also notes the value of the hot desert collections in their higher yield of unusual meteorite types, other than irons, in comparison to modern falls and finds. Coupled to quality curation and accessibility for research, this influx of new meteorite material has changed the nature of meteorite research.

John Wasson summarized data on Antarctic iron meteorites emphasizing the relatively high abundance, 40%, of ungrouped irons in the collection. The high abundance of ungrouped irons was attributed to the numbers of smaller iron meteorites in the collection since smaller objects are more likely to occupy orbits different from that of the parent asteroid, or as Wasson puts it, "tend to wander farther from home."

Combining Mössbauer data to indicate degree of weathering of Antarctic meteorite samples with terrestrial age data, Bland and colleagues show a peak in oxidation-frequency distribution significantly lower than found for meteorites from hot deserts, inconsistent with the contention that the meteorite-rich blue ice areas are static accumulations and that the meteorite populations represent a mature weathering signature. Indeed many of the meteorites examined still retain some fusion crust. The gradients in terrestrial ages for meteorites in specific icefields (Jull et al., 1998) are also consistent with a lower weathering index. The terrestrial age spectrum is interpreted as a result of ice movement, a hypothesis that, if correct, can be used to make

estimates of flow rates for catchment areas, and to allow estimates of meteorite flux over 10^5 – 10^6 years.

The summary data on meteorites collected from two major areas in Libya that have yielded over 850 meteorites with terrestrial ages up to 30,000 years, were presented by Weber and colleagues. An estimate of 1.2 meteorites per square kilometer is a lower limit as the searching relies on visual observation from a vehicle. Pairing can be established for the less common meteorites but is a problem for ordinary chondrites, particularly the H5s and L6s. Assuming 60% pairing for the ordinary chondrites results in an above-average abundance of ordinary chondrites for this region. However, this anomaly is removed if pairing in the ordinary chondrites, is normalized to the carbonaceous chondrites where pairing can be more reliably established and is as high as 77%. Using this approach the Libyan meteorite abundances resemble those from other sites except in the low abundance of irons.

The collections from the Nullarbor Plains in Australia were documented by Bevan and colleagues. Terrestrial meteorites ages have been used in this region as a guide to palaeoclimate over the last 30,000 years in this region of remarkable surface stability. As in the Libyan desert, irons are in low abundance (although three irons make up 99% of the total recovered meteorite mass) a factor that may be influenced by human intervention. The pairing problem is minimized in Nullarbor as samples appear to have remain totally undisturbed since their fall. The population statistics closely resemble the Antarctic data and differs only slightly from the Libyan data. In comparison to modern falls, the Nullarbor population has an above-average number of the less-common chondrite types, perhaps reflecting the ease of recognition in this environment or the skill and experience of the finders. The recovery of meteorites from the Nullarbor has slowed to a trickle due to an unfortunate disease that has eliminated the rabbit population of Australia. The rabbits had been maintaining the Nullarbor in a nonvegetative state. With their absence, the desert has been reclaimed by grasses that mask the meteorites and prevent their recovery.

Verish and colleagues have been investigating the playa lakes in the Mojave Desert in southern California, report on meteorite finds from several of these, and raise the prospect of further finds from other dry lakes in the region. The Lucerne Dry Lake is the source for 17 specimens from at least 7 separate meteorites and the extent of pairing is notably low.

Kring and his associates report on the recovery of approximately 3000 specimens of the Gold Basin L4 chondrite from an area of 225 square kilometers in the Mojave Desert. A detailed reconstruction of the palaeo-environment since the fall 14,000 years ago indicates that

most of the weathering of the samples occurred early, in the wetter warmer portion of the Wisconsin glaciation.

Buchanan and coworkers were able to determine the extent of pairing among howardites and polymict eucrites from the broader Elephant Moraine collecting region in Antarctica, a determination that could be made with certainty after consideration of data on bulk, matrix, and mineral compositions combined with estimates of terrestrial alteration. Such determinations among the more abundant ordinary chondrites will require a more detailed geochemical database than is currently available.

The workshop was enriched by the accounts, brought together by Ursula Marvin, of the discovery and subsequent history of the Cape of Good Hope iron in South Africa, of the largest known meteorite, Hoba in Namibia, and of the great iron meteorite shower, Gibeon, also in Namibia.

The 1999–2000 ANSMET field party will cover a lot of ground this season, with the major target being several icefields in the Walcott Névé region. The Walcott Névé region lies just north of the headwaters of the Beardmore Glacier, and just south of the Law Glacier. This area has been a prolific source of meteorites for ANSMET field parties, including well-known meteorite sources such as the Lewis Cliff ice tongue, the Queen Alexandra Range (also known as the Foggy Bottom area), and the MacAlpine Hills icefields. During the 1999–2000 season, the primary target will be an area informally called “Foggy Bottom” at the south end of the Walcott Névé, where 5 previous seasons of work have recovered over 3400 meteorites. Other targets this season are the Goodwin Nunataks icefields (near Foggy Bottom), the MacAlpine Hills icefield, the Miller Range, and the Geologists Range.

A successful meteorite recovery expedition was held following the 1999 Meteoritical Society meeting in Johannesburg. Expedition members (Sara Russell, Phil Bland, Matt Genge of the Natural History Museum, Mike Zolensky of NASA JSC) returned to the same general area searched by Arch Reid, Peter Jakes, and Mike Zolensky in 1990, being ancient slightly dissected desert pavement surfaces immediately southwest of Walvis Bay, Namibia. During the previous expedition, during which three meteorites were recovered, basins were primarily searched. During the 1999 expedition, similar basins were initially searched, with no success. However, searches of the flat, desert paved plains *above* the basins provided approximately one dozen meteorites. This is apparently an ancient exposed surface, with no subsequent concentration process operating. Further expeditions to this area might be warranted. The meteorites recovered by this expedition are currently on loan to the natural history Museum in London, but are ultimately the property of the Namibian Geological Survey.

The papers presented are a sample of the diversity of studies based on the principal meteorite collection areas of the Antarctic, the Sahara, and the Nullarbor desert regions. These, and other regions yet to be investigated, provide the

stable land surfaces coupled to high preservation potential to act as accumulation surfaces over extended periods of time, as witnessed by the spectrum of meteorite terrestrial ages from these localities. We have yet to achieve a complete understanding of all the processes that result in meteorite preservation, but it should not be difficult to predict and to search some of the areas with greatest potential. We have scratched the surface of the populations from the hot and cold desert regions and in so doing have added substantially to the quantity and to the diversity of our meteorite collections, a timely development in meteoritics that has helped fill a gap in the availability of samples returned from other solar system bodies.

WEATHERING EFFECTS

In the field of meteorite research, ever-increasing insights about asteroidal and planetary parent bodies are being pried from these precious stones through progressively detailed studies and the application of ever more powerful analytical techniques. However, increased caution must be exercised when interpreting many of these mineralogical, chemical or isotopic features as the extent and pervasiveness of terrestrial alteration and contamination becomes increasingly apparent.

From the moment a meteorite enters the Earth's atmosphere it is subjected to an environment far removed from the conditions it formed in, or in which it has subsequently been “stored,” and therefore is prone to reaction as it attempts to regain chemical equilibrium with its new surroundings. Therefore, to identify and interpret the indigenous features it is first necessary to identify and exclude any terrestrial features. At first glance, many of these terrestrial features may appear obvious. However, details of these effects are very important, particularly where they overlap with the indigenous features we are attempting to study. This task is made even more challenging by the wide range of different environments from which meteorites have been recovered, and the different reactions and processes that have affected them.

Discussion of these aspects began with a study of the REE abundances in the shergottite DaG 476 by G. Crozaz. In this Saharan meteorite there is evidence for considerable mobilization of LREE from the host merrillites into surrounding minerals and into crack infill material in this heavily weathered meteorite, to an extent considerably greater than that seen in similar meteorites collected in Antarctica.

A study of weathering effects on ordinary chondrites from Antarctica was presented by K. Welten. The levels of oxidized metal present in the nonmagnetic fractions of H chondrites from Frontier Mountain suggested two populations of meteorites from this site. One group, displaying low degrees of weathering, may have resided within the ice until very recently, whereas a second, more abundant population, with much higher weathering rates,

would have spent a considerable proportion of their terrestrial residence on the surface of the ice. Such observations highlight the diversity of weathering issues, even from a single environment.

In contrast to this diversity, evidence from two recent falls allowed M. Zolensky to argue that apparently distinct features may in fact have a common origin. The observation of abundant halite in Zag and Monahans (1998) was used to suggest that the efflorescences commonly seen in Antarctic meteorites are not terrestrial contamination but rather due to dissolution and reprecipitation of indigenous halite. Similarly, the CI chondrite Orgueil displays evidence that the cracks filled with hydrous magnesium sulfates are due to a similar remobilization of material after the polished mounts were prepared.

Two other talks in this session highlighted an additional complication to the study of terrestrial weathering, namely differences in the populations between modern falls and meteorites from hot and cold deserts. Talks by M. Lipschutz and by T. Nakamura considered details about the metamorphosed carbonaceous chondrites found only in Antarctic, and to a lesser extent in hot desert collections. The former presented arguments outlining a metamorphic sequence based upon volatile element depletions while the later discussed evolution of textures, noble gas abundances, and the organic carbon components.

TERRESTRIAL AGE DETERMINATIONS

Jull described recent progress in the use of ^{14}C and ^{14}C - ^{10}Be for determinations of meteorite terrestrial ages. They note a predictable exponential drop off in meteorite populations from hot deserts with terrestrial ages to at least 30 ka, although they have documented varying weathering rates for different deserts. They discussed the new dating technique using both ^{14}C and ^{10}Be , in which the effects of shielding can be corrected. Since both of these nuclides are produced by spallation of oxygen, their depth dependence is similar, and their production rate is independent of chemistry, the ^{10}Be production rate can be used to correct the ^{14}C production rate, yielding improved terrestrial ages. Neupert et al. (*Meteoritics & Planet. Sci.*, 32, A98, 1997) and Kring et al. (*LPS XXIX*, 1998) have already reported some results using this procedure.

Nishiizumi provided an update on efforts to determine the terrestrial ages of a huge number of Antarctic meteorites. They have measured these in 270 new meteorites using ^{36}Cl , and report that they have reduced the typical 70-ka errors for these determinations to 40 ka, by using nuclide pairs, such as ^{41}Ca - ^{36}Cl and ^{36}Cl - ^{10}Be . They find terrestrial ages up to 2 Ma, with the Allan Hills meteorites representing the oldest population, although many of the Lewis Cliff Ice Field meteorites have old ages also. Interestingly, they find no correlation of terrestrial age with location on the Lewis Cliff ice field, which certainly

complicates use of terrestrial ages to refine models of ice stranding and movement dynamics.

In related work, Welten reported on efforts to determine the terrestrial ages of meteorites for which the concentration of ^{14}C had decayed to the point where it cannot be used. For these meteorites, the concentration of cosmogenic ^{36}Cl and ^{41}Ca were measured. As the original ratio of these nuclides in the metal phase in chondrites is constant and well determined, the measured ration in the meteorite finds can be used as a measure of terrestrial age.

INTERPLANETARY DUST PARTICLES

Flynn showed that the largest interplanetary dust particles (IDPs) captured in the stratosphere are not chemically identical to the same sized micrometeorites recovered from polar ices. One might have thought that they would be identical. Instead, they find that the large stratospheric IDPs have chondritic Ni/Fe ratios within a factor of 3, and that about one-third have depletions in Zn and Ge generally related to evaporative loss during atmospheric entry. In contrast, almost all the polar micrometeorites show greater than 3 \times decrease of Ni/Fe below chondritic levels, and significant depletions in Ge and Se. Most of the polar micrometeorites, including all the ones from Antarctica, showed enrichments in Zn, as well as Pb. Discussion at the workshop suggested that these chemical changes in the polar micrometeorites are consistent with leaching of sulfides in the terrestrial environment, and contamination by terrestrial Pb. An unresolved question is why these polar micrometeorites, being larger than most IDPs, have not lost significant Zn during atmospheric ablation. It is possible that the polar micrometeorites are truly different than the large stratospheric IDPs, and sample different bodies.

Nyquist offered a new interpretation of the origin of I-type cosmic spherules based on abundances of Fe, Cr, and Ni reported by Herzog (*GCA*, 63, in press, 1999), and calculated fractionation factors of these elements during atmospheric ablation. The isotopic fractionation for these three elements is large, indicating evaporative losses on the order of 80–85%. The calculated preatmospheric Fe/Ni and Cr/Ni ratios are inconsistent with derivation of the I-type spherules from iron meteorites (the conventional hypothesis). Nyquist suggests that these spherules could have originated as independent metal grains from CO chondrite parent asteroids, or perhaps from other asteroids not sampled as meteorites.

During discussion at the workshop, T. Nakamura described how the Japanese have recently returned from Antarctica with a large quantity of polar micrometeorites. These were collected by scientists of the National Institute of Polar Research (NIPR) in the course of their recent expedition to recover meteorites. These micrometeorites are now being curated at the NIPR, in a new specially constructed clean room facility, and are receiving a preliminary

characterization by a consortium of Japanese meteoriticists. It is anticipated that these samples will presently be made available for distribution to investigators worldwide. The Japanese are making a determined effort to develop techniques for analysis of nanogram-sized materials in preparation for the return of the Muses-C mission asteroid samples, which will consist of a few grams of dust and chips.

NOBLE GASES AND COSMIC-RAY EFFECTS

In meteorites noble gas components of different origin can be characterized by a specific isotopic or elemental composition. Some have been produced *in situ* in the meteoritic material such as *radiogenic* or *cosmogenic* gases. Others are *trapped* gases that are incorporated into meteoritic material when formed, or were implanted as solar-wind ions.

Cosmogenic noble gas nuclides are used to determine the irradiation history of meteorites (cosmic-ray exposure ages). A combination with cosmogenic radionuclides produces information on possible complex irradiation histories, the size of the meteoroid, and its terrestrial age. Such information is also valuable if pairing of meteorites is considered, a major problem of meteorites from hot and cold deserts when statistical considerations are applied. The material of many of these meteorites is altered by weathering effects on Earth. These effects are more pronounced in specimens from hot deserts compared to Antarctic meteorites or to modern falls. Therefore, the influence of weathering on the noble gas and radionuclide record of meteorites was an important topic for discussion in this workshop.

Meteorites finds from the Antarctic have generally smaller masses than those found in other areas (see, e.g., Grady, this volume), and effects of solar cosmic rays are expected not to be negligible in small meteoroids. R. Reedy reported calculations of production rates of solar-proton-produced nuclides in such bodies. He concluded that small objects in space — which may result in small meteorites — could have enhanced cosmogenic nuclide concentrations due to this effect.

The influence of weathering on solar-wind-implanted gases in regolithic breccias — in this case the lunar meteorite DaG 262 — were discussed by I. Franchi. He and his co-workers have studied the release of N and Ar in stepped heating experiments and compared it to other lunar

meteorites. Only small differences in the gas profiles of three lunar meteorites are observed, but they are distinct from those of returned lunar samples. Presently, it is not possible to attribute this difference to terrestrial weathering or shock metamorphism.

A special experiment to explain a deficit of cosmogenic Ar in some enstatite chondrites was described by A. Patzer. She carried out experiments simulating the weathering of meteorites in the field. As a result it was shown that the concentration of cosmogenic Ar did decrease after treatment with water.

S. Merchel discussed the irradiation history of five Saharan meteorites with low cosmogenic radionuclide concentrations. The E4 chondrite Acfer 287 has suffered a complex irradiation history with a recent irradiation of 2.9 Ma as a meteoroid after being irradiated for a longer time, possibly at the surface of its parent body. A similar scenario could explain the cosmogenic nuclides of Dar al Gain 055. Hammadah al Hamra 056 and 096 are possibly pieces from very large meteoroids (preatmospheric radius about 120 cm), while Hammadah al Hamra 096 obviously was a rather small meteoroid with a maximum radius of 15 cm.

L. Schultz reported new noble gas measurements on 15 meteorites recently found in Libya. He discussed possible pairings and noted that trapped Kr and Xe is influenced by adsorbed terrestrial atmospheric gases. R. Wieler described the results of noble gas measurements of 16 meteorites from the Antarctic and from hot deserts. He reported on noble gas systematics in meteorites, exposure ages, and possible pairings.

S. Murty discussed the noble gases and N content of Dar al Gani 476, a new SNC meteorite from Libya. He confirmed an exposure age of 1.1 ± 0.1 Ma for this meteorite, which is different from that of all other SNCs. The trapped gases (including N) are mainly a mixture of Chassigny-type gas (martian mantle?) and terrestrial contamination. One temperature step, however, shows a high $^{129}\text{Xe}/^{132}\text{Xe}$, indicating some martian atmospheric gas.

D. Sears reviewed natural and induced thermoluminescence data for samples collected at different Antarctic ice fields. He concluded that all ice fields have sampled similar meteorite populations with similar temperature histories on Earth. Variations in some TL data among meteorites from different ice fields probably reflect differences in weathering.

REPOSITORIES OF DESERT METEORITES

At present, meteorites collected in deserts can be obtained by qualified investigators. The following information is provided to facilitate these loans.

ANSMET

Antarctic meteorite samples are available to research scientists of all countries, regardless of their current state of funding for meteorite studies. These expeditions result from a unique agreement between the National Science Foundation, the Smithsonian Institution, and NASA. In this arrangement the NSF provides the funding and support for collection activities, and NASA and the Smithsonian provide the curatorial and meteorite expertise.

Meteorite recovery expeditions have been held on a generally yearly basis since 1976. Samples collected by these expeditions are available from the Meteorite Working Group (MWG). The MWG is a peer-review committee that meets twice a year to guide the collection, curation, allocation, and distribution of the U.S. collection of Antarctic meteorites. Issuance of samples does not imply a commitment by any agency to fund the proposed research. Requests for financial support must be submitted separately to the appropriate funding agencies. As a matter of policy, U.S. Antarctic meteorites are the property of the National Science Foundation and all allocations are subject to recall.

Each request should accurately refer to meteorite samples by their respective identification numbers and should provide detailed scientific justification for proposed research. Specific requirements for samples, such as sizes or weights, particular locations (if applicable) within individual specimens, or special handling or shipping procedures should be explained in each request. Requests for thin sections that will be used in destructive procedures such as ion probe, etch, or even repolishing must be stated explicitly. Consortium requests should be initialed or countersigned by a member of each group in the consortium. All necessary information should probably be condensable into a one- or two-page letter, although informative attachments (reprints of publication that explain rationale, flow diagrams for analyses, etc.) are welcome.

Requests should be sent to:

Secretary, Meteorite Working Group
Mail Code SN2
NASA Johnson Space Center
Houston TX 77058, USA

Samples can be requested from any meteorite that has been made available through announcement in any issue of the *Antarctic Meteorite Newsletter* (beginning with 1 (1) in June 1978). Many of the meteorites have also been described in five *Smithsonian Contr. Earth Sci.*: Nos. 23,

24, 26, 28, and 30. A table containing all classifications as of December 1993 is published in *Meteoritics* 29(1), pp. 100–142. Back issues of the *Antarctic Meteorite Newsletter* can be obtained from the above address.

NIPR

The National Institute for Polar Research (NIPR) in Tokyo has successfully managed numerous expeditions to the Antarctic and collected thousands of meteorite fragments, and more recently polar micrometeorites. These searches have occurred since 1976 in the Yamato, Belgica, and Sør Rondane Mountains. Information on many of these meteorites has been published in the *Meteorite News* (published by the NIPR), and the abstracts and papers resulting from the annual Symposia on Antarctic Meteorites, hosted by the NIPR. These Antarctic meteorites are the property of the National Institute for Polar Research, and allocations are generally only made for a period of 1 to 2 years.

All requests for meteorite samples are reviewed by the Committee on Antarctic Meteorites, which meets approximately twice a year. Each request should accurately refer to meteorite samples by their respective identification numbers and should provide detailed scientific justification for proposed research. Specific requirements for samples, such as sizes or weights, particular locations (if applicable) within individual specimens, or special handling or shipping procedures should be explained in each request. Requests for samples or thin sections that will be used in destructive procedures such as ion probe, etch, or even repolishing must be stated explicitly.

Requests for meteorite samples and additional information should be addressed to:

Dr. Hideyasu Kojima
Curator of Meteorites
Department of Antarctic Meteorites
National Institute of Polar Research
9-10, Kaga 1-chome, Itabashi-ku
Tokyo 173, Japan

EUROMET

There have been several Euromet expeditions to Antarctica, generally held within the larger framework of German (GANOVEX) and Italian (PNRA) National Antarctic Programs. Part of the EUROMET meteorites are at the moment at the Open University at Milton Keynes, UK. Each request should accurately refer to meteorite samples by their respective identification numbers and should provide detailed scientific justification for proposed research. Specific requirements for samples, such as sizes or

weights, particular locations (if applicable) within individual specimens, or special handling or shipping procedures should be explained in each request. Requests for samples or thin sections that will be used in destructive procedures such as ion probe, etch, or even repolishing must be stated explicitly.

Requests for meteorite samples and additional information should be addressed to:

Dr. Robert Hutchison
Department of Mineralogy
The Natural History Museum
Cromwell Road
London SW7 5BD, UK

WAMET

For the past decade Prof. Alex Bevan has led numerous expeditions through the Nullarbor Plain in western Australia, recovering thousands of meteorite fragments. EUROMET has participated in several of the most recent recovery expeditions.

The disposition of these meteorites is controlled by the Meteorite Commission of Western Australia, which arranges for peer review of all requests. The WAMET meteorites are the property of the Western Australian Museum, and all allocations are considered loans. Each

request should accurately refer to meteorite samples by their respective identification numbers and should provide detailed scientific justification for proposed research. Specific requirements for samples, such as sizes or weights, particular locations (if applicable) within individual specimens, or special handling or shipping procedures should be explained in each request. Requests for samples or thin sections that will be used in destructive procedures such as ion probe, etch, or even repolishing must be stated explicitly.

Information on these collections and the availability of samples can be obtained from:

Prof. Alex Bevan
Department of Mineralogy
Western Australian Museum
Francis Street
Perth, Western Australia 6000

SAHARAN DESERT METEORITES

The new desert collections from the Sahara are distributed among many private collectors. Information on repositories may be found in METBASE 4.0, recently released by Jörn Koblitz.

ACKNOWLEDGMENTS

We thank all participants of the workshop who contributed valuable research papers and participated in discussions. In the course of the preparation for the workshop able assistance was received from L. Franke (Mainz). Before and during the meeting help by Dr. Gill Drennan (Johannesburg) and Dr. Paul Buchanan (Houston) is greatly appreciated.

We thank Prof. Uwe Reimold and Brenda Lacey-Smith (Johannesburg) for selecting Kwa-Maritane as the meeting place and for their efforts to make the local organization so perfect. All sponsoring agencies, especially the Lunar and Planetary Institute, Houston, the Department of Geology of the University of the Witwatersrand, and the Max-Planck-Institut für Chemie, Mainz, are thanked for technical, logistical, and financial help.

THE NATURAL THERMOLUMINESCENCE SURVEY OF ANTARCTIC METEORITES: ORDINARY CHONDRITES AT THE GROSVENOR MOUNTAINS, MACALPINE HILLS, PECORA ESCARPMENT AND QUEEN ALEXANDRA RANGE, AND NEW DATA FOR THE ELEPHANT MORaine, ICE FIELDS. Paul H. Benoit and Derek W.G. Sears. Cosmochemistry Group, University of Arkansas, Fayetteville, Arkansas 72701 USA. E-mail: pbenoit@comp.uark.edu.

Introduction

The natural TL survey of Antarctic meteorites was started in 1987 at the request of the Antarctic Meteorite Working Group in order to provide an initial description of radiation and thermal histories [1]. It was intended to be a complement to the mineralogical and petrographic surveys performed at the Johnson Space Center and the Smithsonian Institution. All ANSMET samples recovered since then, besides those that were heated throughout by atmospheric passage, have been measured. To date this amounts to about 1200 samples. As the data for each ice field reaches a significant level, we have been conducting a thorough examination of the data for that field with a view to (1) identifying pairing, (2) providing an estimate of terrestrial age and residence time on the ice surface, (3) looking for differences in natural TL between ice fields, (4) looking for variations in natural TL level with location on the ice, (5) looking for meteorites with natural TL levels outside the normal range. Pairing is a necessary first step in ensuring the most productive use of the collection, while geographical variations could perhaps provide clues to concentration mechanisms. Samples with natural TL values outside the normal range are usually inferred to have had either small perihelia or recent changes in orbital elements. In addition, induced TL data have enabled us to (5) look for evidence for secular variation in the nature of the flux of meteorites to Earth, and (6) look for petrologically unusual meteorites, such as particularly primitive ordinary chondrites, heavily shocked meteorites, or otherwise anomalous meteorites. To date we have published studies of the TL properties of 167 ordinary chondrites from Allan Hills [2], 107 from Elephant Moraine [3] and 302 from Lewis Cliff [4] and we have discussed the TL properties of fifteen H chondrites collected at the Allan Hills by Euromet after a storm during the 1988 season [5]. We now have additional databases for a reasonable number of ordinary chondrites from Grosvenor Mountains (39 meteorites), MacAlpine Hills (70 meteorites), Pecora Escarpment (60 meteorites), and Queen Alexandra Range (173 meteorites) and we have data for a further 101 samples from Elephant Moraine. The results are summarized in Table 1. We also have fairly minimal databases (10-15 meteorites) for Dominion Range, Graves Nunataks, Reckling Peak and Wisconsin Range that will not be discussed here.

Discussion

Pairing. Our criteria for pairing of individual meteorites are based on the variation in natural TL and TL sensitivity in multiple samples of individual modern falls and seem fairly robust [6-9], especially when combined with mineralogical, petrographic, isotopic and geographic data. However, our estimates for the amount of pairing at a given ice field are probably conservative because of our bias against small samples. Small samples (<20 g, *i.e.* those that cannot provide a chip >5 mm from any potential surface) cannot be measured because their natural TL was probably drained by heating during atmospheric passage. Of the 471 ordinary chondrites in the current database not previously discussed, 246 are probably paired samples so that the collection represents no more than an additional 224 individual falls, or ~50% of the total number of samples. The prevalence of pairing varies considerably between ice fields. Our earlier work found the incidence of pairing at the Allan Hills, Elephant Moraine and Lewis Cliff fields to be 23%, 32% and 14%, respectively. The new Elephant Moraine samples have a pairing incidence of 58%, considerably higher than the previous data. About 18% of the Grosvenor Mountains, 30% of the MacAlpine Hills and 45% of the Pecora Escarpment meteorites are paired. Typical pairing groups consist of two or three meteorites. In contrast, pairing at Queen Alexandra Range is about 70%, mostly because of two major showers QUE 90205 (39 members) and the possibly related QUE 90207 (55 members).

With the exception of Queen Alexandra Range, our fall-to-specimen ratio of 1.1 to 1.2 is lower than expected. Ikeda and Kimura suggested that fall-to-specimen ratios for Antarctic ordinary chondrites should be 1:2 to 1:6 (*i.e.* 50% to ~80% of the fragments are paired) on the basis of mass distributions [10], with some variation among petrologic type and chemical class, and Scott has made a similar suggestion [11]. In some part, this might reflect our bias against small samples. Consistent with this, there is more pairing in the 1990 and 1992 data for Elephant Moraine, which includes a greater proportion of small samples than in the 1987 study [3, 12].

Paired fragments have been removed in data comparisons in the remainder of our discussion.

Natural TL distributions. Meteorites from the present ice fields exhibit similar natural TL distributions to each other and to those observed in our earlier studies of Allan Hills, Elephant Moraine, and Lewis Cliff ordinary chondrites and modern falls (Fig. 1). The distributions show a broad peak between 5 and 100 krad, and a long tail extending to

lower values and short tail to higher values. At all ice fields, 15-20% of the meteorites have TL levels <5 krad, the one exception being Queen Alexandra Range and Pecora Escarpment where the proportion is ~30%. About 10% of the samples have natural TL >100 krad, slightly higher in the case of Allan Hills. Meteorites with natural TL of <5 krad we suggest had perihelia <0.85 AU for their last $\sim 10^5$ years in space [13], while samples with natural TL >100 krad probably underwent rapid orbital evolution from >1.2 AU perihelia to 1.0 AU [5]. The Allan Hills, Queen Alexandra and Pecora Escarpment natural TL distributions are unusual for the large numbers of meteorites with values between 5 and 20 krad, although pairing may be confusing the data for Queen Alexandra Range. Meteorites with natural TL in the 5 to 20 krad range probably had long surface exposures. Conversely, the large number of meteorites with natural TL >100 krad at Grosvenor Mountains suggests a high population of meteorites with short surface exposure times at this field. However notwithstanding these details, meteorites at the various ice fields generally experienced fairly similar terrestrial histories and sampled similar meteorite populations.

Geographical factors. We have previously reported variations in natural TL with location on the ice for the Allan Hills and Lewis Cliff Ice Fields that we suggested reflected different meteorite concentration mechanisms and ice sheet behavior [2, 4]. There were variations in the natural TL of meteorites at Elephant Moraine, but these were thought to be the result of a major shower and of no wider significance [3]. Of the present ice fields, we have made a preliminary examination of the meteorites from Pecora Escarpment but not the other fields, either because we have not reached this point in our study or because maps are not yet available. At Pecora Escarpment we found that meteorites paired on the basis of natural TL and TL sensitivity were either found in tight groups on the ice or linear arrays [14] but we have yet to explore the implications, if any, for ice movement studies in this region.

TL sensitivity distributions. Unlike ordinary chondrites of petrologic type 3-4, unshocked equilibrated ordinary chondrite falls display a factor of only ~ 10 in TL sensitivity and observed falls have TL sensitivities 10-100 times Dhajala [15]. Most of the equilibrated ordinary chondrites in the present study have TL sensitivities 0.1 to 1.0. However, since their TL sensitivity can be increased to levels similar to modern falls by gentle acid-washing, it is clear that these values have been decreased by weathering. Presumably weathering coated the feldspar grains with rust [16].

There are significant differences in the TL sensitivity distributions for each ice field (Fig. 2), with a tendency to increase along the series Lewis Cliff, Allan Hills, MacAlpine Hills, Elephant Moraine, Pecora Escarpment, Queen Alexandra Range, Elephant Moraine (with our previous and present data being in good agreement), and Grosvenor Mountain. Furthermore, the distribution becomes flatter as the mean TL sensitivity increases. If we accept on the basis of petrographic data that these differences in distribution do not represent differences in shock or metamorphic history, then we would have to conclude that there are systematic differences in weathering among these ice fields and that the most weathered meteorites are to be found at the Lewis Cliff and the least weathered at Grosvenor Mountains. It remains to be seen whether these differences are related to size, but it seems unlikely that they are related to terrestrial or surface exposure age because the natural TL distributions are so similar for the various sites.

Highly shocked equilibrated ordinary chondrites exhibit TL sensitivities typically <0.1 (relative to Dhajala), reflecting destruction of the feldspar phosphor by shock-heating [17]. These meteorites are rare and only eight are in the present collection, MAC 88162, MAC 87310, MAC 87302, QUE 93410, QUE 94202, EET 92501, GRO 95543, and GRO 95509.

Conclusions

We have reviewed natural and induced TL data for about 1200 ordinary chondrite samples collected by ANSMET, six major ice fields being reasonably well sampled. We find that pairing, while common in the collection, may not be as prevalent as previously thought (generally less than about 50%). Natural TL distributions for equilibrated ordinary chondrites are similar for the six major ice fields, suggesting that they have generally sampled similar meteorite populations and have experienced similar terrestrial histories. Variations in natural TL with location on the ice can sometimes shed new light on ice movements and meteorite concentration mechanisms, but the details vary with ice field and the data for most ice fields have yet to be examined in detail. Induced TL sensitivity varies with ice field, most probably reflecting differences in weathering. These differences are not simply related to terrestrial age or surface residence time, but it is unclear at the moment as to whether they are related to size or local conditions. The natural TL survey has identified a number of meteorites that arrived to Earth on small perihelia orbits, a few that appear to have only recently acquired Earth-crossing orbits, and even fewer that have been heavily shock-heated.

Table 1. Summary of natural TL properties of Antarctic ordinary chondrites by ice field (present work unless otherwise noted).

| Ice Field | No. | % paired | % with dose | | | Meteorites <5 krad | Meteorites >100 krad | Geog. cont? [†] |
|-----------------------|-----|----------|-------------|------|------|--|--|--------------------------|
| | | | <5 | 5-20 | >100 | | | |
| Allan Hills [2] | 167 | 23 | 22.7 | 9.0 | 18.6 | see [2] | see [2] | Yes |
| Elephant Moraine [3] | 107 | 32 | 28.4 | 1.3 | 12.3 | see [3] | see [3] | No |
| Elephant Moraine | 101 | 58 | 15.6 | 32.8 | 6.3 | 90054, 90488, 92034, 92041, 96035, 96058, 96061, 96134, 96140, 96351 | 90372, 92035, 92040, 96136 | Unk |
| Lewis Cliff [4] | 302 | 14 | 13.1 | 22.3 | 7.5 | see [4] | see [4] | Yes |
| Grosvenor Mountains | 44 | 18 | 9.1 | 25.0 | 9.1 | 95543, 95527, 95540, 95531 | 85203, 85213, 95518, 95520 | Unk |
| MacAlpine Hills | 70 | 30 | 20.4 | 12.2 | 12.2 | 87302, 87307, 87308, 87310, 87311, 87312, 87315, 88116, 88118, 88134 | 87305, 88115, 88119, 88122, 88128, 88129 | Unk |
| Pecora Escarpment | 60 | 45 | 27.3 | 21.2 | 6.1 | 91009, 91017, 91022, 91023, 91027, 91030, 91057, 91062, 91067 | 91001, 91134 | Unk |
| Queen Alexandra Range | 173 | 70 | 30.8 | 26.9 | 3.8 | 87400, 90204, 90205, 90266, 93027, 93028, 93034, 93072, 93080, 93410, 94242, 94244, 94247, 94477, 94623, 94716 | 93046, 93021 | Unk |

* Pairing corrected.

[†] Geographical control, *i.e.* natural TL varies systematically with location on the ice. Unk, unknown.

Acknowledgements. We are grateful to the membership of the Meteorite Working Group (particularly Lou Rancitelli, Gary Huss, William Cassidy and Ralph Harvey) and the staff of the JSC Meteorite Processing Laboratory for support and encouragement over the lifetime of the Natural Thermoluminescence Survey, to the many associates who have helped run the laboratory, to Charles Melcher, Steven Sutton and Robert Walker for originally suggesting its establishment, and the National Science Foundation and National Aeronautics and Space Administration for its funding.

References.

- [1] Hasan F.A., Haq M., and Sears D.W.G. (1987) *Proc. Lunar Planet. Sci.* 17th, *J. Geophys. Res., suppl.*, 92, E703-E709. [2] Benoit P.H., Sears H. and Sears D.W.G. (1993) *J. Geophys. Res.* 98, 1875-1888. [3] Benoit P.H., Roth J., Sears H., and Sears D.W.G. (1994) *J. Geophys. Res.* 99, 2073-2085. [4] Benoit P.H., Sears H., and Sears D.W.G. (1992) *J. Geophys. Res.* 97, 4629-4647. [5] Benoit P.H. and Sears D.W.G. (1993) *Earth Planet. Sci. Lett.* 120, 463-471. [6] Vaz J.E. (1971) *Nature Phys. Sci.* 230, 23-24. [7] Lalou C., Nordemann D., and Labyrie J. (1970) *C.r. Hebd. Seanc. Acad. Sci. (Paris) Serie D* 270, 2401-2404. [8] Benoit P.H. and Chen Y. (1996) *Rad. Meas.* 26, 281-289. [9] Ninagawa K., Hashikawa Y., Kojima H., Matsunami S., Benoit P. H. and Sears D. W. G. (1998) *Antarct. Meteorit. Res.* 11, 1-17. [10] Ikeda Y. and Kimura M. (1992) *Meteoritics* 27, 435-441. [11] Scott E.R.D. (1984) *Proc. Symp. Antarctic Meteor.* 9th, 102-125. [12] Benoit P.H. and Sears D.W.G. (1999) *Lunar Planet. Sci.* 30, Abstract #1052. [13] Benoit P. H. and Sears D. W. G. (1997) *Icarus*, 125, 281-287. [14] Benoit P.H. and Sears D.W.G. (1998) *Lunar Planet. Sci.* 29, Abstract #1454. [15] Sears, D.W., Grossman, J.N., Melcher, C.L., Ross, L.M. and Mills, A.A. (1980) *Nature*, 287, 791-795. [16] Benoit P.H., Jull A.J.T., McKeever S.W.S., and Sears D.W.G. (1993) *Meteoritics* 28, 196-203. [17] Haq M., Hasan F.A., and Sears D.W.G. (1988) *Geochim. Cosmochim. Acta* 52, 1679-1689.

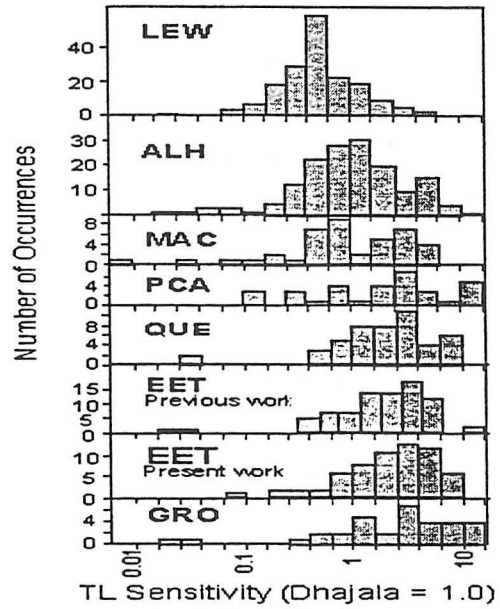
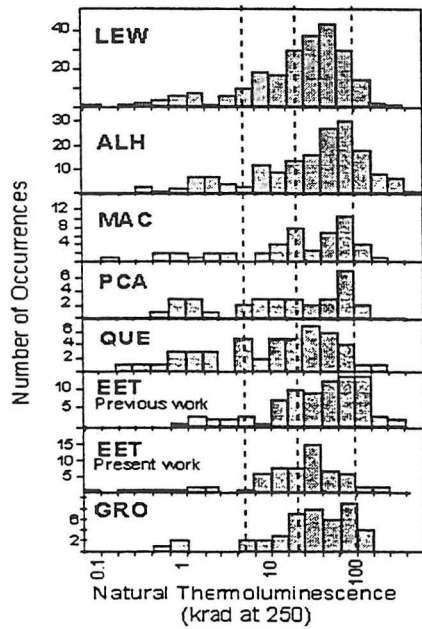


FIG. 1 (LEFT). Distribution of natural TL levels for equilibrated ordinary chondrites in the current study, subdivided by collection site. Potentially paired samples have been removed. Data distributions are fairly similar among the ice fields.

FIG. 2 (RIGHT). Distribution of TL sensitivity for equilibrated ordinary chondrites in the current study, subdivided by collection site. Potentially paired samples have been removed. TL sensitivity for meteorite finds partially reflects degree of weathering, low sensitivity reflecting high degrees of weathering [12]. Very low TL sensitivities (<0.1 relative to Dhajala) probably reflect high degrees of shock processing.

METEORITES FROM THE NULLARBOR, AUSTRALIA: AN UPDATE. A. W. R. Bevan¹, P. A. Bland², and A. J. T. Jull³. ¹Department of Earth and Planetary Sciences, Western Australian Museum of Natural Science, Perth, Western Australia 6000. ²Department of Mineralogy, The Natural History Museum, London SW7 5BD, UK. ³NSF AMS Facility, University of Arizona, Tucson, Arizona 85721, USA

The gibber plains of the Nullarbor in Australia are important meteorite accumulation sites [1,2,3]. Situated on the border between Western Australia and South Australia, the Nullarbor consists of flat-lying limestones of Early Miocene age exposed over a total area of *ca.* 240,000 km² and covered with a thin calcareous loam. Prolonged aridity has allowed the accumulation of meteorites in the region, and a physiographically stable surface over the last 30 ka combined with low weathering rates are model circumstances for the estimation of the meteorite flux with time. Moreover, quantification of weathering effects in ordinary chondrites from the Nullarbor is providing a new palaeoclimatic tool [4].

Similar to Antarctica, the masses of most stony meteorites from the Nullarbor are 100 g or less, with a peak in the mass distribution between 10-50 g. Statistical analysis of meteorite types from the Nullarbor shows that stony meteorites are most abundant with chondrites accounting for 92.7% of the total. Only 1.5% of distinct meteorites so far described from the Nullarbor are irons, which is much less than that (*ca.* 5%) predicted from the modern flux of meteorites. The small number of distinct irons from the Nullarbor is difficult to explain and human interference cannot be ruled out. Nevertheless, out of the four irons known, three, Mundrabilla, Haig, and Watson make up more than 99% of the total mass of meteorites collected from the Nullarbor.

¹⁴C terrestrial ages for chondritic meteorites from the Nullarbor indicate an age range from present day to *ca.* 35 ka [5]. Evidence suggests that meteorites are lying on, or near to, the surfaces on which they fell and that physiographically, the region has remained essentially undisturbed for at least the last 30 ka. For this reason, the Nullarbor has provided important data on the flux of meteorites over the accumulation period [3,6]. One significant factor affecting flux calculations using meteorite accumulations is the determination of the number of distinct falls represented in the population. The lack of transportation processes in the Nullarbor allows confident 'pairing' of meteorites. Consequently, most paired meteorites are detected. Statistics confirm that there are few undetected pairs in the population of meteorites so far described from the Western Australian Nullarbor [3].

The constitution of the population of meteorites by type from the Nullarbor is very similar to the Antarctic population but slightly different from the Saharan population. Mass frequencies of stony meteorite types are also very similar in most accumulation sites. However, compared with modern falls, the Nullarbor population includes a high proportion of rare and anomalous chondritic meteorites. This may be related to the period of accumulation of Nullarbor meteorites, to their ease of recognition in that setting compared with the rest of the world, or may result from meteoroid streams [7].

References: [1] A. W. R. Bevan (1992), Records of the Australian Museum Suppl. **15**, 1-27; [2] A. W. R. Bevan (1996), Journal of the Royal Society of Western Australia **79**, 33-42; [3] A. W. R. Bevan et al. (1998), in "Meteorites: Flux with Time and Impact Effects" (eds M. M. Grady et al.) Geol. Soc. London Spec. Pub. **140**, 59-73. [4] P. A. Bland et al. (1998), Geochim. Cosmochim.

Acta **62**, 3169-3184. [5] A. J. T. Jull *et al.* (1995), ^{14}C terrestrial ages and weathering of meteorites from the Nullarbor Region, Western Australia. Lunar & Planetary Institute Technical Report **95-02**: 37-38; [6] P. A. Bland *et al.* (1996), Monthly Notices of the Royal Astronomical Society **283**, 551-565; [7] G. W. Kallemeyn *et al.* (1991), Geochim. Cosmochim. Acta **55**, 881-892.

ICE FLOW AS THE PRINCIPAL SINK FOR ANTARCTIC METEORITES. P. A. Bland¹, A. J. T. Jull², A. W. R. Bevan³, T. B. Smith⁴, F. J. Berry⁵, and C. T. Pillinger⁶, ¹Department of Mineralogy, Natural History Museum, Cromwell Road, London, SW7 5BD, U.K., ²NSF Accelerator Facility for Radioisotope Analyses, University of Arizona, Tucson, Arizona 85721, U.S.A., ³Western Australian Museum, Francis Street, Perth, Western Australia 6000, ⁴Dept. of Physics, ⁵Dept. of Chemistry, ⁶Planetary Science Research Institute, The Open University, Walton Hall, Milton Keynes MK7 6AA, U.K.

INTRODUCTION

It has previously been shown that Mössbauer spectroscopy is capable of providing a quantitative measure of weathering in ordinary chondrite (OC) meteorites [1,2]. Used in conjunction with ¹⁴C terrestrial ages, we have used this method to constrain weathering rates for individual hot desert meteorite populations [3]. Typically, oxidation over time may be effectively modelled using an appropriate power-law, suggesting an initial rapid weathering phase, followed by more gradual oxidation [4]. By quantifying oxidation over time, and modelling the effect of oxidation in destroying samples (from oxidation-frequency distributions) we can derive a decay-rate for meteorites in an accumulation, or a weathering half-life of a meteorite in a population. This, combined with a knowledge of the number of individual meteorites on the ground today, enables an estimate of the flux of meteorites over the lifetime of the site [3]. Hot desert OC's typically show a peak in their oxidation-frequency distribution at 40% (ie. 40% of the iron in a meteorite is ferric): until this point oxidation is accommodated by available porosity; after this point porosity is exceeded and the sample erodes [3,5]. If this interpretation is correct, the oxidation-frequency distribution describes the response of OC's to a given amount of chemical weathering, and should be similar between different sites.

Ordinary chondrites at the Allan Hills, despite their far longer residence times, are found to have a peak in their oxidation-frequency distribution at 10-15%, 25-30% lower than hot desert OC's [6] (see Figure 1). In addition (and contrary to earlier studies [1]), although the data show more scatter than is typical of hot desert populations, we have shown that there is a correlation between weathering and terrestrial age for the Allan Hills meteorites, allowing an (approximate) estimate of the rate of weathering over time [6]. The plot of oxidation over time, although indicating much slower weathering rates than for hot desert meteorites, is qualitatively similar in its form: it can be modelled using an appropriate power-law, and shows an initial rapid weathering phase (Figure 2).

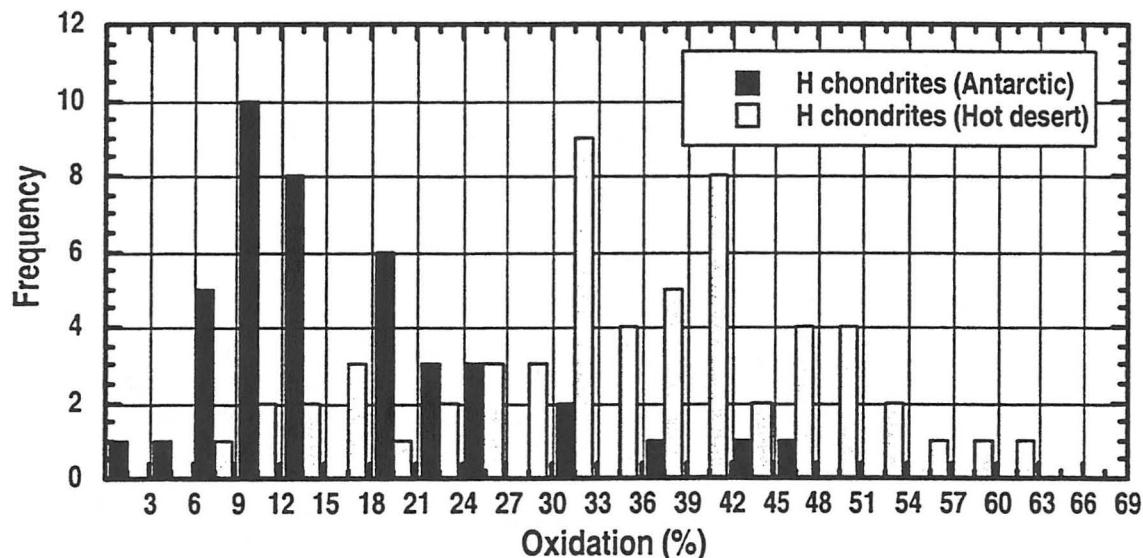


Figure 1. Percentage oxidation (ferric iron as a percentage of total iron, determined by Mössbauer spectroscopy) as a frequency distribution comparing H and chondrites recovered from hot desert regions and the Allan Hills (data derived from [6]).

WEATHERING AND ICE FLOW AT ALLAN HILLS: P.A. Bland, T.B. Smith, F.J. Berry and C.T. Pillinger

RESULTS

Our initial work on the Antarctic population compared Mössbauer spectroscopy analyses of meteorites to terrestrial ages, typically measured using the ^{36}Cl method. We suggested that the scatter in the data may be a result of the large error associated with the ^{36}Cl method, rather than differences in exposure time on the ice as has previously been supposed [e.g. 1]. ^{14}C offers more precise terrestrial ages, but is only effective in dating samples with ages <40 ka. However, given the comparatively rapid initial weathering phase that we observe, it is possible that we might observe a correlation between weathering and terrestrial age, even over the narrow window accessible by ^{14}C dating. We therefore chose to analyse by Mössbauer spectroscopy a suite of Allan Hills OC's with terrestrial ages measured using the ^{14}C method.

Although there is some scatter, we observe a correlation between weathering and ^{14}C terrestrial ages in both H and L(LL) chondrites from the Allan Hills (Figure 3). This data represents a snapshot of the initial weathering phase in these meteorites - from our earlier study, after the first ~ 50 ka or so, the increase in oxidation with time is extremely slow.

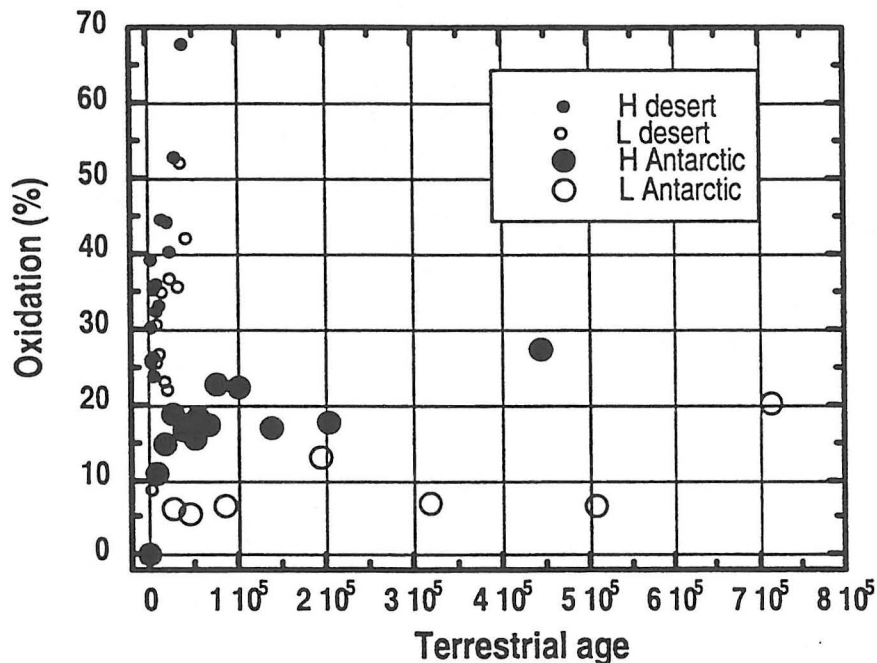


Figure 2. Oxidation vs. terrestrial ages in H and L(LL) chondrites recovered from both hot desert regions, and from the Allan Hills. Data are binned by terrestrial age so that 5-6 data points fall in each bin.

These analyses confirm our previous work, and enable us to more accurately constrain Antarctic weathering rates. Taken together with the ^{36}Cl /Mössbauer data, these results indicate that weathering rates in Antarctica are extremely slow, approximately 3 orders of magnitude lower than values typical for hot desert meteorites.

DISCUSSION

Mössbauer spectroscopy measurements of meteorites can be thought of as quantifying, at least in part, the chemical alteration that a sample experiences: the conversion of Fe-Ni metal and ferrous iron in a fresh fall to ferric iron-containing alteration products. Our studies of hot desert meteorites suggest that it is the chemical alteration of a sample, and eventual volume expansion, brecciation, and subsequent fragmentation, that is the principal 'sink' for meteorites in a hot desert accumulation. What then is the situation in Antarctica?

Allan Hills meteorites show a peak in oxidation-frequency distribution 20-25% lower than hot desert meteorites. Taking this data at face value, this would suggest that an Antarctic meteorite is likely to be destroyed by a much lower amount of weathering than a hot desert sample. Possibilities to account for this might be physical weathering

WEATHERING AND ICE FLOW AT ALLAN HILLS: P.A. Bland, T.B. Smith, F.J. Berry and C.T. Pillinger

processes such as freeze-thaw action or wind abrasion, but only if physical and chemical weathering were strongly correlated. In addition, neither process appears entirely satisfactory as a sink for meteorites. Experimental evidence [7] indicates that in most cases after 300 freeze-thaw cycles fragmentation virtually stops: meteorites exposed on the surface of Antarctic blue ice fields may experience several cycles of freeze-thaw each season [8], so we might expect an average chondrite to be saturated after <100 years, a tiny fraction of most measured terrestrial ages. Also, many Antarctic meteorites, including old terrestrial age meteorites, commonly retain some fusion crust, suggesting that wind abrasion is not a significant factor. Therefore, we suggest that the shift to lower weathering values that we see in the oxidation-frequency distribution for Allan Hills OC's arises from some other process ie. the distribution does not reflect a 'mature' steady-state population with weathering as the sink. We have observed a similar feature in the Saharan population, where the oxidation-frequency distribution is shifted to lower values, probably because the accumulation surface appears to be quite young: the population has not had time to acquire a 'mature' weathering signature. We suggest that a similar reason applies in Antarctica: given that blue ice regions are not static zones of accumulation [9] but subject to some horizontal flow, we propose a model in which the observed oxidation-frequency distribution is largely a result of ice movement, rather than weathering.

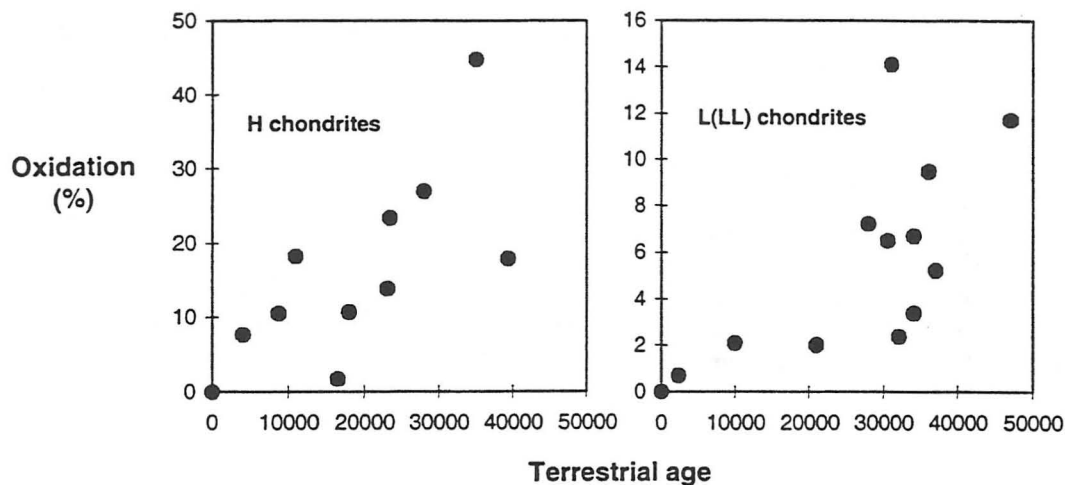


Figure 3. Oxidation vs. ^{14}C terrestrial ages in H and L(LL) chondrites from the Allan Hills.

There is an independent line of evidence that supports our interpretation. At the Allan Hills Main Icefield, there is a gradient of increasing terrestrial to the far NE edge of the Icefield [10]. Similarly, Jull et al. [11] observes a gradient of increasing numbers of young meteorites with distance from the Allan Hills: with the Far Western Icefield > Middle Western > Main Icefield. These data are consistent with an ice stream slowing down as it approaches the Allan Hills barrier, and carrying older meteorites out of the zone of accumulation ie. it is ice flow, and not weathering, which governs the terrestrial age distribution in Antarctic meteorite accumulations.

If this model is realistic then a comparison of the oxidation-frequency distribution in an area with the overall oxidation-terrestrial age plot for Antarctic OC's should allow a lifetime for an accumulation to be estimated, as well as an averaged horizontal ice flow rate. For the whole Allan Hills population, we calculate an average horizontal flow rate (integrated over the lifetime of the population) of approximately 1m yr^{-1} (this would be less in the Main Icefield, and more further away). We note that this is of a similar order to other estimates [9]. Aside from any palaeoclimatic value that this data has, knowing the averaged flow rate should allow us to constrain a catchment area for these samples, and knowing the catchment area, we can refine estimates of meteorite flux. If an improved dataset confirms our model, this work may allow a comparison between Antarctic meteorites and other populations, and an estimate of the flux of meteorites over ca. 10^5 - 10^6 years. The recognition that weathering is not the significant process in removing meteorites from Antarctic accumulations has the additional implication that there may be extremely old terrestrial age meteorites in areas where ice flow is not a factor: we recommend a detailed search of the Dry Valleys. Although identifying meteorites will clearly be more difficult in this region, the recovery of a population of samples with terrestrial ages of several million years (as seems possible from our data), would be of great interest to the research community.

WEATHERING AND ICE FLOW AT ALLAN HILLS: P.A. Bland, T.B. Smith, F.J. Berry and C.T. Pillinger

REFERENCES

- [1] BURNS R. G. et al. (1995) Weathering in Antarctic H and CR chondrites: Quantitative analysis through Mössbauer spectroscopy. *Meteoritics* **30**, 625-633.
- [2] BLAND P. A. et al. (1996) Flux of meteorites to the Earth and weathering in hot desert ordinary chondrite finds. *Geochim. Cosmochim. Acta* **60**, 2053-2059.
- [3] BLAND P. A. et al. (1996) The flux of meteorites to the Earth over the last 50,000 years. *Monthly Notices R. Astron. Soc.* **283**, 551-565.
- [4] BLAND P. A. et al. (1998) Rapid weathering in Holbrook: An ^{57}Fe Mössbauer spectroscopy study. *Meteoritics and Planetary Science* **33**, 127-129.
- [5] BLAND P. A. et al. (1998) Climate and rock weathering: a study of terrestrial age dated ordinary chondritic meteorites from hot desert regions. *Geochim. Cosmochim. Acta* **62**, 3169-3184.
- [6] BLAND P. A. et al. (1998) Calculating flux from meteorite decay rates: A discussion of problems encountered in deciphering a 10^5 to 10^6 year integrated meteorite flux at Allan Hills and a new approach to pairing. In: Grady M. M., Hutchison R., McCall G. J. H. and Rothery D. A. (eds) *Meteorites: Flux with Time and Impact Effects*. *Geol. Soc. London, Spec. Pub.* **140**, 43-58.
- [7] LAUTRIDOU J. P. and OZOUF J. C. (1982) Experimental frost shattering: 15 years of research at the Centre de Geomorphologie du C.N.R.S. *Prog. Phys. Geog.* **6**, 215-232.
- [8] SCHULTZ L. (1986) Allende in Antarctica: Temperatures in Antarctic meteorites. *Meteoritics* **21**, (Abstract), 505.
- [9] ANNEXSTAD J. O. (1985) Meteorite concentration mechanisms in Antarctica. *LPI Technical Report* **86-01**, 23-25.
- [10] NISHIZUMI K. et al. (1989) Update on terrestrial ages of Antarctic meteorites. *Earth and Planetary Science Letters*, **93**, 299-313.
- [11] JULL A. J. T., CLOUDT S. and CIELASZYK E. (1998) ^{14}C terrestrial ages of meteorites from Victoria Land, Antarctica, and the infall rates of meteorites. In: Grady M. M., Hutchison R., McCall G. J. H. and Rothery D. A. (eds) *Meteorites: Flux with Time and Impact Effects*. *Geol. Soc. London, Spec. Pub.* **140**, 75-91.

PAIRING AMONG THE EET87503 GROUP OF HOWARDITES AND POLYMICT EUCRITES. P. C. Buchanan¹, D. J. Lindstrom¹, and D. W. Mittlefehldt²

¹Mail Code: SN2, NASA Johnson Space Center, Houston, Texas 77058 USA; e-mail: pbuchana@ems.jsc.nasa.gov.

²C23, Lockheed Martin SO, 2400 Nasa Rd. 1, Houston, Texas 77058 USA.

INTRODUCTION

The ten HED polymict breccias EET82600, EET87503, EET87509, EET87510, EET87512, EET87513, EET87518, EET87528, EET87531, and EET92022 were found over a broad area in the Elephant Moraine collecting region of Antarctica. Locations are scattered among the Main (Elephant Moraine), Meteorite City, and Texas Bowl icefields and the Northern Ice Patch (Fig. 1). It was previously suggested that these polymict breccias are paired [e.g., 1]. However, degree of terrestrial alteration among these meteorites varies from relatively pristine (type A) to extensively altered (type B/C) and there are textural, mineralogical, and compositional differences. This study is a re-evaluation of the pairing of these meteorites.

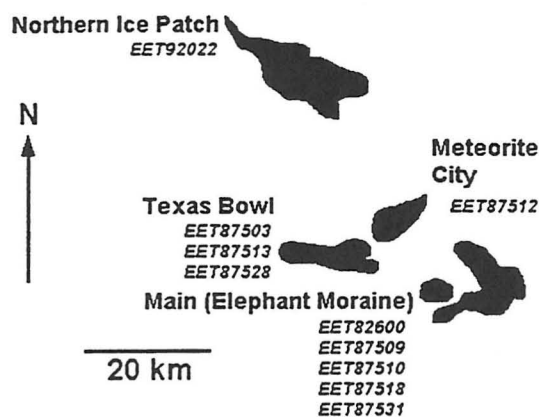


Fig. 1. Generalized map of the Main (Elephant Moraine), Meteorite City, and Texas Bowl icefields and the Northern Ice Patch.

PREVIOUS WORK

Based on initial descriptions of the meteorites, EET87503, EET87509, EET87510, EET87512, EET87513, EET87518, and EET87531 were originally thought to be paired [1]. Based on geochemical data, Mittlefehldt and Lindstrom [2] suggested that EET82600 is a member of this group and that EET87513 is unrelated. This is consistent with TL sensitivity data [3]. In contrast, Sears et al. [4] proposed that EET87509 and EET87513 are paired, but that EET87531 and EET87518 are part of a separate group. Grossman and Score [5] suggested that EET92022 is also a member of the EET87503 group.

DATA

Below are short descriptions of these meteorites organized by icefield. Relevant data are summarized in Table 1.

Table 1.

| Meteorite type* | mass (g) [#] | alteration [#] |
|---|-----------------------|-------------------------|
| TEXAS BOWL ICEFIELD | | |
| EET87503 howardite | 1734.5 | A |
| EET87513 howardite | 394.5 | A/B |
| EET87528 | 40.5 | A |
| METEORITE CITY ICEFIELD | | |
| EET87512 howardite | 181.6 | B/C |
| NORTHERN ICE PATCH | | |
| EET92022 howardite | 9.7 | A |
| MAIN (ELEPHANT MORAINÉ) ICEFIELD | | |
| EET82600 polymict eucrite | 247.1 | Ae |
| EET87509 polymict eucrite | 583.9 | B |
| EET87510 | 250.3 | B |
| EET87518 | 349.6 | B |
| EET87531 polymict eucrite | 527.2 | B |

* based on data presented in this study

[#] from [1]

Texas Bowl Icefield

EET87503 is a howardite (Fig. 2) and displays minimal amounts of terrestrial alteration (type A) [1]. The outside of the meteorite has a glassy, unaltered fusion crust and the interior is relatively fresh with minor iron oxide staining. Geochemical data suggest minor alteration in the outer portions of this large stone [2]. Included within this polymict breccia are a wide variety of clasts, including those with variolitic and porphyritic textures, fragments of earlier breccias apparently formed by impact, and fragments of brown glass.

EET87513 is relatively unaltered (type A/B) [1] with glassy fusion crust. Iron oxide staining is present, particularly close to the outer surface of the meteorite. Degree of terrestrial alteration is slightly greater than EET87503. Petrographic analysis indicates that this meteorite is composed of a mixture of diagenetic and eucritic components. Matrix feldspars range in composition from An₇₇ to An₉₄. Matrix pyroxenes range from magnesian orthopyroxenes to iron-rich pyroxenes similar to those found in main group or Nuevo Laredo-trend eucrites. A histogram of Mg# of matrix pyroxenes is plotted in Fig. 2 [6]. This spectrum of compositions indicates that the meteorite contains greater than 20%

diagenetic material. Mittlefehldt and Lindstrom [2] suggest it contains ~35% diagenetic material. Hence, the meteorite is properly classified as a howardite.

EET87513 contains a wide variety of lithic clasts, including a relatively large fragment of CM chondrite [7]. Other lithic clasts in this meteorite include fragments of recrystallized diogenites, cumulate eucrites, and equilibrated eucrites that are similar in composition to Juvinas [6].

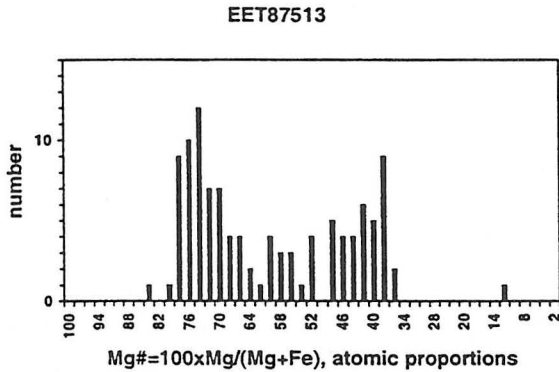
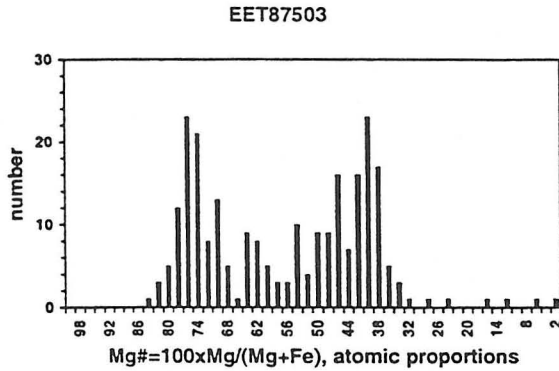


Fig. 2. Histogram of Mg# of matrix pyroxenes for EET87503 and EET87513.

Meteorite City Icefield

EET87512 is a howardite with a large diagenetic component (Fig. 3). Iron oxide staining is pervasive throughout the meteorite and it is extensively altered (type B/C) [1]. The glassy fusion crust is still present, although partially altered. Fragments of brown glass in the matrix of the meteorite also are altered. Mineral fragments throughout the meteorite display evidence of shock, including undulatory extinction. Veins running through the meteorite and containing fine-grained, iron oxide-stained material may represent fractures that originally contained glass and were altered in the terrestrial environment.

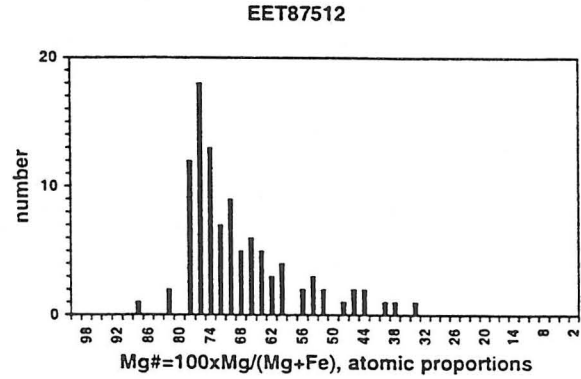


Fig. 3. Histogram of Mg# of matrix pyroxenes for EET87512.

Northern Ice Patch

EET92022 is a howardite with a large diagenetic component (Fig. 4) [1]. Alteration is minimal (type A) and it has a glassy fusion crust. There is a small amount of iron oxide staining around opaque grains in the matrix and in the mesostasis of eucrite clasts. Clasts include porphyritic materials with phenocrysts composed of skeletal, zoned pyroxene grains within a groundmass composed of long, thin laths of pyroxene and plagioclase radiating from these phenocrysts.

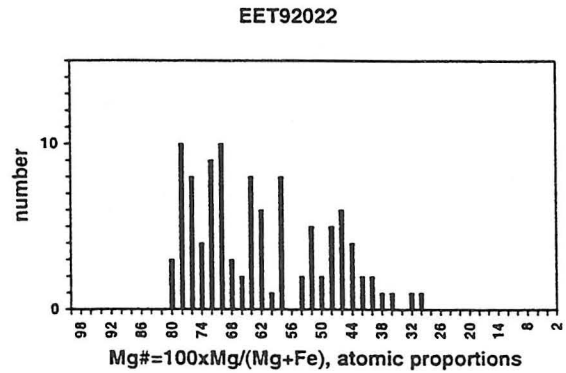


Fig. 4. Histogram of Mg# of matrix pyroxenes for EET92022.

Elephant Moraine Icefield

EET82600 has evaporite deposits on the surface (type Ae) [1]. Mittlefehldt and Lindstrom [2] suggested that trivalent REE were redistributed from the outside to the inside of the meteorite. Petrographic examination indicates that the interior is relatively unaltered with minimal iron oxide staining. The meteorite is a polymict eucrite (Fig. 5).

EET87509 is moderately altered (type B) and displays a weathering rind that is ~1 cm in thickness [1]. Fusion crust of this meteorite has been pervasively altered and is dull grey in colour. Evaporite deposits cover several surface areas, including fractures, and there is iron oxide staining throughout the meteorite. Electron microprobe analyses of matrix minerals indicate that it contains <10% magnesian orthopyroxene (Fig. 5) and should be classified as a polymict eucrite.

Petrographic examination of thin sections indicates that this breccia is finer-grained than EET87503. The meteorite contains a variety of lithic clasts with a large proportion representing quenched or quickly cooled volcanic rocks. A fragment of porphyritic material is composed of large zoned, skeletal pyroxene grains contained in a very fine-grained groundmass composed of pyroxene and plagioclase needles that radiate outward from the phenocrysts [6]. Also contained within the brecciated matrix of EET87509 are brown glass fragments that range in size from 80 μ m to 300 μ m. Some of these fragments contain microphenocrysts (30-100 μ m) of plagioclase (An91-93) and of skeletal pyroxene (zoned from Wo8En53 to Wo9En43) [6].

EET87510 is moderately altered (type B) [1]. Iron oxide staining is present around opaque grains in the interior of the meteorite. However, the fusion crust appears relatively unaltered.

EET87518 is pervasively altered (type B) [1]. The fusion crust is still recognizable, though significantly altered. Surface areas without fusion crust are slate grey in colour and are extensively altered. There are moderate amounts of iron oxide staining throughout the interior of the meteorite. Petrographic examination indicates numerous fragments of brown glass and vitrophyres that are composed of phenocrysts in a groundmass of brown glass. Some of this brown glass displays evidence of alteration. Also present in this meteorite are fragments of lithified earlier breccias.

EET87531 displays iron oxide staining throughout and is pervasively altered (type B) [1] with a slate grey colour. Fusion crust is still discernable, but is extensively altered. The matrix of the meteorite contains brown glass fragments. Large proportions of the lithic clasts contained in this meteorite are quickly cooled materials, including vitrophyres and porphyritic eucrites. Clasts representing lithified earlier breccias are also present. The matrix of the meteorite is finer-grained than that of EET87503.

Analysis by electron microprobe of matrix minerals indicates that this meteorite contains pyroxenes that range to magnesian compositions.

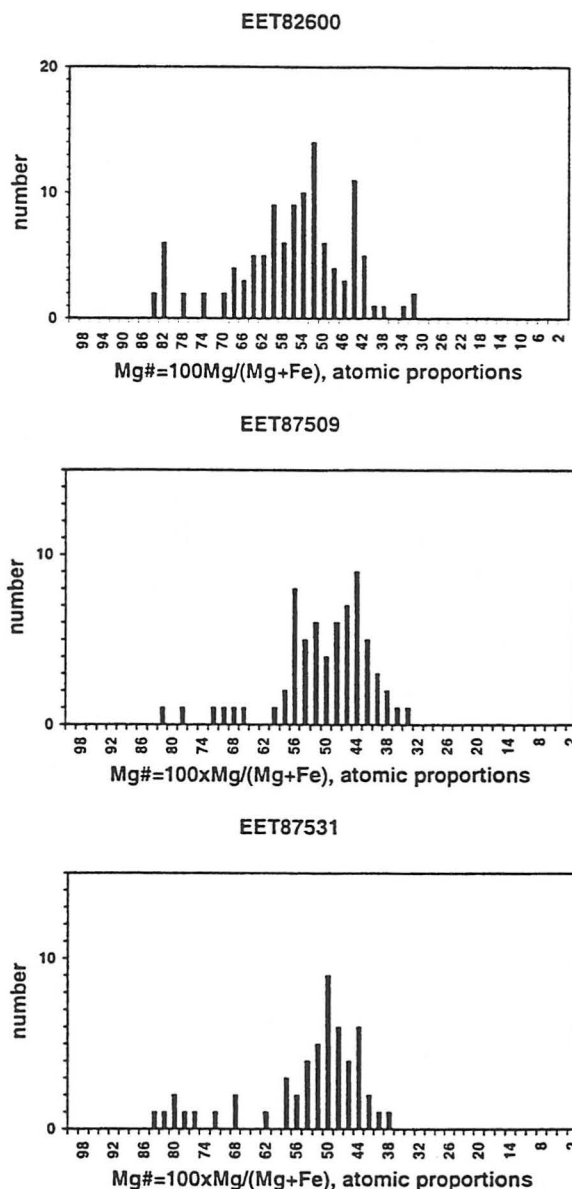


Fig. 5. Histogram of Mg# of matrix pyroxenes for EET82600, EET87509, and EET87531.

However, magnesian orthopyroxenes with diagenetic compositions are less than 10% in volume (Fig. 5) [6]. This spectrum of compositions is similar to that of EET87509 and is different from that of EET87513. EET87531 is a polymict eucrite.

DISCUSSION

Meteorites of the EET87503 group display several correlated features (Table 1). Degree of terrestrial alteration is correlated with location. Those meteorites found on the Texas Bowl Icefield and the Northern Ice Patch are relatively unaltered. EET87512, found on the Meteorite City Icefield, is

extremely altered. Those meteorites found on the Main (Elephant Moraine) Icefield vary from relatively unaltered to moderately altered. Where geochemical and mineralogical information are available, there is also a correlation between the location and petrologic type. EET87503 and EET87513, which were found on the Texas Bowl Icefield, are howardites and contain significantly larger proportions of diogenitic components than EET82600, EET87509, and EET87531. These latter meteorites should be classified as polymict eucrites because they contain less than 10% diogenite. EET87512 from the Meteorite City Icefield and EET92022 from the Northern Ice Patch contain the largest proportions of diogenitic material and are distinctly different from meteorites from the Texas Bowl Icefield.

Available bulk composition data confirm these proportions of diogenitic materials. Fig. 3 is a plot of Cr (mg/g) vs. Ca (mg/g) for INAA analyses of whole rock and matrix samples of some of these meteorites. Analyses for EET87503 and EET87513 overlap and have higher Cr abundances than analyses for EET87509, EET87531, and EET82600.

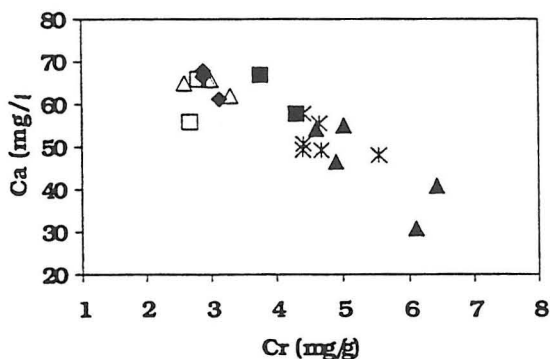


Fig. 6. Cr (mg/g) vs. Ca (mg/g) for whole rock and matrix samples of EET82600 (open squares), EET87503 (filled squares), EET87509 (filled diamonds), EET87513 (stars), EET87531 (open triangles), and other polymict HED breccias (filled triangles).

The group of polymict eucrites (EET82600, EET87509, EET87510, EET87518, and EET87531) from the Main (Elephant Moraine) Icefield may be part of a larger group of paired meteorites, including several collected in earlier years. Freundel et al. [8] reported an ^{38}Ar exposure age of $26.3 \pm 1.9 \times 10^6$ a and a terrestrial ^{81}Kr -Kr age of $173 \pm 29 \times 10^3$ a for EET82600. These ages are similar to those of the polymict eucrite EETA79005 and the howardite EETA79006, which were also found on the Main Icefield. Delaney et al. [9] and Freundel et al. [8] concluded that these meteorites probably are paired.

CONCLUSIONS

EET87503, EET87513, and EET87528 are probably paired and are similar in collection location, degree of terrestrial alteration (type A), and geochemical composition. These meteorites are distinctly different from those found on the Main (Elephant Moraine) Icefield because they are howardites. These data also suggest that the meteorites found on the Main Icefield (EET82600, EET87509, EET87510, EET87518, and EET87531) may form a paired group of polymict eucrites. Geochemical compositions, degrees of terrestrial alteration, and petrologic classifications are similar for these meteorites. EET87512 (Meteorite City Icefield) and EET92022 (Northern Ice Patch) are probably not related to either of these groups. Differences in collection location and degrees of terrestrial alteration suggest that these two meteorites probably are not paired.

References: [1] Score R. and Lindstrom M. M. (1990) *Ant. Met. Newsletter* 13,1. [2] Mittlefehldt D. W. and Lindstrom M. M. (1991) *LPSC XXII*, 901-902. [3] Batchelor J. (1992) Ph.D. dissertation, University of Arkansas, 194 p. [4] Sears D. W. G. et al. (1991) *Geochim. Cosmochim. Acta* 55, 3167-3180. [5] Grossman J. N. and Score R. (1996) *Meteor. Planet. Sci.* 31, A161-A174. [6] Buchanan P. C. (1995) Ph.D. dissertation, University of Houston, 313 p. [7] Buchanan P. C. et al. (1993) *Meteoritics* 28, 659-669. [8] Freundel M. et al. (1986) *Geochim. Cosmochim. Acta* 50, 2663-2673. [9] Delaney J. S. et al. (1984) *Proc. Lunar Planet. Sci. Conf.* 15, JGR 89 supplement, C251-C288.

CHEMICAL ALTERATION OF HOT DESERT METEORITES: THE CASE OF SHERGOTTITE DAR AL GANI 476. Ghislaine Crozaz¹ and Meenakshi Wadhwa².
¹Dept. of Earth and Planetary Sciences and McDonnell Center for the Space Sciences, Washington University, St. Louis, MO 6313, USA; ²Dept. of Geology, The Field Museum, Roosevelt Rd. at Lake Shore Dr., Chicago, IL 60605, USA.

During the last three decades, many cosmochemical studies have been stimulated by the recovery of large numbers of meteorites from Antarctica. Similarly, the more recent discoveries of meteorites in hot deserts significantly increase the number of known meteorites. It is likely that new meteorite types will be found in these hot deserts and that the number of rare meteorites that can be studied in the laboratory using an array of state of the art techniques will be expanded. However, meteorites found in both cold and hot deserts have much longer terrestrial ages than others and, thus, it is critical to ascertain whether their properties reflect processes that occurred prior to their fall on earth or whether some of their characteristics have been modified by their extensive residence on our planet. Here, we study the microdistribution of lanthanides (REE) and use them as indicators of terrestrial alteration. These elements are important because they are commonly used to decipher the petrogenesis and chronology of meteorites.

In Antarctic meteorites, there is clear evidence that weathering can result in REE loss as well as redistribution of the remaining REE. The effect is most pronounced in eucrites [1], but not limited to this type of meteorite, and is most easily diagnosed by the presence of a Ce anomaly, most often in pyroxene (e.g., [2], [3]), and occasionally in whole rock analyses. Terrestrial alteration of Antarctic meteorites partially dissolves Ca-phosphate, the major REE carrier in many meteorites. Some of the REE released by this process are lost from the meteorite and the rest gets deposited in adjacent phases. Pyroxene is frequently affected, particularly when shocked, and Ce anomalies in this mineral, due to the partitioning of the more insoluble Ce⁴⁺

from the other (trivalent) REE, are clear indicators of this process. But, apart from these anomalies, the REE patterns of Antarctic meteorites remain largely unchanged. As we will now show, the effects of weathering in meteorites from hot deserts are likely to be much more severe.

During the course of an ion microprobe study of Dar al Gani 476 (DaG 476), a 2 kg basaltic shergottite found last year in the Lybian Sahara [4], we uncovered clear evidence of terrestrial contamination. DaG 476 is the 13th meteorite believed to come from Mars and the first one recognized as such among Saharan meteorites. We received, from the Max-Planck Institut für Chemie, Mainz, thin section #3 for an ion microprobe study and measured the concentrations of the REE and a number of other trace elements in different mineral phases [5].

The REE budget of basaltic shergottites is always dominated by Ca-phosphate (merrillite) [6], and the same can be said for DaG 476. As in other shergottites, the LREE are depleted in this mineral and a significant negative Eu anomaly is present. REE patterns for 4 different grains are identical within errors but, surprisingly, the REE pattern for an additional merrillite grain located close to a fracture differs in having a relatively elevated La concentration. A significant variation in REE pattern is not expected as, presumably, all merrillite grains formed essentially simultaneously at the end of the crystallization sequence of the DaG 476 parent melt. In addition, some analyses of minerals like olivine and pyroxene, which have much lower REE concentrations than merrillite, show pronounced LREE enrichments that are not compatible with their formation from a typical basaltic shergottite melt. These

enrichments clearly point to contamination of these minerals by a LREE-rich component of terrestrial origin.

In order to confirm this suggestion, we analyzed material filling fractures in this heavily weathered meteorite. Smooth, homogeneous, pure carbonate areas have very low REE concentrations. However, we found "grungy" Ca-rich areas that are strikingly LREE-rich and contain a host of elements, including P, F, Rb, and Sr. In Fig. 1, we show the REE pattern of such an area, with the highest REE concentrations observed. Note that the REE abundances are plausible estimates as we cannot accurately measure the Ca (normalizing element) content in the volume sampled by the ion microprobe analysis.

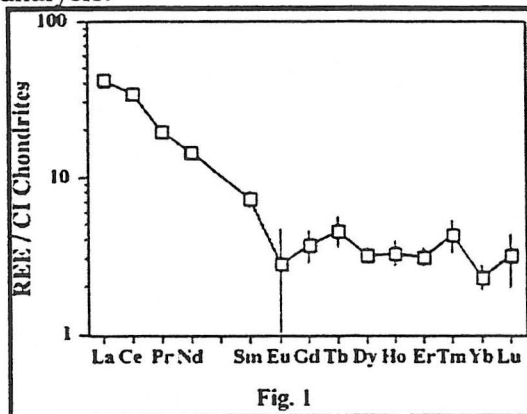


Fig. 1

The CI normalized La/Nd ratio of this analysis is similar to that of average continental crust [7]. Although significant REE enrichments were only found in Ca-rich areas also containing P, the LREE and P are not linearly correlated. However, there is a striking association of Rb and Sr with the LREE component.

Last January, Barrat *et al.* [8] reported observations pertinent to the question addressed here. These authors obtained whole rock elemental abundances for samples of the Saharan diogenite Tatahouine recovered immediately after its fall, in 1931, as well as samples collected in 1994, 63 years later. Just as we observe for the DaG 476 find, the latter are distinctly

LREE-enriched. In addition, the LREE pattern of 1994 Tatahouine samples are parallel, at lower concentrations, to that of the local soil. Rb and Sr are also greatly enriched in the 1994 samples when compared to those collected immediately after the fall.

DaG 476 is heavily weathered, highly fractured and affected by shock metamorphism, and it has resided on earth much longer than Tatahouine [9]. Although it is possible for whole rock analyses to avoid most of the contamination by carefully selecting samples that show a minimum of visible alteration, it most likely is impossible to avoid terrestrial contamination entirely. As already noted by Zipfel *et al.* [4], the measurement of a DaG 476 whole rock powder showed a much higher K/La ratio than typical of shergottites, probably due to K enrichment during terrestrial weathering. We would add that both elements were enriched during this process, but K to a larger extent than La.

It is also likely that terrestrial LREE contaminated the leachate fractions used by Jagoutz *et al.* [10] to determine the age of formation of DaG 476. In a meteorite whose LREE budget is dominated by merrillite (like the shergottites), we would expect the leachate and whole rock to have very similar Sm/Nd ratios, which they do not in DaG 476. The lower (by ~25%) $^{147}\text{Sm}/^{144}\text{Nd}$ ratio in the leachates than in the whole rock is most likely the result of addition to this shergottite of an easily leachable LREE-rich component. These considerations thus cast doubt on the use of the Sm-Nd chronometer in meteorites that have been significantly affected by terrestrial contamination.

In conclusion, whereas in Antarctic meteorites the effects of terrestrial alteration are more subtle and easier to deal with, such is probably not the case for many hot desert meteorites. Therefore, the consequences of terrestrial weathering will need to be kept in mind as researchers try to extract relevant information from this important source of extraterrestrial objects.

- References:** [1] Mittlefehldt D. W. and Lindstrom M. (1991) *GCA*, 55,77-87. [2] Floss C. and Crozaz G. (1991) *EPSL*, 107, 13-24 [3] Crozaz G. (1995) *LPI Tech. Rpt. 95-02*, 24-25. [4] Zipfel J. *et al.* (1999) *LPSC XXX*, abst.#1206. [5] Wadhwa M. *et al.* (1999) *MAPS*, in press. [6] Wadhwa M. *et al.* (1994) *GCA*, 58, 4213-4229 [7] Faure G. (1998) *Principles and Applications of Geochemistry*. Prentice Hall [8] Barrat J. A. *et al.* (1999) *MAPS*, 34, 91-97. [9] Nishiizumi K. (1999) *LPSC XXX*, abst.#1966 [10] Jagoutz *et al.* (1999) *LPSC XXX*, abst.#1808.

Chemical Compositions of Large Interplanetary Dust Particles from the Stratosphere and Small Antarctic Micrometeorites: Evidence for Element Loss and Addition in the Antarctic Micrometeorites. G. J. Flynn¹, S. R. Sutton², and W. Klöck³. 1) Dept. of Physics, SUNY-Plattsburgh, Plattsburgh NY 12901, 2) Dept. of Geophysical Sciences, The University of Chicago, Chicago IL 60637, 3) Martin Luther University, Halle, Germany.

The largest interplanetary dust particles (IDPs) collected from the Earth's stratosphere overlap in size with the smallest micrometeorites collected from the polar ices. This size overlap, for particles from about 25 to 75 microns in diameter, offers the opportunity to compare particles that were, presumably, identical prior to their respective terrestrial residence, collection, and curation. Differences between the IDPs and the polar micrometeorites are likely to result from contamination or weathering in the respective environments of each particle. This size range from 25 to 75 microns is particularly interesting because the mass-frequency distribution for particles incident on the Earth's atmosphere is sharply peaked in the 10^{-6} to 10^{-5} gram mass range (particles a few hundred microns in diameter). Thus, the 25 to 75 micron diameter IDPs and polar micrometeorites are close in size to the peak in the mass-frequency distribution, and these particles are likely to reflect the composition of the bulk of the interplanetary material accreting onto the Earth.

Samples Analyzed

We distinguish two types of large IDPs, based on their apparent structural strength. The first type of IDP consists of an isolated cluster of fragments on the collection surface. The fragments included in each cluster are, apparently, the remains of a single large IDP that was so weak it fragmented on impact with the collector. The pre-atmospheric sizes of the clusters cannot be determined with certainty since the porosity of the original assembly is not known. However, a cluster generally includes a few fragments ~20 microns in size, more fragments >10 microns in size, and abundant fragments in the 5 to 10 micron size range. This suggests that for most clusters the original particle was greater than 40 microns in diameter. The second type of IDP, presumably stronger, was collected intact, without any evidence of fragmentation.

We used the X-Ray Microprobe at the National Synchrotron Light Source (Brookhaven National Laboratory) to measure the chemical compositions (Fe, Ni, Cu, Zn, Ga, Ge, Se, Br, and Pb) of more than 30 large (all greater than 25 microns in their largest dimension) IDPs and more than 40 cluster fragments from the NASA stratospheric collection. We also measured 12 irregular-shaped micrometeorites collected from the Antarctic ice (Maurette, 1993). Major element chemistry was also measured on each Antarctic micrometeorite by SEM-EDX. For each Antarctic micrometeorite we determined the element/Fe ratio for the elements Ni, Cu, Zn, Ga, Ge, Se, Br, and Pb using the X-Ray Microprobe, and determined the bulk Fe content of each particle using the SEM-EDX. For the large IDPs we measured only element/Fe ratios using the X-Ray Microprobe.

The chemical analyses of 12 Antarctic micrometeorites, in Table 1, were reported by Flynn et al. (1993). The analyses of large IDPs collected intact are described in Flynn et al. (1997) and Flynn et al. (1998). The analyses of cluster fragments are described in Flynn et al. (1996), Flynn and Sutton (1997) and Flynn and Sutton (1998).

Compositions of Antarctic Micrometeorites and Large IDPs

To facilitate comparison with meteorites, CI normalized element abundances are generally employed. The large IDPs of both types are easily separated into two groups based on their CI normalized element abundance patterns. One group has a relatively flat pattern of the volatile elements Cu, Zn, Ga, Ge, and Se. The second group has significant depletions of Zn and Ge with respect to the flat line defined by the other volatile elements. Zinc depletions as extreme as $Zn < 0.01 \times CI$ have been observed in the IDPs. Zinc and Ge depletions have previously been linked to volatile loss during atmospheric entry heating in smaller (~10 micron diameter) IDPs (Thomas et al., 1992; Flynn, 1994). Thus, we take the average composition of the subset of IDPs which do not have Zn and Ge depletions to reflect the pre-atmospheric composition of each type of IDP.

The large IDPs collected intact have a pre-atmospheric composition with the volatile elements Cu, Zn, Ga, Ge, and Se present in approximately the CI abundances (Flynn et al., 1995; Flynn et al., 1998). The cluster fragments have a pre-atmospheric composition with the volatile elements Cu, Zn, Ga, Ge, and Se enriched relative to CI by factors of 2 to 4 (Flynn et al., 1996; Flynn and Sutton, 1997; Flynn and Sutton, 1998).

Entry Heating

About 1/3rd of the large IDPs collected intact show evidence of Zn and Ge loss on atmospheric entry. This is consistent with an atmospheric entry velocity just above Earth escape velocity, implying a main-belt asteroidal

source for the large IDPs (Flynn, 1995). Cluster fragments show a similar fraction with Zn depletions. However, since the pre-entry density of these particles is not known, we cannot infer an atmospheric entry velocity for the cluster particles.

The Antarctic micrometeorites differ from both types of large IDPs in that none of the 12 Antarctic micrometeorites shows any evidence of Zn depletion. This suggests either the 12 Antarctic micrometeorites selected for this study were not significantly heated on entry, consistent with their irregular (rather than rounded) shapes, or that diffusion inhibits element loss in these larger particles.

Ni Contents

The large IDPs, whether heated or unheated, all have Ni/Fe falling within a factor of 3 of the CI value. Almost all of the Antarctic micrometeorites show significant depletions of Ni. Only 3 of the 12 Antarctic micrometeorites have Ni/Fe within a factor of 3 of the CI value, and each of those had Ni/Fe <0.5xCI. Brownlee (1985) has suggested the pervasive Ni-depletion in micrometeorites results from separation of a Ni-rich metal nugget formed during melting on atmospheric entry. However, we measured only irregular-shaped, apparently unmelted, Antarctic micrometeorites. In addition, all 12 of the Antarctic micrometeorites we measured had Zn concentrations above the CI value, suggesting little volatile loss. Thus, the Ni depletion in these polar micrometeorites is not due to melting during the entry heating pulse.

Terrestrial Alteration of Antarctic Micrometeorites

Meteorites collected in the Antarctic are known to have experienced significant terrestrial alteration, including contamination with Pb and halogens as well mineral alteration. Because of their higher ratio of surface area to volume, the Antarctic micrometeorites are likely to be even more susceptible to contamination and alteration than the much larger Antarctic meteorites.

Element Loss from Polar Micrometeorites

The Ni depletion in these polar micrometeorites is accompanied by depletions in S, Ge and Se, a pattern suggesting the loss of a sulfur-bearing phase during residence in or extraction from the ice (Flynn et al., 1993; Presper et al., 1993). The relatively high Zn contents of the 12 Antarctic micrometeorites would appear to require that the bulk of the Zn not reside in the same host phase as the missing S, Ni, Ge, and Se. Pyrrhotite, the most common sulfur-bearing phase in the CI meteorites (Kerridge et al., 1979), contains relatively high concentrations of Ni (1.41 %), and Se (65 ppm), but little Zn (36 ppm) [analysis of Orgueil pyrrhotite by Greshake et al., 1998], and is, thus, a plausible candidate for the sulfur-rich phase that was lost from the Antarctic micrometeorites.

The observation of apparent element loss from the Antarctic micrometeorites raises the concern that other element abundances may also have been altered by terrestrial weathering.

Element Addition to Antarctic Micrometeorites

Each of the 12 Antarctic micrometeorites has a very high Pb content, ranging from 40 to 900 ppm, compared to a CI content of 2.5 ppm. Few of the large IDPs contain Pb at or above the detection limit of ~10 ppm. Unless the Antarctic micrometeorites have a Pb content remarkably distinct from that of the large IDPs, the high Pb contents must reflect contamination in the Antarctic micrometeorites. Substantial Pb contamination has been reported in interior samples from Antarctic meteorites (Misawa et al., 1992), and these small Antarctic micrometeorites are likely to be susceptible to similar contamination. This apparent addition of a relatively large amount of Pb to the Antarctic micrometeorites raises the concern that some or all of the other elements we have measured may have been similarly contaminated.

Modeling the Original Composition of Polar Micrometeorites

To relate the polar micrometeorites to other materials such as the large IDPs and the meteorites, it is necessary to reconstruct their pre-alteration chemical compositions. If we assume that only a single sulfur-bearing phase was removed from these polar micrometeorites, then we can model the pre-alteration composition of these particles by adding in the composition of that sulfur-bearing phase. Because of the reported similarity of the polar micrometeorites to hydrated carbonaceous chondrite meteorites, we begin with the assumption that the missing sulfur-bearing phase was pyrrhotite, the most common sulfur-bearing phase in the CI meteorites. Greshake et al. (1998) have reported chemical compositions, measured using the X-Ray Microprobe, for 20 pyrrhotite grains

extracted from the Orgueil CI carbonaceous chondrite. We averaged the 20 individual pyrrhotite compositions, and include that average in Table 1.

We model the pre-alteration composition of the Antarctic micrometeorites as a mixture of the average composition measured for the 12 Antarctic micrometeorites and the average composition of the Orgueil pyrrhotites. If we require the pre-alteration S content to equal that of CM meteorites ($S = 3.3\%$), we must mix 6% pyrrhotite with 94% Antarctic micrometeorite. The resulting composition, shown in Table 1 as A(94)P(6), is significantly deficient in Ni ($Ni = 0.32\%$) compared to the CM Ni content ($Ni = 1.2\%$) or the CI Ni content ($Ni = 1.1\%$). If we require the pre-alteration S content to equal the CI meteorite content ($S = 5.4\%$), we must mix 10% Orgueil pyrrhotite with 90% Antarctic micrometeorite. This gives a composition shown in Table 1 as A(90)P(10). Again, this mixture results in a significant deficiency in Ni ($Ni = 0.40\%$) compared to 1.1% Ni in the CI meteorites. Instead of fixing the pre-alteration S content, we can require the modeled pre-atmospheric composition result in a CI concentration of Ni ($Ni = 1.1\%$). In this case we are required to mix 73% pyrrhotite with 27% Antarctic micrometeorite, shown in Table 1 as A(27)P(73). This results in a S content of 35% and an Fe content of 43%. While the first two models are generally consistent with the pyrrhotite content of hydrated meteorites, the model with 73% pyrrhotite results in both a pyrrhotite abundance and a S content inconsistent with any stone meteorite.

This indicates that we cannot produce model pre-alteration composition of the Antarctic micrometeorites which matches either type of unheated large IDP or the CI or CM meteorites by the addition of a single sulfur-rich phase having an Orgueil pyrrhotite composition. Either the original sulfur-rich phase had a significantly higher Ni content than Orgueil pyrrhotite or an additional phase, possibly Ni-rich metal, was also removed from the Antarctic micrometeorites.

Comparison of Polar Micrometeorites and Large IDPs

Most of the large IDPs collected intact are platy in morphology and depleted in Ca, relative to CI, suggesting they are hydrated particles. We determined the mineralogies of four of the large IDPs collected intact which were included in our chemical analyses. Three were dominated by smectite and the fourth contained abundant cronstedite and Mg-rich serpentine (Flynn et al., 1995). Thus it seems likely that the large IDPs collected intact are mostly hydrated particles. The cluster particles are generally more porous than the large IDPs collected intact, and, in the cases for which mineralogy is available, the cluster particles usually contain anhydrous silicates.

All but one (B1 #2, which was lost after the X-Ray Microprobe analysis) of the 12 Antarctic micrometeorites included in this study were examined by TEM for mineralogical characterization. None of the Antarctic micrometeorites contained recognizable hydrated phases, such as the smectites and serpentines frequently found in IDPs, but 3 were so fine-grained that no mineral identification was possible (Flynn et al., 1993).

The high average Cu ($5.9\times CI$), Zn ($4.1\times CI$), and Ga ($3.6\times CI$) contents of the 12 Antarctic micrometeorites included in this study distinguish them from the large IDPs collected intact, which have approximately CI concentrations of these volatiles. The average Cu, Zn, and Ga contents of the 12 Antarctic micrometeorites are more similar to the cluster fragments, which generally show enrichments of the volatile elements to 2 to $4\times CI$. However, the cluster fragments show similar enrichments in Ge and Se, which are present, on average, in the Antarctic micrometeorites at $0.5\times CI$ and $0.6\times CI$ respectively.

The effect of adding 10% Orgueil pyrrhotite to the Antarctic micrometeorite composition is to reduce the Cu content (to about $3.7\times CI$), but the Se only increases to about the CI level ($0.9\times CI$) and Ge remains significantly depleted ($0.5\times CI$). This results in an element abundance pattern that is more similar to the cluster IDPs than to the large IDPs collected intact. However, the polar micrometeorites are quite compact, resembling the large micrometeorites collected intact, rather than the more porous cluster fragments.

Conclusions

The Antarctic micrometeorites differ in composition from IDPs and CI or CM meteorites in that they have extremely low contents of Ni ($0.25\times CI$) and S ($0.1\times CI$) and an extremely high content of Pb ($110\times CI$). They appear to have experienced terrestrial alteration that removed S, Ni, Ge, and Se and which added Pb. These alterations make it difficult to compare the polar micrometeorites with IDPs or meteorites, and raise the serious concern that the concentrations of other elements, whose abundances seem reasonable, may likewise have been altered.

On average, the Antarctic micrometeorites have factor of 3 to 6 times higher Cu, Zn, and Ga contents than the large "unheated" IDPs collected intact. If this Cu, Zn, and Ga is indigenous, then the Antarctic micrometeorites are chemically distinct from the large IDPs collected intact from the Earth's stratosphere. These high contents of Cu, Zn, and Ga are more similar to compositions of the cluster IDPs collected from the stratosphere.

No simple mixture of the recovered Antarctic micrometeorites and Orgueil pyrrhotites can simultaneously match the Ni/Fe and S/Fe ratios of carbonaceous chondrite meteorites or "unheated" large IDPs. This indicates that either the sulfur-rich phase removed from the Antarctic micrometeorites contains significantly more Ni than Orgueil pyrrhotites or that an additional phase, possibly Ni-rich metal, was removed from the Antarctic micrometeorites by terrestrial weathering.

Our selection of irregular-shaped polar micrometeorites appears to have very efficiently discriminated against heated polar micrometeorites. None of the 12 Antarctic micrometeorites show the Zn and Ge depletions that are observed in about 1/3rd of the large IDPs collected from the Earth's stratosphere.

References:

- Brownlee, D. E. (1985) in *Ann. Rev. Earth. Planet. Sci.*, 13, 147-172.
 Flynn, G. J. (1994) in *Analysis of Interplanetary Dust*, AIP Conf. Proc. 310, AIP Press, 127-144.
 Flynn, G. J. (1995) *Meteoritics*, 30, 504-505.
 Flynn, G. J., S. R. Sutton, W. Klöck (1993) *Proc. NIPR Symp. Antarct. Meteorites*, 6, 304-324.
 Flynn, G. J., S. Bajt, S. R. Sutton, and W. Klöck (1995) *Lunar & Planet. Sci. XXVI*, LPI Houston, 407-408.
 Flynn, G. J., S. R. Sutton, and S. Bajt (1996) *Meteoritics*, 31, A45-A46.
 Flynn, G. J. and S. R. Sutton (1997) *Lunar & Planet. Sci. XXVIII*, LPI Houston, 363-364.
 Flynn, G. J., S. R. Sutton, K. Kehm, and C. M. Hohenberg (1997) *Meteoritics & Planet. Sci.*, 32, A42-A43.
 Flynn, G. J., S. R. Sutton, K. Kehm, and C. M. Hohenberg (1998) *Meteoritics & Planet. Sci.*, 33, A51.
 Flynn, G. J. and S. R. Sutton (1998) *Meteoritics & Planet. Sci.*, 33, A49-A50.
 Greshake, A., W. Klock, P. Arndt, M. Maetz, G. J. Flynn, S. Bajt, and A. Bischoff (1998) *Meteoritics & Planet. Sci.*, 33, 267-290.
 Kerridge, J. F. et al., (1979) *Earth Planet. Sci. Lett.*, 43, 359.
 Maurette, M., C. Olinger, M. Christophe Michel-Levy, G. Kurat, M. Pourchet, F. Brandstatter, and M. Bourot-Denise (1991) *Nature*, 351, 44-47.
 Misawa, K., M. Tatumoto, and K. Yanai (1992) *Proc. NIPR Symp. Antarct. Meteorites*, 5, 3-22.
 Presper, T., G. Kurat, C. Koeberl, H. Palme, and M. Maurette (1993) *Lunar Planet. Sci. XXIV*, 1177-1178.
 Thomas, K. L. et al. (1992) *Lunar & Planet. Sci. XXIII*, LPI Houston, 1427-1428.

Table 1: Chemical Compositions of Irregular-Shape Antarctic Micrometeorites

| Particle | S (%) | Fe (%) | Ni (%) | Cu (ppm) | Zn (ppm) | Ga (ppm) | Ge (ppm) | Se (ppm) | Br (ppm) | Pb (ppm) |
|------------------|-------|--------|--------|----------|----------|----------|----------|----------|----------|----------|
| B1 #2 | ---* | 18.5* | 0.21 | 690 | 2900 | 96 | 45 | 17 | 30 | 130 |
| B1 #4 | 0.3 | 26.9 | 0.03 | 780 | 2200 | 100 | 4 | 36 | 30 | 230 |
| B1#5 | 0.6 | 21.2 | 0.52 | 170 | 920 | 7 | 23 | 10 | 11 | 100 |
| B1 #7 | 0.2 | 27.5 | 0.43 | 670 | 870 | 13 | 5 | 5 | 3 | 210 |
| B1 #8 | 0.4 | 27.3 | 0.19 | 350 | 550 | 6 | 5 | <2 | 4 | 150 |
| B1 #17 | 1.2 | 21.4 | 0.25 | 630 | 2300 | 100 | 20 | 14 | 50 | 900 |
| B1 #19 | 0.1 | 8.2 | 0.30 | 110 | 370 | 1 | 4 | 4 | 12 | 40 |
| B1 #20 | 0.2 | 25.9 | 0.06 | 240 | 1100 | 20 | 42 | 9 | 21 | 130 |
| B1 #22 | 1.45 | 19.1 | 0.48 | 290 | 570 | 2 | 4 | 22 | 16 | 50 |
| B3 #1 | 0.5 | 14.8 | 0.11 | 3400 | 1500 | 28 | 36 | 5 | 48 | 440 |
| B3 #2 | 0.3 | 32.8 | 0.14 | 1100 | 1700 | 35 | 5 | 13 | 52 | 890 |
| B3 #3 | 0.4 | 31.0 | 0.61 | 400 | 440 | 9 | 12 | 15 | 26 | 40 |
| Avg. 12 | 0.5 | 22.9 | 0.28 | 736 | 1285 | 35 | 17 | 13 | 25 | 276 |
| CI Norm. | 0.1 | 1.2 | 0.25 | 5.9 | 4.1 | 3.6 | 0.5 | 0.6 | 7.6 | 110 |
| Avg. Pyr. # | 48.3 | 50.2 | 1.41 | 85 | 36 | n.d. | n.d. | 65 | n.d. | n.d. |
| Modeled Mixtures | | | | | | | | | | |
| A(94)P(6) | 3.4 | 24.5 | 0.35 | 696 | 1210 | 33 | 16 | 16 | 24 | 260 |
| CI Norm. | 0.6 | 1.3 | 0.32 | 5.6 | 3.8 | 3.4 | 0.5 | 0.8 | 6.9 | 104 |
| A(90)P(10) | 5.5 | 25.6 | 0.39 | 670 | 1160 | 32 | 15 | 18 | 23 | 248 |
| CI Norm. | 1.0 | 1.4 | 0.35 | 5.4 | 3.7 | 3.3 | 0.5 | 0.9 | 6.6 | 99 |
| A(27)P(73) | 35.4 | 42.8 | 1.10 | 260 | 373 | 10 | 5 | 31 | 7 | 75 |
| CI Norm. | 6.6 | 2.3 | 1.00 | 2.1 | 1.2 | 1.0 | 0.2 | 1.5 | 2.0 | 30 |

* Particle B1 #2 was lost prior to EDX. Fe assumed to be the CI concentration, no S data available.

* Average composition of 20 pyrrhotite grains extracted from the Orgueil CI chondrite from Greshake et al. (1998). n.d. indicates the element was not detected. The detection limit is ~2 ppm. Elements not detected were assumed to have zero abundance in computing mixtures.

THE INFLUENCE OF TERRESTRIAL WEATHERING ON IMPLANTED SOLAR GASES IN LUNAR METEORITES

I.A. Franchi, A.V. Verchovsky and C.T. Pillinger

Planetary Sciences Research Institute, Open University, Walton Hall, Milton Keynes, MK7 6AA, UK.

The recent discovery of two large lunar meteorites in the Dar al Gani (DaG) region of the Libyan Sahara desert (DaG 262 and DaG 400) have sparked considerable and wide ranging interest in lunar material. The addition of lunar meteorites to the collections of extra-terrestrial material have greatly complemented the suite of samples returned by the Apollo and Luna missions almost 30 years ago, extending the range of materials available for investigation. However, care may be required in interpreting variations seen in the lunar meteorite population and also any differences with the returned lunar samples. As has been noted previously in the comparison of ordinary chondrite populations from Antarctica, hot deserts and observed falls, variations between the populations may be attributed to their interaction with the different terrestrial environments they have been exposed to rather than indigenous, pre-atmospheric differences [e.g. 1, 2]. In the case of the lunar samples this effect may be even more extreme as all the lunar meteorites are finds whereas the returned lunar samples were collected and subsequently stored in as near to ideal conditions as practically possible. Other factors related to the high levels of radiation damage suffered by materials in the lunar regolith may also make certain aspects of the lunar meteorites susceptible to terrestrial weathering. The particular interest behind this paper is how terrestrial weathering may have influenced the abundance and release characteristics of the implanted solar gases.

A thorough description of the mineralogy, chemistry and isotope systematics of DaG 262 was presented by Bischoff *et al.* [3], describing this meteorite as a mature, anorthositic regolith breccia with highland affinities. The results of a similar study of DaG 400 indicates that it is chemically, mineralogically and texturally very similar to DaG 262 [4] but that the later found meteorite contains very much lower abundances of solar gases [5]. The variation in the solar gases led both sets of workers to conclude that DaG 262 and DaG 400 were not paired. That only three lunar meteorites have been found outside Antarctica, and the two from the northern hemisphere are within 25km of each other in the Libyan Sahara, suggests that a pairing of DaG 262 and DaG 400 is statistically probable, particularly given the high level of similarity between these two meteorites. In part it was the possibility that terrestrial weathering could have resulted in the marked difference in the abundance of implanted gases between these two meteorites that led to this investigation. However, it should be noted that recent results

have shown that Dar al Gani 262 and 400 have in fact very different terrestrial exposure ages of 18kyr and 80kyr respectively clearly indicating different fall events [6]. Nonetheless, the results discussed below reveal striking differences between lunar meteorites and returned lunar samples which may be related to weathering effects and show that great care may be required when comparing noble gas abundances of weathered finds.

One of the most striking features about the implanted solar gases in DaG 262 reported by Bischoff *et al.* [3] was the release profile of N and Ar during stepped heating extraction. In this sample the N and Ar were released as a single discrete component with a peak release at 1200°C (Fig 1). In contrast, analyses of a wide range of returned lunar materials by high resolution stepped heating extractions always reveals a bimodal release of N and Ar [e.g. 7, 8] with peak releases at around 800°C and 1200°C (e.g. Fig 2), the relative proportions of the two releases ranging from 5:1 to less than 1:1 depending on the nature of the sample, from fine soil fraction through to breccia and glassy agglutinates. Brilliant *et al.* [9] presented evidence that the high temperature release, coincident with melting of the sample, was associated with "internal" surfaces – *i.e.* reworked material such as agglutinates and glassy breccias *etc.*, and the release at 800°C associated with the un-reworked grains – *i.e.* those openly exposed to the environment. The question then arises as to why the release profile from the lunar meteorite DaG 262 should be different to the asteroidal regolith and returned lunar samples? Two possible explanations were briefly discussed by Bischoff *et al.* [3] – a redistribution of the implanted gases following shock event(s) and loss of gas due to weathering processes.

Shock metamorphism or even melting should have an affect on the abundance and location of the implanted gases within a sample, perhaps sufficient to homogenise the bimodal release typically seen in returned lunar samples to the single, high temperature release seen in DaG 262. Although DaG 262 contains abundant glassy material and veins the maximum shock pressures experienced by the meteorite post-lithification were not more than 20 GPa [3] – hardly exceptional in comparison with other lunar breccias. The noble gases in DaG 262 do show a light-gas depleted fractionation relative to returned lunar material, although whether the magnitude of this fractionation is compatible with either a quantitative loss of the com-

ponent typically released around 800°C or relocation of this component to a site comparable to that of the high temperature component remains unresolved.

The scenario employing terrestrial weathering affecting the noble gas and nitrogen signature of the meteorite is based on the fact that the implanted gases, at least in the lightly- or un-reworked grains, reside in a very radiation damaged, thin layer less than 1µm thick on the surface of each grain. Such radiation damaged rims would be expected to be relatively more prone to terrestrial weathering compared to the bulk of the sample. Indeed, DaG 262 displays evidence of pervasive, high levels of contamination ranging from penetrating carbonate veins, abundant organic carbon and elevated levels of minor and trace elements typical of terrestrial contamination [3] clearly demonstrating that it has suffered considerably during its long residence in the Sahara desert. Partial or complete loss of implanted gases from the grain rims would leave only those gases protected from the weathering reagents (O₂, H₂O, etc.) – i.e. those gases on “internal” surfaces. The net result of this process would be to remove the release of N and Ar seen around 800°C leaving only the release peaking at 1200°C. Evidence from other gases analysed by high resolution stepped heating experiments (He and Ne) is limited as the higher diffusion rates of these gases usually results in a single, broad release of gas even in pristine returned lunar samples.

Comparison of the release profile from a lunar meteorite observed to fall would clearly be of great benefit to resolving the magnitude of the effect of terrestrial weathering on such implanted gases. However, as noted above all known lunar meteorites are intact finds from either Antarctica or hot deserts. Instead, for comparison 3 Antarctic meteorites with relatively low weathering grades, ALHA 81005 and MAC 88105 (weathering grade A/B), and QUE 94281 (B) have been analysed by high resolution stepped heating with analyses of He, N, Ne and Ar to determine what similarities or differences they exhibit with DaG 262 (see Fig 3). The abundances of all the gases extracted are comparable to previous results and, more importantly, the release profiles are similar to the release profile of DaG 262. ALHA 81005 and QUE 94281, with gas contents similar to DaG 262 are very similar with a single release peaking at 1200°C for both N and Ar. MAC 88105, with a much lower total gas content, displays a single release of Ar around 1200°C, although the small amounts of N released relative to the system blank and the low temperature contamination somewhat mask the release profile at higher temperatures. The noble gas and N abundance patterns from these meteorites are similar to that of DaG 262, with perhaps slightly more fractionated He/Ar ratios.

There appears to be little difference in the nature of the gas release profiles of the 4 lunar meteorites analysed by high resolution stepped heating to date. If weathering is the key to this difference then this may indicate the efficiency and speed at which such effects occur given the different storage and weathering conditions of the meteorites studied. It is interesting to note that of the gas-rich meteorites the least weathered specimen, ALHA 81005, does display the most pronounced evidence for a release around 800°C, suggesting that not all the implanted gases in the radiation damaged rims has been lost. That the release profiles from the lunar meteorites are so distinct from the returned lunar samples clearly shows that considerable differences exist between the two suites of samples. Although it is not presently possible to discriminate between the effects of terrestrial weathering and shock metamorphism as the process responsible for the differences some support for the weathering hypothesis comes from the Ne isotopic composition. The Ne extracted from these meteorites shows that it is primarily a mixture of cosmogenic with SEP neon rather than with SW neon (e.g. Fig 4). Such behaviour is consistent with the more deeply implanted SEP component being more resistant to weathering than the bulk SW component. Similarly, strongly weathered gas-rich ordinary chondrites also display a pronounced SEP signature in comparison with fresh falls [10]. Detailed petrographic comparison of rim material in returned and meteoritic lunar samples should yield further information on this problem, as will the recovery of a new fall of a lunar meteorite.

References:

- [1] M.M. Grady *et al.* (1989). *Meteoritics* **24**, 147-154.
- [2] C. Koebrel and W.A. Cassidy (1991) *Geochim. Cosmochim. Acta.* **55**, 3-18.
- [3] A. Bischoff *et al.* (1998) *Meteor. Planet. Sci.* **33**, 1243-1257.
- [4] J. Zipfel *et al.* (1998) *Meteor. Planet. Sci.* **33**, A171.
- [5] P. Scherer *et al.* (1998) *Meteorit. Planet. Sci.* **33**, A135-136.
- [6] K. Nishiizumii *et al.* (1999) Presentation at *Workshop on Extraterrestrial Materials from Cold and Hot Deserts*, Kwa-Maritane, South Africa.
- [7] D.R. Brilliant (1999) Ph.D Thesis.
- [8] S.S. Assonov *et al.* (1999) *Proc. Third Conf. Luna Exploration* Submitted.
- [9] D.R. Brilliant *et al.* (1994) *Meteoritics* **29**, 718-723.
- [10] R. Wieler *et al.* (1999). Presentation at *Workshop on Extraterrestrial Materials from Cold and Hot Deserts*, Kwa-Maritane, South Africa.

Fig 1 Argon release profile of Dar al Gani 262. Data from [3]

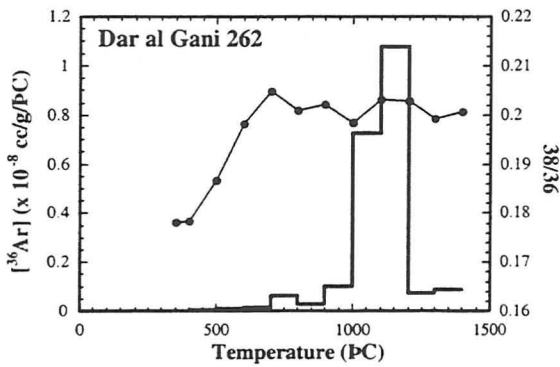


Fig 3 Argon release profile of ALHA 81005, MAC 88105 and QUE 94281

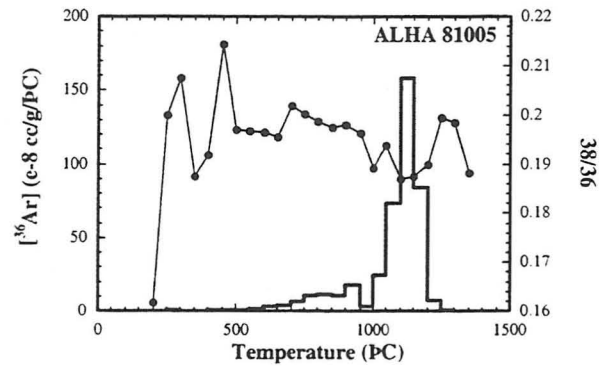


Fig 2 Argon release profile of Apollo 12023 soil, <1mm soil fraction. Data from [7].

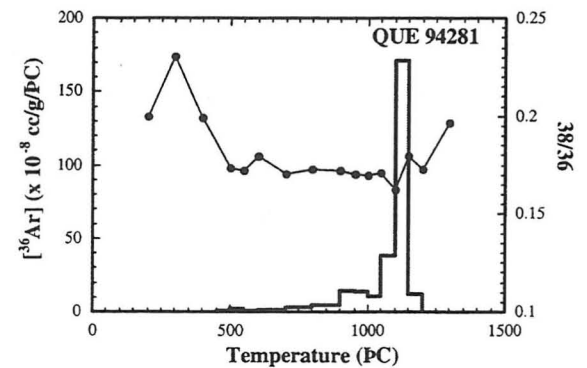
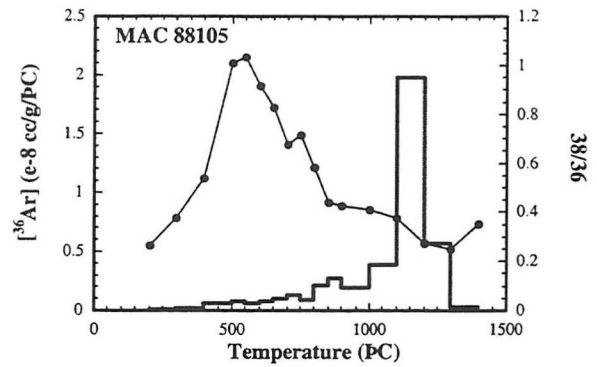
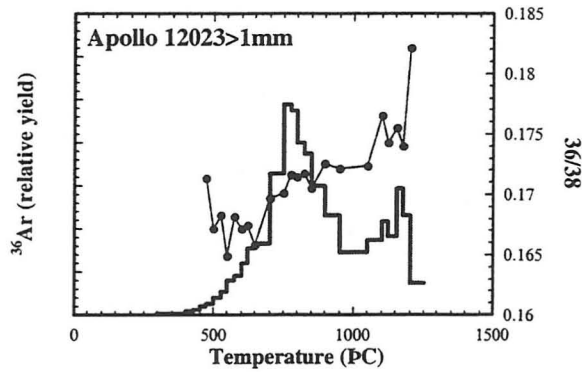
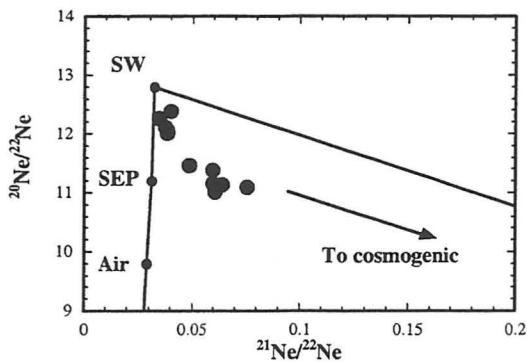


Fig 4 Neon isotopic composition of QUE 94281



Meteorites from Cold and Hot Deserts: How Many, How Big, and What Sort? Monica M. Grady, Department of Mineralogy, The Natural History Museum, Cromwell Road, London SW7 5BD, UK.

In the 5 years since the first workshop on meteorites from cold and hot deserts, there has been a big rise in the number of meteorites returned from desert localities. The number of meteorites found in the Sahara has grown three-fold, several new Antarctic localities have yielded plentiful harvests (e.g. Grosvenor Mountains, Queen Alexandra Range), and return visits to well-documented Antarctic sites have also resulted in many additional meteorites (e.g. Elephant Moraine). Although classification of new meteorites is regularly reported in the *Meteoritical Bulletin*, the total number of different types from all localities has not been published for many years. The present Symposium provides an opportunity to draw together statistical data for meteorites from cold and hot deserts, for comparison with data for modern falls; data are taken from the (almost published) 5th Edition of the *Catalogue of Meteorites*. All numbers are correct as of 1st May 1999.

The breakdown of different meteorite types is shown in Table 1. Table 2 summarises the occurrence frequency of different meteorite types for the most productive collection areas; Figure 1 gives the mass frequency distribution for hot deserts, and Figure 2 for cold deserts. The mass frequency distribution for modern falls is plotted on both figures for comparison. Note that no correction is made for pairing. It has long been recognised that one consequence of the ease with which meteorites are located on the ice is that the mean size of meteorites in the Antarctic collection is smaller than that of modern falls and finds. This effect is readily visible in Figures 1 and 2; Table 3 lists the median and modal specimen weights for each locality. A further characteristic of desert meteorite collections is that there are more rare and unusual meteorite types compared to modern falls and finds, an effect that is illustrated in Table 2.

Modern Falls: there are 1003 recorded meteorite “falls”, stretching back over 500 years to the first well-authenticated fall, Ensisheim in 1492. Recovered weights are recorded for 860 of the falls, and range from 144mg (Vilna, Canada, 1967) to over 27 tonnes (Sikhote-Alin, Russia, 1947), with a median weight of 3kg (mode at 1 kg).

Antarctic finds: 17474 meteorites (uncorrected for pairing) have been returned from Antarctica, approximately half this number from the Yamato Mountains region by Japanese expeditions and half from Victoria Land by U.S. and European collecting parties.

Saharan finds: 1508 meteorites (uncorrected for pairing) have been collected from the Sahara Desert, mainly by private collectors. The three most productive areas are the Reg el Acfer in Algeria (320 meteorites), and Dar al Gani (256) and Hammadah al Hamra (520) in Libya. A further 206 specimens have been returned from an unknown location within the desert (“Sahara X” in the figures and tables); the mass frequency distribution for this locality is almost identical to that of the Dar al Gani region.

Nullarbor Region: the Nullarbor Region in Western and South Australia was the first desert area from which meteorites were recovered on a regular basis, the first searches taking place in the early 1960s. Since regular expeditions started in the late 1980s, over 280 specimens have been found.

Table 1: Summary of Classified Meteorites

| <i>Class</i> | <i>Fall</i> | <i>Find</i> | <i>NHM</i> | <i>Total</i> | <i>Class</i> | <i>Fall</i> | <i>Find</i> | <i>NHM</i> | <i>Total</i> |
|-----------------------|-------------|-------------|------------|--------------|-------------------------|-------------|--------------|-------------|--------------|
| STONES | | | | | | | | | |
| Chondrites | | | | | | | | | |
| UNGR | 0 | 9 | 4 | 9 | L-Group | | | | |
| Carbonaceous | | | | | L | 12 | 39 | 5 | 51 |
| CI | 5 | 0 | 3 | 5 | L3 | 6 | 310 | 15 | 316 |
| CM | 15 | 145 | 17 | 160 | L3-4 | 1 | 7 | 0 | 8 |
| CO | 5 | 79 | 8 | 84 | L3-5 | 0 | 5 | 0 | 5 |
| CV | 6 | 40 | 8 | 46 | L3-6 | 2 | 4 | 4 | 6 |
| CR | 3 | 75 | 2 | 78 | L4 | 22 | 395 | 38 | 417 |
| CK | 2 | 71 | 2 | 73 | L4-5 | 0 | 16 | 1 | 16 |
| CH | 0 | 11 | 1 | 11 | L4-6 | 0 | 2 | 0 | 2 |
| UNGR | 0 | 9 | 3 | 9 | L5 | 64 | 1149 | 88 | 1213 |
| UNCL | 0 | 91 | 0 | 91 | L5-6 | 1 | 51 | 2 | 52 |
| Total | 36 | 521 | 44 | 557 | L6 | 242 | 3790 | 311 | 4032 |
| Enstatite | | | | | L6-7 | 0 | 7 | 0 | 7 |
| E | | | | | L7 | 0 | 15 | 0 | 15 |
| E | 0 | 2 | 0 | 2 | L/LL | 1 | 38 | 9 | 39 |
| E3 | 0 | 19 | 0 | 19 | Total | 351 | 5828 | 473 | 6179 |
| E4 | 0 | 5 | 0 | 5 | LL-Group | | | | |
| E5 | 0 | 8 | 0 | 8 | LL | 1 | 25 | 0 | 26 |
| E6 | 0 | 4 | 0 | 4 | LL3 | 9 | 62 | 7 | 71 |
| Total | 0 | 38 | 0 | 38 | LL3-6 | 2 | 4 | 1 | 5 |
| EH | | | | | LL4 | 7 | 56 | 7 | 63 |
| EH | 2 | 8 | 2 | 10 | LL4-5 | 0 | 2 | 0 | 2 |
| EH3 | 2 | 96 | 4 | 98 | LL4-6 | 1 | 12 | 1 | 14 |
| EH4 | 2 | 7 | 4 | 9 | LL5 | 14 | 182 | 15 | 196 |
| EH5 | 2 | 4 | 2 | 6 | LL5-6 | 0 | 31 | 0 | 31 |
| EH6 | 0 | 2 | 0 | 2 | LL5-7 | 0 | 1 | 0 | 1 |
| Total | 8 | 117 | 12 | 125 | LL6 | 35 | 368 | 31 | 403 |
| EL | | | | | LL7 | 1 | 8 | 2 | 9 |
| EL | 0 | 3 | 1 | 3 | Total | 70 | 751 | 64 | 821 |
| EL3 | 0 | 8 | 0 | 8 | Rumurutiites | | | | |
| EL4 | 0 | 0 | 0 | 0 | R | 1 | 16 | 1 | 17 |
| EL5 | 0 | 2 | 0 | 2 | Total Chondrites | | | | |
| EL6 | 6 | 18 | 11 | 24 | | 789 | 13917 | 1168 | 14706 |
| Total | 6 | 31 | 12 | 37 | Achondrites | | | | |
| Kakangari-type | | | | | ACAP | 1 | 11 | 1 | 12 |
| K | 1 | 2 | 2 | 3 | ANGR | 1 | 3 | 1 | 4 |
| Ordinary | | | | | AUB | 9 | 35 | 10 | 44 |
| UNGR | 1 | 0 | 0 | 1 | BRACH | 0 | 7 | 2 | 7 |
| UNCL | 0 | 40 | 0 | 40 | DIO | 9 | 84 | 8 | 93 |
| H-Group | | | | | EUC | 24 | 171 | 23 | 195 |
| H | 15 | 61 | 2 | 76 | HOW | 20 | 73 | 22 | 93 |
| H3 | 7 | 181 | 18 | 188 | LOD | 1 | 13 | 1 | 14 |
| H3-4 | 1 | 15 | 1 | 16 | LUN | 0 | 18 | 1 | 18 |
| H3-5 | 2 | 9 | 1 | 11 | SNC | 4 | 10 | 6 | 14 |
| H3-6 | 2 | 8 | 0 | 10 | URE | 5 | 86 | 11 | 91 |
| H4 | 57 | 1293 | 116 | 1350 | WIN | 1 | 10 | 4 | 11 |
| H4-5 | 0 | 83 | 4 | 83 | UNGR | 1 | 3 | 0 | 4 |
| H4-6 | 0 | 8 | 1 | 8 | UNCL | 1 | 1 | 0 | 2 |
| H5 | 137 | 3140 | 268 | 3277 | Total | 77 | 525 | 90 | 602 |
| H5-6 | 2 | 79 | 7 | 81 | Other Stones | | | | |
| H6 | 92 | 1677 | 138 | 1769 | UNGR | 0 | 5 | 0 | 5 |
| H7 | 0 | 5 | 0 | 5 | UNCL | 72 | 5776 | 0 | 5848 |
| H/L | 0 | 5 | 0 | 5 | TOTAL STONES | | | | |
| Total | 315 | 6564 | 556 | 6879 | | 938 | 20223 | 1258 | 21161 |

| <i>Class</i> | <i>Fall</i> | <i>Find</i> | <i>NHM</i> | <i>Total</i> |
|--------------------|-------------|-------------|------------|--------------|
| IRONS | | | | |
| IAB | 5 | 126 | 71 | 131 |
| IC | 0 | 11 | 10 | 11 |
| IIAB | 6 | 96 | 47 | 102 |
| IIC | 0 | 8 | 5 | 8 |
| IID | 3 | 13 | 14 | 16 |
| IIE | 1 | 17 | 10 | 18 |
| IIIAB | 11 | 218 | 155 | 229 |
| IIICD | 3 | 38 | 24 | 41 |
| IIIE | 0 | 13 | 10 | 13 |
| IIIF | 0 | 6 | 4 | 6 |
| IVA | 4 | 60 | 38 | 64 |
| IVB | 0 | 13 | 12 | 13 |
| UNGR | 7 | 93 | 54 | 100 |
| UNCL | 8 | 103 | 11 | 111 |
| TOTAL IRONS | | | | |
| | 48 | 815 | 465 | 863 |

| <i>Class</i> | <i>Fall</i> | <i>Find</i> | <i>NHM</i> | <i>Total</i> |
|--------------------------|-------------|-------------|------------|--------------|
| STONY-IRONS | | | | |
| MES | 7 | 59 | 23 | 66 |
| PAL | 5 | 45 | 27 | 50 |
| TOTAL STONY-IRONS | | | | |
| | 12 | 104 | 50 | 116 |
| UNKNOWN TYPE | | | | |
| | 5 | 7 | 0 | 12 |
| GRAND TOTAL | | | | |
| | <i>Fall</i> | <i>Find</i> | <i>NHM</i> | <i>Total</i> |
| | 1003 | 21149 | 1773 | 22152 |

Table 2: Occurrence frequency (%) of meteorite types according to collection locality

| | Iron | St.-Iron | Achond | H | L | LL | E | C | Other |
|--------------------|------|----------|--------|------|------|------|------|------|-------|
| Fall | 5.0 | 1.3 | 8.1 | 34.1 | 37.9 | 7.6 | 1.5 | 3.9 | 0.5 |
| Hot Desert | | | | | | | | | |
| DaG | 0.2 | 0.0 | 3.3 | 46.2 | 31.7 | 7.5 | 0.0 | 9.0 | 2.1 |
| HH | 0.0 | 0.0 | 1.6 | 44.5 | 41.4 | 9.0 | 0.0 | 1.2 | 2.3 |
| Sahara X | 0.0 | 1.5 | 1.9 | 23.3 | 30.6 | 11.7 | 24.8 | 1.5 | 4.9 |
| Acfer | 0.3 | 0.6 | 0.3 | 50.6 | 30.1 | 9.8 | 0.3 | 6.0 | 1.9 |
| Nullarbor | 1.1 | 0.4 | 6.8 | 40.0 | 41.1 | 4.6 | 0.7 | 2.9 | 2.5 |
| Cold Desert | | | | | | | | | |
| Yamato | 0.2 | 0.1 | 6.4 | 52.5 | 29.9 | 5.2 | 1.2 | 4.0 | 0.5 |
| Asuka | 0.0 | 2.2 | 18.3 | 23.7 | 28.0 | 11.8 | 1.1 | 14.0 | 1.1 |
| Frontier | 0.0 | 0.0 | 3.2 | 73.0 | 21.4 | 1.5 | 0.0 | 0.3 | 0.6 |
| ANSMET | 0.8 | 0.4 | 2.8 | 41.3 | 45.0 | 5.0 | 1.0 | 3.4 | 0.3 |
| ALH | 0.8 | 0.2 | 3.6 | 60.5 | 26.1 | 3.5 | 1.1 | 3.8 | 0.4 |
| EET | 0.5 | 0.1 | 3.3 | 16.7 | 69.1 | 2.8 | 0.8 | 6.6 | 0.1 |
| QUE | 0.1 | 0.8 | 1.3 | 30.6 | 54.5 | 10.8 | 0.5 | 1.3 | 0.0 |
| LEW | 0.4 | 0.1 | 2.8 | 63.6 | 26.4 | 4.2 | 0.5 | 1.7 | 0.3 |

Includes K-type, R and ungrouped meteorites. Unclassified meteorites are not included in the totals

Table 3: Median and Modal weights for different collection areas

| | Median | Mode (g) |
|--------------------|--------|----------|
| Fall | 3000 | 1000 |
| Hot desert | | |
| DaG | 223 | 90 |
| HaH | 513 | 184 |
| Sahara X | 252 | 50 |
| Acfer | 238.5 | 105 |
| Nullarbor | 94.3 | 74 |
| Cold desert | | |
| Yamato | 6.27 | 2.1 |
| Asuka | 27.176 | 0.904 |
| Frontier | 5.99 | 1.2 |
| ANSMET | 18.3 | 0.5 |
| ALH | 18.3 | 4.9 |
| EET | 22.7 | 1.4 |
| QUE | 11.7 | 0.5 |
| LEW | 11.1 | 3.8 |

Figure 1: Hot Deserts

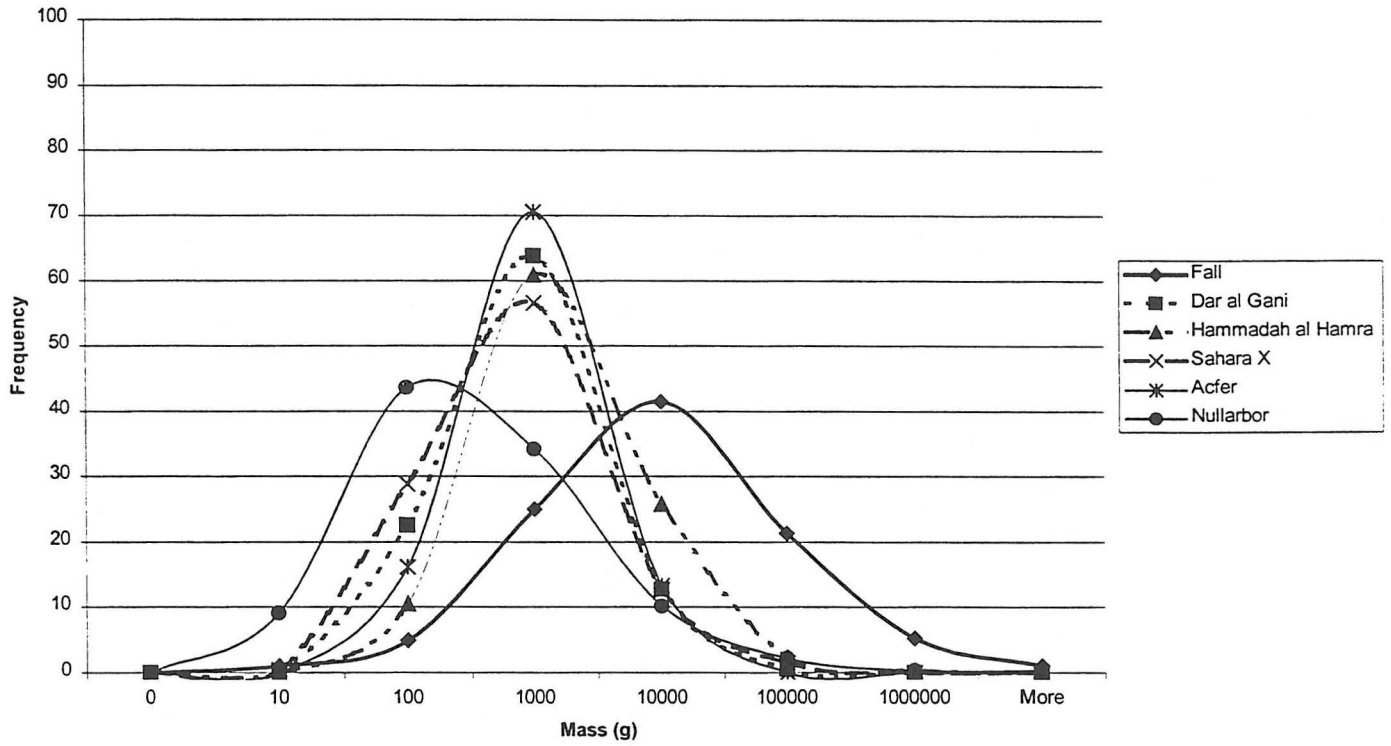
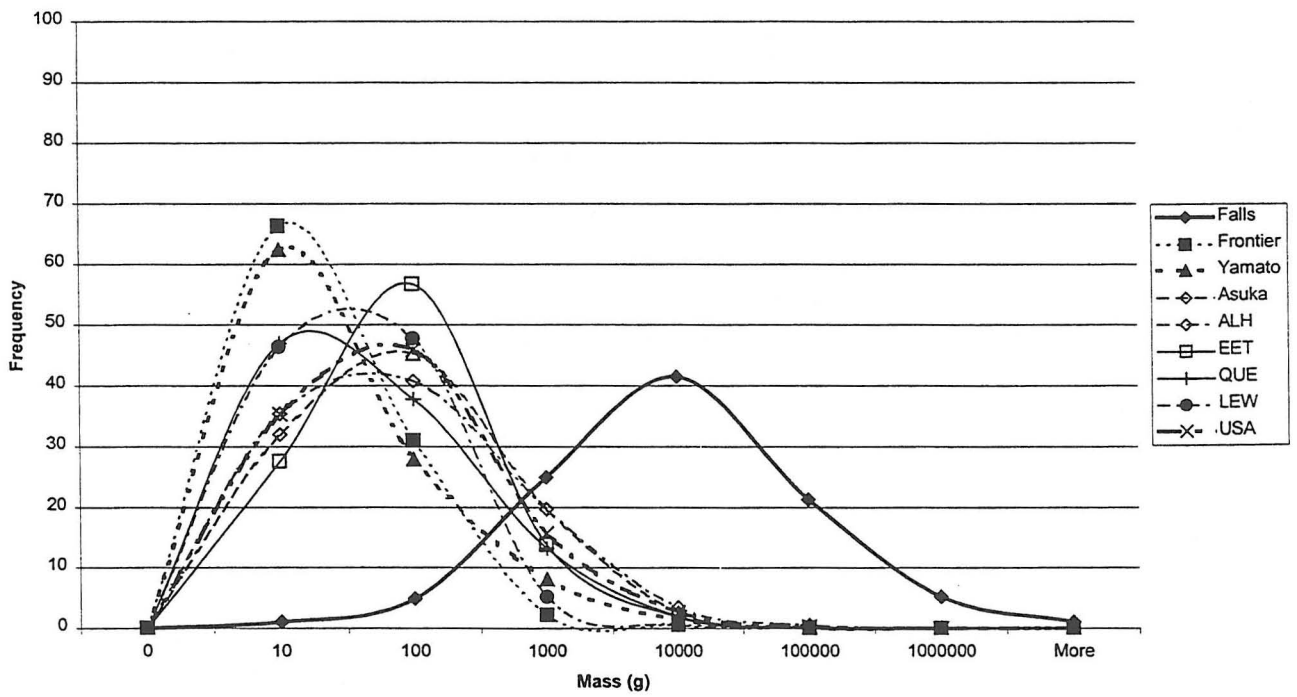


Figure 2: Cold Deserts



USING ^{14}C AND ^{14}C - ^{10}Be FOR TERRESTRIAL AGES OF DESERT METEORITES. A. J. T. Jull¹, P.A. Bland², S. E. Klandrud¹, L. R. McHargue¹, A. W. R. Bevan³, D. A. Kring⁴ and F. Wlotzka⁵. ¹NSF Arizona AMS Facility, University of Arizona, Tucson, AZ 85721, USA. ²Natural History Museum, London SW7 5DB, England. ³Western Australian Museum, Perth, WA 6000, Australia. ⁴Lunar and Planetary Laboratory, University of Arizona, Tucson, AZ 85721, USA ⁵Abteilung Kosmochemie, Max-Planck-Institut für Chemie, 55122 Mainz, Germany.

The arid regions of the world appear to be great storage locations for meteorites, where they can survive for long periods of time in such environments [1]. Large numbers of meteorites have been recovered from diverse areas of arid and semi-arid regions of North Africa, Arabia, North America and Western Australia. The cold desert of Antarctica is a further storehouse of meteorites [2]. One of the first recognized areas for collections of meteorites was Roosevelt County, New Mexico [3]. The Nullarbor region of Australia and the northern Sahara Desert in Africa are also prolific sources of meteorites [4].

The study of the terrestrial ages of these meteorites gives us useful information concerning the storage and weathering of meteorites and the study of fall times and terrestrial age. The most useful for many meteorite collection areas is ^{14}C ($t_{1/2}=5730$ years). For the Nullarbor and for some other locations, we can show an approximately exponential drop-off of number of meteorites with increasing terrestrial age. Jull et al [1,4] and Wlotzka et al [5] have reported on terrestrial ages of meteorites from North Africa and this region. Different climatic regimes and local geology can affect the distribution of terrestrial ages of meteorites from areas such as the Sahara desert and Roosevelt County, as weathering occurs at different rates depending on sample chemistry and local climatic effects [6].

In general, the Nullarbor and Sahara meteorites show an approximately exponential decrease of number of finds with terrestrial age to at least 30kA. Since weathering gradually destroys meteorites, in a given population of finds the resulting distribution should show some kind of exponential dependence on age. The distribution of meteorite terrestrial ages is easily understood in the case of a collection where all meteorites fell directly on the collection area. The meteorites then should eventually disintegrate and therefore, the number will decrease with increasing age, and so there should be more young meteorites than older ones. This is the expected distribution based on a simple first-order model of meteorite accumulation [7]. However, due to other effects, many sites do not show this simple relationship. Many stony meteorites can survive in desert environments for long periods of time [6]. Some interesting achondrites have also been recovered from these desert regions, although the vast majority are ordinary chondrites. Several interesting lunar and Martian meteorites have been recovered from these "hot" deserts.

In this paper, we explore the usefulness and limitations of using ^{14}C for terrestrial age determinations and we also introduce a method of dating using both ^{14}C and ^{10}Be . Since both of these radionuclides are produced by the same spallation reactions on oxygen, their production in meteorites is almost always at a constant ratio. This allows us to correct for shielding effects, the only assumption being that the exposure age of the meteorite is sufficient to saturate ^{10}Be . This exposure age can also be verified by noble-gas data. Both ^{14}C and ^{10}Be can be measured by accelerator mass spectrometry (AMS) at the Arizona AMS Laboratory. For ^{14}C measurements, a

sample of ~0.1 to 0.3g of the meteorite is crushed and treated with phosphoric acid to remove terrestrial carbonate weathering products. The washed and dried powder is then mixed with iron chips (~5g) and heated to melting in an RF furnace, in a flow of oxygen. The combusted products are collected and the amount of CO₂ determined, and then reduced to graphite over an Fe catalyst. For ¹⁰Be, the sample is also cleaned in acid to remove weathering carbonates. It is then dissolved in HF-HNO₃ and a carrier of Be added. ¹⁰Be is then extracted using standard solvent-extraction and ion exchange procedures. The Be(OH)₂ so produced is heated to ~900°C to produce BeO. The BeO is mixed with Ag to make an accelerator target.

Neupert et al. [8] correlated ¹⁴C, ²⁶Al and ¹⁰Be in some A \acute{c} fer meteorites, and used the results to estimate shielding-corrected terrestrial ages. Since both ¹⁴C and ¹⁰Be are produced by spallation of oxygen, their depth dependence is very similar, and also the production ratio is independent of chemistry. An excellent example of the use of the ¹⁴C-¹⁰Be method is shown by Kring et al. [9,10] for the large fall of the Gold Basin meteorites. In figure 1, we compare the results obtained for both of these radionuclides on splits of the same samples. Three groups of samples are plotted, including Gold Basin data [10], and a group of well-characterized Western Australian meteorites. Samples at saturation for both nuclides should plot in the range of the two lines through the origin, which represent our best estimate of the production ratio of ¹⁴C/¹⁰Be based on studies of artificial irradiations and recent falls [11].

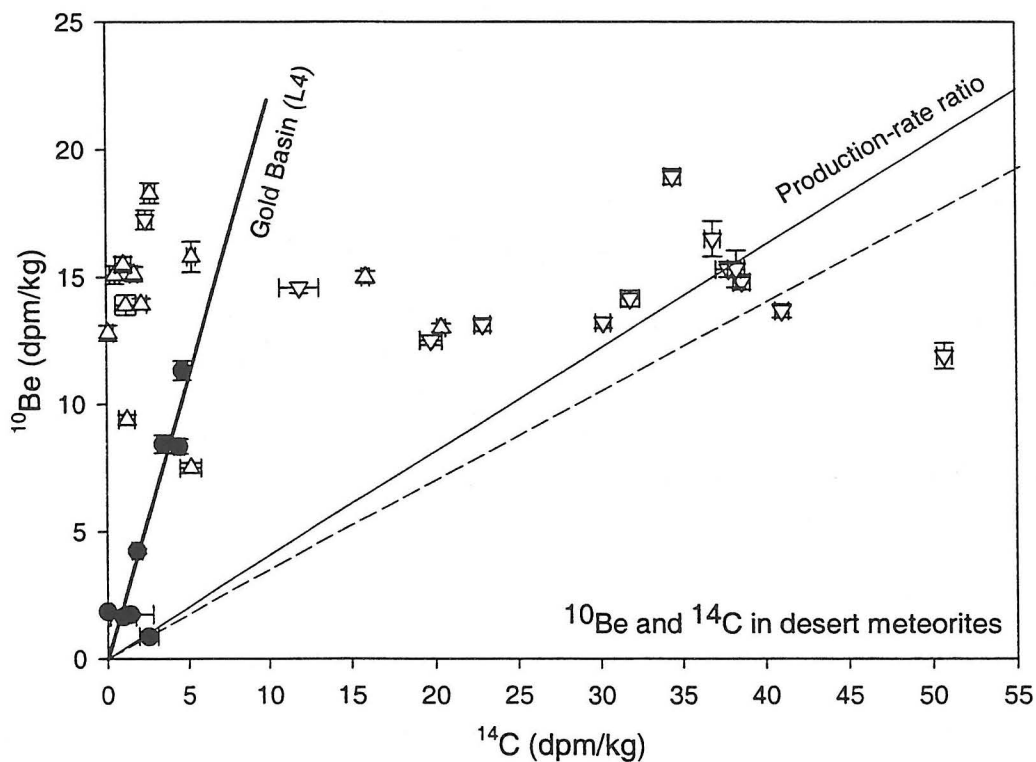


Figure 1: Distribution of ¹⁰Be and ¹⁴C contents of desert ordinary chondrites from Western Australia, both well-classified (∇) and non-classified (Δ) compared to a series of samples from the large Gold Basin, Arizona (\bullet) fall [9,10].

The Gold Basin samples plot along a line going through the origin, which is consistent with samples from the same object, but varying amounts of shielding [10]. The Western Australian meteorites generally show lower shielding and higher ^{10}Be production in the range 13-18 dpm/kg ^{10}Be . Only one sample (Mundrabilla 005) plots to the right of the production-rate line, which indicates saturated ^{14}C but low ^{10}Be . This should be consistent with a short exposure age and undersaturation of ^{10}Be for this meteorite. All the other samples are remarkably well-behaved and the ^{10}Be production rate can then be used to correct the ^{14}C production rate to give a better estimate of terrestrial age, than possible using ^{14}C alone. In conclusion, ^{14}C measurements of desert meteorites, either alone or in combination with other nuclides, is a critical tool in understanding the terrestrial ages of meteorites from arid regions.

References: [1] A. J. T. Jull et al. (1995), Workshop on meteorites from cold and hot deserts, LPI Tech. Rep. 95-02, 37-38. [2] A. J. T. Jull et al. (1998), in "Meteorites: flux with time and impact effects" (eds. M. M. Grady, et al.), Geol. Soc. London Spec. Pub. 140, 75-91. [3] E. R. D. Scott et al. (1986), *Meteoritics*, 21, 151-308. [4] A. J. T. Jull et al. (1993), *Meteoritics*, 28, 376-377. [5] F. Wlotzka et al. (1995), Workshop on meteorites from cold and hot deserts, LPI Tech Rep.95-02, 72-73. [6] P. A. Bland et al. (1998), *Geochim. Cosmochim. Acta.*, 62, 3169-3184. [7] A. J. T. Jull et al. (1993), *Meteoritics*, 28, 188-195. [8] U. Neupert et al. (1997), *Meteoritics Planet. Sci.*, 32, A98-99. [9] D. A. Kring et al. (1998), *Lunar Planet. Sci.* 29, CD-ROM. [10] D. A. Kring et al (1999), this workshop. [11] A. J. T. Jull et al. (1994), *Meteoritics*, 29, 649-651.

THE GOLD BASIN STREWN FIELD, MOJAVE DESERT, AND ITS SURVIVAL FROM THE LATE PLEISTOCENE TO THE PRESENT. David A. Kring¹, A. J. Timothy Jull², and Phil A. Bland³, ¹Lunar and Planetary Laboratory, University of Arizona, 1629 E. University Blvd., Tucson, AZ 85721 USA (kring@lpl.arizona.edu), ²NSF Arizona Accelerator Mass Spectrometer Facility, University of Arizona, Tucson, AZ 85721 USA, ³Department of Mineralogy, Natural History Museum, Cromwell Road, London, SW7 5BD, U.K.

Introduction: The Gold Basin strewn field occurs in the Mojave Desert of northwestern Arizona. When we first reported the find last year [1], approximately 2000 specimens had been recovered over a 160 km² area. More recent fieldwork has increased the number of samples to ~3000 over an area of about 225 km² [2]. The area is currently part of the arid American Southwest, but climatic conditions have fluctuated since the time the meteorite fell. In this paper, we explore those changes and how they affected the weathering of the meteorite, comparing and contrasting these effects, where possible, with the effects seen among meteorites found in other hot desert regions of the world.

The Gold Basin Meteorite: The Gold Basin meteorite is an L4 chondrite dominated by olivine (Fa_{24±1}), pyroxene (Wo₁En₇₉Fs₂₀), and a metal-sulfide assemblage that has clearly been weathered [1]. The samples are sometimes found buried, up to 10 inches deep, in a fine-grained loose soil where they are occasionally partially or wholly encased in caliche. Many samples have also been recovered from the surface where they are only partially buried in a desert pavement.

Rare stones are completely surrounded by fusion crust, but most samples have partial fusion crusts and fractured faces. The fusion crust is variably preserved. Sometimes it is still vividly black, but in other cases it is patchy and/or has turned a rusty red color. Rusty halos around metal grains exposed in the fractured surfaces are also visible in hand specimens. Samples recovered from the desert pavement are sometimes coated with desert varnish.

In thin-section, the silicate phases are stained red and the metal-sulfide assemblages are being converted to oxides. The weathering state of the meteorite is typically W2 to W3 [3], although it varies from W1 to W4 in the strewn field. This is probably a function of where each stone landed. Some samples are on mountain slopes, while others are in drainage systems. The nature of the soil and depth of burial also vary.

Current Environment: The original two samples of the meteorite were found adjacent to White Elephant Wash which drains the White Hills (up to 1577 m high), Senator Mountain (1563 m), and Golden Rule Peak (1177 m). This is a dry wash that only runs after rare storms. Total annual precipitation has not been

measured in the area, but it is probably about 5 inches, supporting only sparse Joshua trees (*Yucca brevifolia*) and desert scrub. White Elephant Wash drains into the Hualapai Wash (also dry), which, in the vicinity of the strewn field, leads north to the Colorado River (now Lake Mead) and south to a closed basin with the Red Lake playa. The conjunction of the White Elephant and Hualapai washes is at an elevation of about 730 m. The strewn field is immediately west of the Colorado Plateau.

These washes intermittently produce new sand and gravel deposits, but are also dissecting poorly consolidated fanglomerates of Quaternary age. The Quaternary sediments in the area also include older sands and gravels, talus, colluvium, and landslide deposits [4]. Almost all samples have been found above the washes in what look like thin modern soils on top of the Quaternary sediments and an Early Proterozoic gneiss. However, meteorites have also been found directly on bedrock and in sediments or soils covering the Tertiary Hualapai Limestone Member of the Muddy Creek Formation, an Early Proterozoic porphyritic monzogranite, and an Early Proterozoic leucogranite complex. The locations of the samples, particularly those on bedrock, indicate they have not been significantly transported after impact.

Age of Fall: To determine how long the samples were exposed to weathering processes, we used a combination of ¹⁴C and ¹⁰Be techniques [see 5] to measure the age of the fall. A total of 13 samples were analyzed. Twelve of these samples are consistent with a terrestrial age of 14.3 ± 0.8 ka. One sample appears to be a recent fall. The 14 ka age is not an unusually old one for meteorites recovered from hot deserts. Roosevelt County meteorites from neighboring New Mexico, for example, have ages ranging from 7 to >46 ka [e.g., 6].

Extent of Oxidation: Nine samples were examined using Mossbauer spectroscopy to determine how much of the iron has been oxidized to Fe³⁺ and the relative proportions of the paramagnetic component (mostly akaganeite) and the magnetically ordered component (mostly magnetite and maghemite). The oxidation ranges from 25.6 to 42.0% and has an average of 33.1 ± 5.1%. The disparity is larger than that found among samples from the Nullarbor Region, but similar

to the sort of variation seen among samples from the Sahara. The ratio of paramagnetic to magnetically ordered Fe^{3+} ranges from 0.74 to 0.96. The range in oxidation and the variation in the amount of paramagnetic vs. magnetically ordered Fe^{3+} suggests either different burial or drainage conditions over the area, consistent with observations made in the field where the samples were collected. The amount of oxidation in the Gold Basin samples (30 to 35%) is less than that (40 to 45%) in samples with similar ages that were recovered in Roosevelt County, New Mexico, and more like that found in samples from the Sahara Desert and Nullarbor Region [6].

Paleoenvironmental Reconstruction: The terrestrial age of the meteorite indicates it fell during the Late Pinedale portion of the Wisconsin Glaciation, which was, in general a wetter period than today which caused, in turn, a shift in the distribution of vegetation in the region. Caves near the Gold Basin strewn field contain plant pollen and macrofossils in packrat middens and sloth dung that can be used to evaluate the extent of these effects, including Rampart Cave (535 m elevation; from 10.05 ± 0.35 to 14.81 ± 0.22 ka), Muav Cave (similar to Rampart), and Gypsum Cave (610 m elevation; from 8.5 to 11.7 ka) [7,8]. Despite the wetter conditions implied, however, data from these sites suggest they may not have been sufficiently different to have replaced Joshua trees with woodland species in the Gold Basin area (730 m) at the time of the fall.

Isotopic measurements of the ground water reservoir in the Black Mesa basin on the nearby Colorado Plateau also suggest wetter conditions [9]. Peak recharge in the basin appears to have been 14 to 17 ka, near the time of the Gold Basin fall. These recharge rates are 2 to 3 times higher than present rates, when temperatures are estimated to have been 5 to 6 °C cooler. These conditions successfully supported a much different animal population than that seen today, and probably included camels (*Camelops hesternus*), bison (*Bison bison*), mastodons (*Mammuthus americanus*), Harlan's ground sloth (*Glossotherium harlani*), and mammoths (*Mammuthus columbi*) (see [10] and references therein). These animals may have also co-existed with a human population, because there is definite evidence of early humans in this part of the world at least 13 ka. Consequently, the Gold Basin event may have been a witnessed fall. Most of the Late Pleistocene megafauna became extinct about 11 ka, either due to the climate changes, overhunting, or a combination of these and other factors. At that same time, recharge in the Black Mesa basin began to decrease precipitously until it reached a value that was

only 50% of the present one about 5 ka when temperatures were 2 to 4 °C warmer than today [9]. Consequently, it appears that the Gold Basin samples first experienced wetter conditions than those seen today, then encountered a drier period, and finally a slight increase in moisture in modern times. Based on analyses of the weathering of the Holbrook meteorite [11], which fell in Arizona in 1912, the bulk of the weathering of Gold Basin samples may have occurred within the first 500 yrs after they fell, a process that may have been enhanced by exposure to the wettest conditions seen by the meteorite since it fell.

References: [1] Kring D.A., Jull A.J.T., McHargue L.R., Hill D.H., Cloudt S., and Klandrud S. (1998) Gold Basin meteorite strewn field: The "fossil" remnants of an asteroid that catastrophically fragmented in Earth's atmosphere. *Lunar Planet. Sci. XXIX*, Abstract #1526, Lunar and Planetary Institute, Houston (CD-ROM). [2] Krieger J. (1999) personal communication. [3] Wlotzka F. (1993) A weathering grade scale for the ordinary chondrites. *Meteoritics* **28**, 460. [4] Theodore T.G., Blair W.N., and Nash J.T. (1987) Geology and Gold Mineralization of the Gold Basin-Lost Basin Mining Districts, Mohave County, Arizona. *U.S. Geol. Surv. Prof. Pap.* **1361**, 167 p. [5] Jull A.J.T., Bland P.A., Klandrud S.E., McHargue L.R., Bevan A.W.R., Kring D.A., and Wlotzka F. (1999) Using ^{14}C and ^{10}Be for terrestrial ages of desert meteorites. This volume. [6] Bland P.A., Sexton A.S., Jull A.J.T., Bevan A.W.R., Berry F.J., Thornley D.M., Astin T.R., Britt D.T., and Pillinger C.T. (1998) Climate and rock weathering: A study of terrestrial age dated ordinary chondritic meteorites from hot desert regions. *Geochim. Cosmochim. Acta* **62**, 3169-3184. [7] Wells P.V. and Berger R. (1967) Late Pleistocene History of Coniferous Woodland in the Mohave Desert. *Science* **155**, 1640-1647. [8] Van Devender T.R. and Spaulding W.G. (1979) Development of vegetation and climate in the southwestern United States. *Science* **204**, 701-710. [9] Zhu C., Waddell R.K. Jr., Star I., and Ostrander M. (1998) Responses of ground water in the Black Mesa basin, northeastern Arizona, to paleoclimatic changes during the late Pleistocene and Holocene. *Geology* **26**, 127-130. [10] Kring D.A. (1997) Air blast produced by the Meteor Crater impact event and a reconstruction of the affected environment. *Meteoritics Planet. Sci.* **32**, 517-530. [11] Bland P.A., Berry F.J., and Pillinger C.T. (1998) Rapid weathering in Holbrook: An iron-57 Mossbauer spectroscopy study. *Meteoritics Planet. Sci.* **33**, 127-129.

THERMALLY MOBILE TRACE ELEMENTS IN CARBONACEOUS CHONDRITES FROM COLD AND HOT DESERTS. M.E. Lipschutz, Department of Chemistry, Purdue University, W. Lafayette, IN USA 47907-1393.

Introduction: Some decades ago, Anders and co-workers [1, 2] used RNAA to classify a number of trace elements as being volatile during nebular condensation and accretion into primitive objects based upon their strong depletion in (equilibrated) ordinary chondrites relative to C1 chondrites. Such elements, e.g. Ag, Bi, Cd, Cs, In, Se, Te, Tl, Zn and others, exhibit nearly constant, C1-normalized atomic abundances in C2 (CM2) and in C3 chondrites. They interpreted the near-constancy of these abundances according to a 2-component model in which volatiles were introduced into carbonaceous (and other) chondrites as C1 material which was diluted with differing proportions of high-temperature (i.e. volatile-free) components. In this view, mean volatile element abundances of 0.48 in C2 and 0.24-0.29 x C1 in C3 chondrites indicated that C2 and C3 chondrites are, respectively, about 1:1 and 1:2-3 mixtures of C1-like and high temperature materials [1, 2]. More recently, Xiao and Lipschutz [3] found that C1-normalized abundances of such volatile elements are nearly constant in most C2-6 chondrites (i.e. 25 non-Antarctic meteorites, nearly all falls, and 36 Antarctic finds) consistent with a 2-component mixing model. However, rather than being quantized, mean volatile element contents in each chondrite define a continuum from 0.92-0.14 x C1 for these 61 chondrites [3].

A few carbonaceous chondrites - the first having been the NIPR consortium samples B-7904, Y-82162 and Y-86720 - show an altered pattern: many of the volatile elements in each exhibit the usual constancy of C1-normalized atomic abundances, but modified by further depletion of Cd and other elements like Tl and Bi [4, 5]. These are the most mobile trace elements, i.e. those most readily vaporized and lost from primitive meteorites during week-long heating at $\geq 400^\circ\text{C}$ under low ambient pressures (initially 10^{-5} atm H_2), simulating metamorphic conditions in a primitive parent body [6]. Similarities between mobile element data for B-7904, Y-82162 and Y-86720 [4, 5] with those for Murchison heated at $500\text{-}700^\circ\text{C}$ [7], suggest that these Antarctic C1- and C2-like chondrites were metamorphosed at temperatures like these in the interiors of their parent bodies. Metamorphic temperatures inferred from RNAA data and textural/mineralogic alterations are internally consistent, agreeing with those evident in heated Murchison samples [8]. These 3 chondrites were also heated late in their histories since all have lost cosmogenic ^3He , presumably during close solar approach, and B-7904 and Y-86720 seem also to have lost substantial proportions of radiogenic ^4He and ^{40}Ar , cf. data in [9].

Similarities in spectral reflectance data for C-, G-, B- and F- asteroids, for these meteorites and for heated Murchison samples suggest that thermally metamorphosed interior materials in these asteroids were excavated by impacts and re-deposited on them, forming their present surfaces [10-12]. Establishment of the thermal metamorphic histories of carbonaceous chondrites, then, is essential to establishing the evolution and present-day nature of C-type and related asteroids.

Current Status: In the light of these and other data for B-7904, Y-82162 and Y-86720, we have re-examined older results [3] and have been quantifying mobile trace elements in additional carbonaceous chondrites (including the first few Hot Desert samples) exhibiting characteristics conceivably of metamorphic origin.

Wang and Lipschutz [13] considered RNAA data for 17 C2-C3 chondrites from Antarctica and found that nearly half (4C2, 3CO3 and a CV3) exhibited loss of Cd, at least,

during parent body metamorphism. An additional CM2 chondrite, Y-793321, exhibited petrographic and other evidence for mild thermal metamorphism but no trace element loss, suggesting milder heating at lower temperatures [8]. More recently, we quantified mobile trace elements in an additional 15 C2-3, with 5 more in progress. The compositional data suggest that at least 3 of the 15 have been metamorphosed.

Thermally metamorphosed C2-3 chondrites identified thus far, and estimated alteration temperatures are: Y-793321(CM2) \leq 500°C \leq EET 90043(C2) \leq ALH A81003(CV3) \sim A-881655(CM2) \leq ALH 85003(CO3) \sim Y-82054(CM2) \sim LEW 85332(CO3) \sim Y-790992(CO3) \sim Y-793495(CR2) $<$ PCA 91008(C2) $<$ Acfer 082(CV3) $<$ B-7904(CM2) \sim Y-82162(CI) $<$ Y-86720/Y-86789(CM2) pair \leq 700°C $<$ EET 96010(CV3) \leq 900°C. Confirmatory petrographic and other studies are needed for many of these. Newly measured C2-3 chondrites that exhibit no obvious trace element losses are: Y-791198(CM2); Y-794080(CM2); Y-81020(CO3); Y-82098(CM2); Y-86695(CM2); A-881334(CM2); MAC 88100(CM2); LEW 90500(C2); PCA 91084(C2); WIS 91600(C2); GRO 95645(C2); EET 96007(C2); EET 96016(C2); EET 96018(C2); Nova 002(CV3).

At present, we have data for mobile trace elements in 86 carbonaceous chondrites; 22 non-Desert, mainly falls, 2 from Hot Deserts and 62 from Antarctica (46 from Victoria Land and 16 from Queen Maud Land). Fourteen (one Hot Desert meteorite, 6 from Victoria Land and 7 from Queen Maud Land - including the Y-86720/Y-86789 pair as a single meteorite) have lost one or more mobile trace elements during open-system metamorphism in their parent bodies. A fifteenth, from Queen Maud Land, was apparently metamorphosed under conditions in which mobile elements were not lost. These samples derive from at least 5 separate bodies/regions, the parents of the CI, CM, CR, CO and CV chondrites.

It is curious that all thermally metamorphosed carbonaceous chondrites are from deserts, mainly Antarctica, and none is a fall. Can this quirk reflect a time-dependent variation in carbonaceous chondrite sources to near-Earth space, with the contemporary population sampling only unmetamorphosed parent regions?

Acknowledgements: This research was sponsored by NASA grant, NAGW-3396 with aid for neutron irradiations at the University of Missouri Research Reactor by DOE grant DE-FG02-95NE38135.

References: [1] Wolf R., Richter G., Woodrow A.B. and Anders E. (1980) *Geochim. Cosmochim. Acta*, 44, 711-717. [2] Takahashi H., Gros J., Higuchi H., Morgan J.W. and Anders E. (1978) *Geochim. Cosmochim. Acta*, 42, 97-106. [3] Xiao X. and Lipschutz M.E. (1992) *J. Geophys. Res.*, 97, 10197-10211. [4] Paul R.L. and Lipschutz M.E. (1989) *Z. Naturf.*, 44a, 979-987. [5] Paul R.L. and Lipschutz M.E. (1990) *Proc. NIPR Symp. Antarctic Meteorites*, 3, 80-95. [6] Ikramuddin M. and Lipschutz M.E. (1975) *Geochim. Cosmochim. Acta*, 39, 363-375. [7] Matza S.D. and Lipschutz M.E. (1977) *Proc. Eighth Lunar Sci. Conf.*, 1, 161-176. [8] Lipschutz M.E., Zolensky M.E. and Bell M.S. (1999) *Antarctic Meteorite Res.*, 12, 57-80. [9] Schultz L. and Franke L. (1998) *Helium, Neon and Argon in Meteorites: A Data Compilation*, MPI-Chemie Rept.. [10] Hiroi T., Pieters C.M., Zolensky M.E. and Lipschutz M.E. (1993) *Science*, 261, 1016-1018. [11] Hiroi T., Pieters C.M., Zolensky M.E. and Lipschutz M.E. (1994) *Proc. NIPR Symp. Antarctic Meteorites*, 7, 230-243. [12] Hiroi T., Pieters C.M., Zolensky M.E. and Lipschutz M.E. (1996) *Meteoritics Planet. Sci.*, 31, 321-327. [13] Wang M.-S. and Lipschutz M.E. (1998) *Meteoritics Planet. Sci.*, 33, 1297-1302.

Historical Notes on Three Exceptional Iron Meteorites of Southern Africa: the Cape of Good Hope, Gibeon, and Hoba. Ursula B. Marvin, Harvard-Smithsonian Center for Astrophysics, 60 Garden St., Cambridge, MA 02138, USA. E-mail: Marvin@CfA.Harvard.edu

Africa, is among the richest of continents in meteorites from hot deserts. Namibia is the site of the world's largest individual meteorite, the 60-ton Hoba Ni-rich ataxite, and the largest known meteorite strewn field, that of the Gibeon fine octahedrite. In Egypt, history goes back at least as far as ~1340 B.C when an iron dagger with a small content of nickel was placed in the tomb of King Tutankhamen. History also comes up-to-date in northern Africa with recoveries in recent years of thousands of meteorites in the reaches of the Sahara from Libya to Mauretania. This paper will review the histories of three exceptional meteorites from southern Africa.

The Cape of Good Hope Iron

The earliest meteorite discovered in southern Africa was the 135-kg Cape of Good Hope iron, found by a farmer in the Dutch Cape Colony sometime before 1793 [1]. It lay on an open plain west of mouth of the Great Fish River, nearly 700 km east of the geographic Cape of Good Hope. Meteorites were not recognized as such at that time so the farmer assumed it was part of a discarded anchor and forged hoes and plowshares from the metal. At the turn of the 19th century, a soldier-adventurer, Carl Sternberg, acquired the mass and transported it to Cape Town--much to the subsequent regret of the farmer's family who had lost their source of metal [2a]. At Cape Town, the iron was cut into two pieces, the larger of which, weighing 84-kg, was acquired on behalf of the Dutch government and carried to London in 1803 by Colonel Prehn, governor of the Cape Colony (for whom the mineral prehnite is named). From there it was sent to Haarlem.

Meteoritics emerged as a new science during the decade 1793-1803 due to the writings of E. F. F. Chladni in Germany, the occurrence of five witnessed falls, and chemical analyses of fallen stones and irons by E. C. Howard and J.-L. de Bournon in London [3]. Thus, in 1803, the mass in Haarlem was identified as meteoritic by its Ni content. The remaining 50-kg portion of the Cape of Good Hope iron was shipped to London in 1806 where an analysis requested by Sir Joseph Banks, president of the Royal Society, yielded 10% Ni.

This metal took a high polish and could be rolled into sheets thinner than paper. In 1814 the naturalist-mineralogist James Sowerby, who had acquired the mass in London, had a slice hammered at low red heat into a 2-foot curved sword blade. Sowerby sent this sword to Czar Alexander I in appreciation of Russia's stand against Napoleon [4]. (The Czar responded by sending Sowerby a superb emerald ring set with diamonds.) In 1937, an attempt to find Alexander's sword in Russia failed utterly.

Today, the iron is classed as a nickel-rich ataxite containing ~16.3 % Ni. The largest specimen is a 66-kg remnant of the portion originally sent to Haarlem, now in the National Museum at Budapest. A few scraps of Sowerby's forged metal and other small samples are in the British Museum, and ~3.5 kg of pieces are distributed among twenty or so other institutions. Ironically, the South African Museum in Cape Town possesses only one small (55-g) fragment. The historic Cape of Good Hope iron is of special interest for the precedence of its find in southern Africa and its role in an international exchange of gifts between a private individual and a Czar.

The Gibeon Shower of Iron Meteorites

Small samples of iron were acquired by Captain James E. Alexander during his exploration of Great Namaqualand (Namibia) in 1836-1837. He also heard that large masses of iron, up to two feet square, were scattered in the Namib desert about three days journey northeast of the mission at Bethany [5]. Although he did not visit the area, he inscribed "Much Iron" at that site on his map. In Cape Town John F. W. Herschel analyzed 4.6% Ni in one of Alexander's samples and speculated that the irons had fallen in a shower.

The first large iron from the region to reach Cape Town was the 81-kg Lion River mass, collected by a Mr. John Gibbs who carried it by wagon a distance of nearly 800 miles over the worst possible roads [6]. From there, it was shipped to London and purchased on behalf of Professor Charles U. Shepard, curator of meteorites at Amherst College in Massachusetts. Shepard analyzed 6.7% Ni in the metal and described its Widmanstätten figures. He noted that portions of the metal had been hammered off the mass by the Nama peoples who used it for tools and weapons. This was common throughout Namaqualand in contrast to the regions farther south, where the Bantu peoples showed a reverence for meteorites and used them for magic and medicine but not for practical purposes. Possibly the Bantu had seen irons fall from the sky but the Nama had not [7].

By 1910, at least ten irons from the Namib Desert, with a total weight of ~2300 kg, had been shipped to Europe from Cape Town. Coming from widely separated locations; each iron was named for the farm or settlement where it had been found. The heaviest concentration of them occurred a short distance east of the village of Gibeon, which eventually became the locality name

for all the irons once they were fully recognized as shower fragments.

From 1911 to 1913, Dr. Paul Range, the official geologist of German Southwest Africa, collected all the irons he could find, mapped their locations, and sent them to Windhoek, where they were placed in a large pile in the public garden [8]. The original pile consisted of 37 specimens with a total weight of ~12.6 tons. By 1967, several of the specimens had been donated to museums. These included the largest Gibeon iron then known, a 650-kg specimen that went to the South African Museum at Cape Town. The smallest Gibeon specimen recorded up to 1941 was a thin 195-gram individual, 8 cm long, given in 1929 to Leonard J. Spencer of the British Museum by the station master at Gibeon [9].

This size range was puzzling because it lacked the large numbers of small specimens common in strewn fields. A suggestion that most of the small specimens were collected and used by the native peoples seemed unlikely given the sparse population of the region. It now appears that to some extent the large specimens tended to draw attention away from tiny ones. Still under debate are hypotheses that the Gibeon parent body was a stony-iron with a friable matrix that has been dispersed, or was a polycrystalline mass of metal that broke up mainly along grain boundaries of large taenite crystals of which many specimens are composed.

The map prepared by Dr. Range showed that nearly every iron in his survey had been found in place, partially embedded in the Carboniferous Karroo formation or the Tertiary Kalahari chalk. Buchwald [2b] calculated that the Gibeon meteorites fell over an immense elliptical area with a 275-km main axis, trending N35°W, and a short axis of at least 100 km. This is by far the largest meteorite strewn field in the world. As is observed in the vicinity of many

strewn fields, two irons, Bushman Land and Karasburg, proved to be separate falls [2c]. Calculations suggest that a broad, chunky metallic body, measuring about 4 x 4 x 1.5 meters, entered the atmosphere along a N35°W trajectory at a low angle of 10 to 20° from the horizon. While still high in the atmosphere it broke up with such violence that it caused severe thermal alteration, faulting, overfolding, and necking of some (although not all) of the fragments. The well-developed remaglypts on many specimens show that these fragments had a long flight through the atmosphere before entirely losing their cosmic velocity [2c].

The variety of thermal and shock-induced microstructures found in Gibeon specimens is unmatched in any other meteorite except the Canyon Diablo iron of northern Arizona. Canyon Diablo was a crater-forming impact; Gibeon was not. The Brukkaros crater, which lies in the midst of the Gibeon strewn field, was long held suspect as a possible impact feature. However, Brukkaros is not a rimmed bowl excavated in the plain like a typical impact crater. It is 2.1 km in diameter, with a flat floor lying 91 m above the plain and a rim rising to 548 m. In 1974 after an exhaustive study, Ferguson *et al.* declared the crater to be an ancient kimberlite-carbonatite volcano [10].

By 1967, 81 Gibeon irons, totaling nearly 22 tons, had been recorded from the strewn field. Even so, it seemed likely that many more remained to be found. However, that year, by government decree, the native reserves were extended, white properties expropriated, and local knowledge of find sites was lost as farmers left the territory. Gibeon specimens became scarce and difficult to come by. Then, suddenly, about 1994, specimens of Gibeon began appearing for sale at rock and mineral shows. Norton [11] ascribed this new development to the efforts of a young meteorite collector-dealer

who visited a school in Gibeon, displayed a few small chunks of Canyon Diablo, and offered a reward for any similar specimens brought to him. Whole families joined the search, and within a few weeks 30 fragments had been recovered, including a specimen weighing one metric ton--the largest Gibeon iron found to date. Since that time, collectors have searched the desert with metal detectors and had much success with finding meteorites, including many of the small ones that previously seemed to be missing.

In addition to typical iron fragments, this effort has recovered a few rare, tetrahedral and octahedral crystals of metal described in 1997 by Dietrich and König [12]. These authors suggest that the crystals result from the successive splitting-off of thin kamacite lamellae due to the selective corrosion of intervening taenite layers. Alternatively, corrosion may be destroying thin bands of fine-grained plessite rather than the Ni-rich taenite itself [13]. Today, the pile of irons at Windhoek has been disassembled and the irons mounted on pillars of different heights arranged to give the impression of a group of falling bodies.

The Hoba Iron Meteorite

Much of arid Namibia is so remote that this isolated mass of iron, weighing ~60 metric tons, remained undiscovered until 1920. It lies in the north-central part of the country 20 km west of the village of Grootfontein--listed as its find site--and 45 km southeast of the mining district of Tsumeb. When found, the meteorite was embedded in soft, white, porous limestone that overlies granitic bedrock [14]. Its upper surface is nearly square (2.95 x 2.84 m) and flush with the surrounding plain. A trench dug all the way around it in the 1920s revealed that the bottom surface slopes

downward from about 65 cm at one end to 115 cm at the other.

The meteorite is a Ni-rich ataxite averaging ~16.5% Ni and 0.75% Co. A rind of dark brown iron oxide shale, 30-cm thick, covered the sides and bottom of the meteorite. Analyses made in 1932 showed that the metal and the rind contained similar values of Fe, Ni, and Co, indicating that the oxidation proceeded *in situ* without significant leaching away of components [14]. However, in 1995, Golden *et al.* [15], showed that although the Co has remained immobile in the oxide small percentages of Ni have migrated into the adjacent limestone.

Before oxidation, the meteorite would have weighed about 88 metric tons. Few meteorites weighing one ton or more survive impact with the Earth in one piece. Of the three largest known iron meteorites, only Hoba landed as a single body: the 33.4-ton El Chaco iron at Campo del Cielo, Argentina, is one of hundreds of shower fragments, including ten that weigh more than 300 kg apiece; and the 31-ton Ahnighito from Cape York, Greenland, is one of eight irons totaling 58 tons.

Hoba, which struck the Earth weighing ~88 tons, made no sign of a crater or of any shock damage to the bedrock. It's survival as a single, unshocked mass suggests that it entered the atmosphere on a long trajectory at a sufficiently low velocity to allow a soft landing. In 1986, McCorkell *et al.* measured a significantly high content of ^{59}Ni in the metal, assumed that this represented less than one half-life of the isotope, and concluded that the meteorite fell no more than 80,000 years ago [16]. They hypothesized that the mass landed on granitic bedrock and subsequently, during a period of moist climate, was covered by a lake of stagnant water, rich in calcium carbonate, that slowly evaporated, leaving

the mass covered, or nearly so, with surficial limestone.

Early ideas of recovering nickel from Hoba were soon abandoned. However, in 1954, Dr. Brian Mason, then curator of minerals at the American Museum of Natural History in New York, visited the Hoba farm and discussed with the owner the possibility of purchasing the mass to add to the Museum's two other huge iron meteorites—Cape York from Greenland and Willamette from Oregon. The owner was agreeable to a sale. A railroad through Grootfontein and Tsumeb passes within 7 km of the Hoba farm, and Mason had ascertained that the Tsumeb Corporation possessed heavy equipment capable of moving the meteorite to the nearest railhead. But the railroad gauge was only 2 feet, with an axle loading capacity of 4 tons—hardly adequate for transporting a 60-ton mass of nickel-iron [17]. So the Hoba meteorite remains where it landed. Most of the oxide coating has been chipped off the sides, but only a few samples of metal have been removed by means of either an oxyacetylene torch or closely-spaced drill holes. In 1955 the government of Namibia declared Hoba to be a national monument. More recently, a small park with a stone amphitheater has been created around this remarkable iron meteorite.

Africa's Record of Impacts

In addition to these three and many other meteorites, Africa possesses special features including: the strewn field of Ivory Coast tektites and microtektites that were splashed out of the Bostmtwi Crater in Ghana one million years ago; the enigmatic chunks of 29-million year-old Libyan Desert Glass, with no known source crater, scattered over 6,500 km² of the Great Sand Sea of western Egypt; and 15 or more impact features, including the Vredefort dome of South

Africa, the oldest (*ca* 2023 Ma), most deeply eroded (8-11 km) and possibly the largest impact structure in the world, with an estimated original diameter of 250-300 km [18]. Africa preserves a long record of the Earth's encounters with bodies from space.

References: [1] Barrow, J. (1801) *Travels into the Interior of Southern Africa*. I. T. Cadell and W. Davies, London. [2] Buchwald, V. F. (1975) *Handbook of Iron Meteorites*, Univ. Calif. Press, Los Angeles; [2a] Cape of Good Hope 2:407-409. [2b] Gibeon, 2:584-593. [2c] Gibeon, 3:1385-1393. [3] Marvin, U. B. (1996) *Meteoritics & Planet. Sci.* **31**:545:588. [4] Anonymous (1820) *Phil. Mag.* **55**:49-52. [5] Alexander, J. E. (1838) *Jour. Roy. Geog. Soc.* **8**:1-38. [6] Shepard, C. U. (1853). *Amer. Jour. Sci.*, 2nd Series, **XV**:1-4. [7] Frick, C. and Hammerbeck, E. C. I. (1973) *Bull. 57, Dept. of Mines, Geol. Survey of S. Africa*. [8] Range, P. (1913) *Mitteil. Deutsch. Schutzgebieten* **26**:341-343. [9] Spencer, L. J. (1941) *Min. Mag.* **XXVI**:19-35. [10] Ferguson, J., Martin, H., Nicolaysen, L. O.

and Danchin, R. V. (1974) *Proc. Internat. Kimberlite Conf.*, Cape Town, Pergamon Press, 265-280. [11] Norton, O. R. (1998) *Rocks from Space*. Mountain Press Publishing Co. Missoula, Montana. [12] Dietrich, R. and König, S. (1997) *Meteorite!* **3**:28-29. [13] Petaev, M. (1999) Personal communication. [14] Spencer, L. J. (1932) *Min. Mag.* **XXIII**:1-19. [15] Golden, D. C., Ming, D. W. and Zolensky, M. E. (1995) *Meteoritics* **30**:418-422. [16] McCorkell, R. H., Fireman, E. L., and D'Amico, J. [17] Mason, B. (1966) *Meteorite!* **2**:8-11. [18] Gibson, R. L. and Reimold, W. U. (1999) *Field Excursion Through the Vredefort Structure*, Dept. Geology, Univ. of the Witwatersrand, Johannesburg, S. Africa.

SAHARAN METEORITES WITH SHORT OR COMPLEX EXPOSURE HISTORIES. S. Merchel¹, M. Altmaier², T. Faestermann³, U. Herpers², K. Knie³, G. Korschinek³, P.W. Kubik⁴, S. Neumann⁵, R. Michel⁵ and M. Suter⁶, ¹Max-Planck-Institut für Chemie, D-55020 Mainz, Germany, merchel@mpch-mainz.mpg.de; ²Abteilung Nuklearchemie, Universität zu Köln, Otto-Fischer-Str. 12-14, D-50674 Köln, Germany; ³Fakultät für Physik, Technische Universität München, D-85748 Garching, Germany; ⁴Paul Scherrer Institut, c/o ETH Höggerberg, CH-8093 Zürich, Switzerland; ⁵Zentrum für Strahlenschutz und Radioökologie, Universität Hannover, D-30167 Hannover, Germany; ⁶Institut für Teilchenphysik, ETH Höggerberg, CH-8093 Zürich, Switzerland.

Introduction:

Long-lived radionuclides produced by cosmic rays in meteorites provide information that can be used to determine, on the one hand, the spectral distribution and the constancy of the cosmic ray flux and, on the other hand, to study the exposure history of the meteorites themselves.

During the last four years we investigated a set of nearly one hundred meteorite samples with respect to cosmogenic radionuclides [e.g. 1]. Among them we found five meteorites from the Algerian and Libyan Sahara containing rather low radionuclide concentrations (see Table 1). To find out whether those reflect a short or a complex exposure time as meteoroids or “unusual” shielding conditions of the analysed sample, we decided to look at stable cosmogenic nuclides, too. Comparing the complete set of data to theoretical model calculations [2] offers the possibility to reveal the meteorite histories.

Analytical techniques:

Cosmogenic radionuclide concentrations were determined with the highly sensitive technique of accelerator mass spectrometry (AMS), and additionally, for some meteorites in the case of ²⁶Al, via $\gamma\gamma$ -coincidence-counting [3]. The radiochemical separation method used for preparing the AMS targets is described in detail elsewhere [1,4]. Beryllium-10 and ²⁶Al were measured at the PSI/ETH 6 MV tandem accelerator facility at Zurich (e.g. [5]), whereas ⁵³Mn measurements were performed at the 14 MV tandem at Munich [6]. For the conversion of measured radionuclide ratios in activities, we used the following half-lives: ¹⁰Be ($t_{1/2} = 1.51$ Ma), ²⁶Al ($t_{1/2} = 0.705$ Ma), and ⁵³Mn ($t_{1/2} = 3.7$ Ma). Additionally, an aliquot was taken from each sample to determine the cosmophysically relevant main target elements (Al, Ca, Fe, Mg, Mn, and Ni) via ICP-OES (inductively coupled plasma optical emission spectroscopic) analysis.

Results:

Table 1 contains the calculated radionuclide activities which are based on the bulk composition data obtained by ICP-OES analysis of Al and Fe and the AMS measured radioactive/stable-ratios by AMS. The ²⁶Al results

determined via non-destructive $\gamma\gamma$ -counting are also given. Furthermore, a selection of noble gas data is shown, too. The latter data are those which are mainly used in the discussion of the meteorite histories.

Tab. 1: Cosmogenic nuclide data of stony meteorites

| | A287 | DG055 | HH056 | HH064 | HH096 |
|--|---|------------------------------------|------------------------------------|---|------------------------------------|
| class | E4 | C(K)3 | LL6 | AUR | LL(L)3 |
| ¹⁰ Be [dpm/kg] | 11.5 ± 0.4 | 5.0 ± 0.2 | 9.3 ± 0.4 | 9.5 ± 0.4 | 13.3 ± 0.5 |
| ²⁶ Al (AMS) [dpm/kg] | 34.4 ± 1.9 | 28.6 ± 1.8 | 39.3 ± 2.0 | 36.5 ± 3.6 | 48.1 ± 3.5 |
| ²⁶ Al ($\gamma\gamma$) [dpm/kg] | 40.7 ± 2.0 | 28.9 ± 1.4 | | 28.5 ± 1.5 | 51.6 ± 2.6 |
| ⁵³ Mn [dpm/kg Fe] | 82 ± 24 | 90 ± 33 | | | |
| t_{rad} [Ma] | 17.0 (t_3) ^[7] 20.0 (t_{21}) ^[7] 3.0 (t_{38}) ^[7] | 6.3 (t_{21}) ^[8] | 2.2 (t_{21}) ^[9] | 1.5 (t_3) ^[10] 1.3 (t_{21}) ^[10] | 6.2 (t_{21}) ^[9] |
| (²² Ne/ ²¹ Ne) _c | 1.238 ^[7] | 1.081 ^[8] | 1.063 ^[9] | 1.205 ^[10] | 1.094 ^[9] |

Discussion:

We performed model calculations for production rates of ¹⁰Be, ²¹Ne, ²²Ne, ²⁶Al, and ⁵³Mn as described by Michel *et al.* [2] which are based on a mean chemical composition of the meteorite’s class partially amended by the elemental abundances of Al, Ca, Fe, Mg, Mn, and Ni of the individual sample. For the discussion of meteorite histories, one should keep in mind that calculated production rates of ¹⁰Be (for meteoroid radii ≥ 15 cm) are about 10 % lower than experimental ones. This underestimation, as recently mentioned in [1], can be related to uncertainties in standardisation, on the one hand, and the scarcity of abundance data of the main target element oxygen, on the other.

Furthermore, we observed discrepancies of about 10 % in the ²⁶Al experimental data in other meteorite samples [1]. Until solving this problem in an interlaboratory comparison, which is in preparation, we should take this also into account.

Acfer 287. In contrast to the ^{21}Ne and ^3He irradiation age of 20 Ma and 17 Ma, respectively, all three radionuclide activities measured in this sample of the enstatite chondrite seems to be undersaturated. Since a ^{14}C measurement [11] excludes a long terrestrial age ($t_{\text{terr}} = 2.9$ ka), there is one general explanation for this discrepancy: a complex exposure history. As shown in Fig. 1, which is the result of an iterative procedure, the radionuclides consistently recorded a second irradiation stage of (2.9 ± 0.5) Ma duration. The sample investigated was located in a rather unshielded position of a small meteoroid with a maximum radius of 15 cm. The described shielding conditions are also consistent with the high ratio of cosmogenic $^{22}\text{Ne}/^{21}\text{Ne}$. During the first stage the sample must have been irradiated for a long time in a rather shielded position to accumulate the measured ^{21}Ne and ^3He excesses, but this would simultaneously produce a very low cosmogenic $^{22}\text{Ne}/^{21}\text{Ne}$ which would overlay the ratio build up in the much shorter second stage. For that reason and due to the interesting fact that the irradiation age determined from ^{38}Ar concentrations is about the same as the one for the “second stage” deduced from radionuclides, one might also think about a simple irradiation history of *Acfer 287* and mechanisms (maybe SCR induced nuclear reactions) producing additional amounts of the lighter noble gas isotopes ^3He and ^{21}Ne [12].

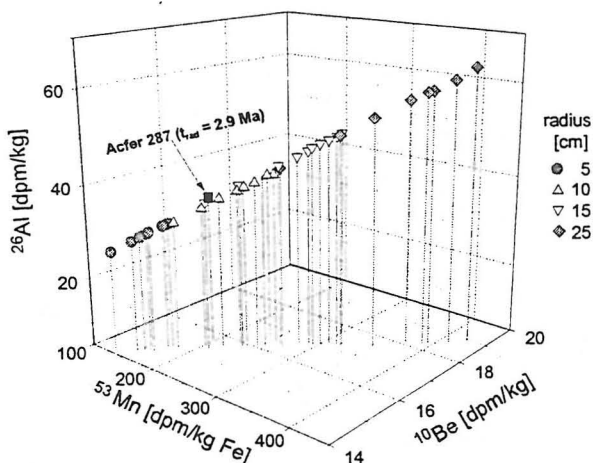


Fig. 1: Theoretical depth- and size-dependent production rates and experimental contents of ^{10}Be , ^{26}Al (AMS), and ^{53}Mn , corrected for an irradiation age of 2.9 Ma, in *Acfer 287*.

Dar al Gani 055. Based on the ^{21}Ne irradiation age of 6.3 Ma [8] of the carbonaceous chondrite *Dar al Gani 055* (DG055) the activities of ^{26}Al and ^{10}Be should be at 99.8 % and 94.5 % of saturation, respectively. We could not find any scenario, which would describe the measured radionuclide concentrations under these conditions. On the contrary the comparison of the

theoretical production rates based on target chemistry of CK/CV chondrites and elemental abundances of DG055 with experimental values requires an irradiation age in the order of 1 Ma (Fig. 2). The best agreement for radionuclide concentrations is reached by assuming an irradiation age of 1.1-1.2 Ma and a terrestrial age of 400-500 ka. We therefore suggest for DG055 a complex exposure history during its way to Earth: a “second stage” reflected by the radionuclide activities and a longer lasting “first stage” which is mainly characterised by the low cosmogenic $^{22}\text{Ne}/^{21}\text{Ne}$.

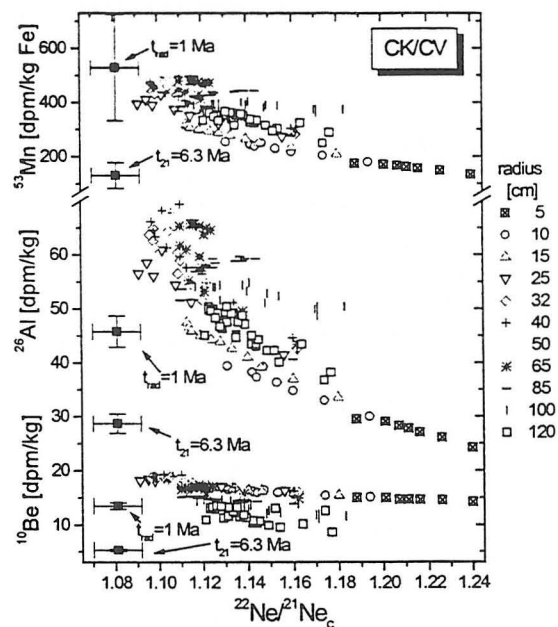


Fig. 2: Theoretical depth- and size-dependent production rates and experimental contents of ^{10}Be , ^{26}Al (AMS), and ^{53}Mn , corrected for an irradiation age of 1 Ma and 6.3 Ma, respectively. Theoretical and experimental values of the irradiation hardness parameter ($^{22}\text{Ne}/^{21}\text{Ne}$)_c are also considered.

Hammadah al Hamra 056/096. At first glance, the low activities of the radionuclides ^{10}Be and ^{26}Al measured in the ordinary chondrites of *Hammadah al Hamra 056* (HH056) and *Hammadah al Hamra 096* (HH096) also seem to be inconsistent with the ^{21}Ne ages determined by Scherer *et al.* [9]. But for these samples the very low values of the irradiation hardness parameter ($^{22}\text{Ne}/^{21}\text{Ne}$)_c hint at rather shielded positions in the meteoroids. By comparing the theoretical production rates of the radionuclides with the noble gas irradiation age corrected experimental values of HH056 and HH096 these “unusual” positions of the investigated samples inside the meteoroids are confirmed (Fig. 3). The preatmospheric radii of HH056 and HH096 were both in the range of 120 cm. But one should keep in mind that not only the model

calculations are validated with meteorites of moderate preatmospheric radii of 15-50 cm, but also the calculation of irradiation ages based on noble gas contents usually fits best for meteoroids with average radii. Therefore, the given irradiation ages should be - due to a possible overestimation of noble gas production rates - regarded as lower limits (especially in the case of HH056).

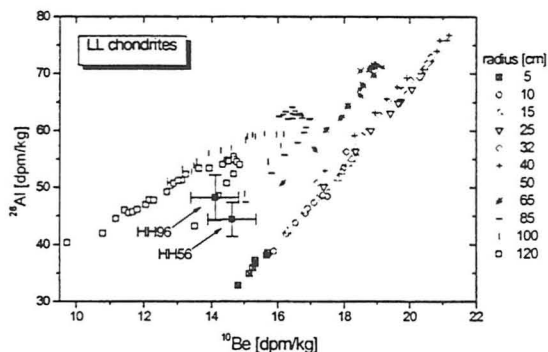


Fig. 3: Theoretical depth- and size-dependent production rates and experimental contents of ^{10}Be and ^{26}Al , corrected for an irradiation age of 2.2 Ma (HH056) and 6.2 Ma (HH096), respectively.

Hammadah al Hamra 064. Even considering the already mentioned discrepancy between ^{26}Al measured with AMS on the one hand and $\gamma\gamma$ -counting on the other, the difference of about 8 dpm/kg for the ureilite Hammadah al Hamra 064 (HH064) is rather large. Generally speaking, if the ^{26}Al concentration from an AMS measurement of a sample of size 150 mg is higher than the ^{26}Al concentration as determined by counting a sample of several grams, this could hint at a sample origin in a rather unshielded position from a small meteoroid. Some of the “AMS- ^{26}Al ” could be produced by solar cosmic ray (SCR) induced nuclear reactions. As we present here only model calculations based on nuclear reactions induced by galactic cosmic rays (GCR) we will rely on the “ $\gamma\gamma$ - ^{26}Al ” data for the further discussion. As can be seen in Fig. 4, the high value of $(^{22}\text{Ne}/^{21}\text{Ne})_c$ strengthens the suggestion for a less-shielded origin of the sample.

As also demonstrated in Figs. 4 and 5, the correction of the measured activity of ^{10}Be and ^{26}Al to saturation values - using the irradiation ages t_{21} and t_3 - results in a consistency between theoretical and experimental values. Therefore, HH064 experienced a single stage exposure of (1.4 ± 0.1) Ma. The investigated sample originated from a small meteoroid with a maximum radius of 15 cm.

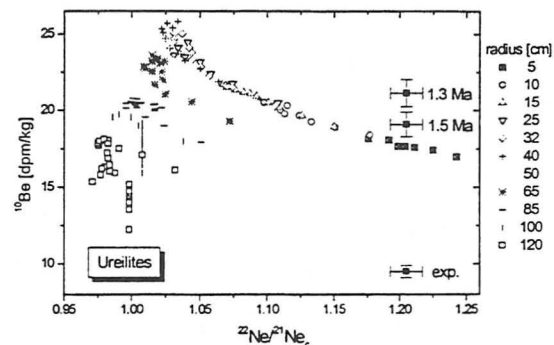


Fig. 4: Theoretical depth- and size-dependent production rates and experimental contents of ^{10}Be , uncorrected and corrected for an irradiation age of 1.3 Ma (t_{21}) and 1.5 Ma (t_3), respectively.

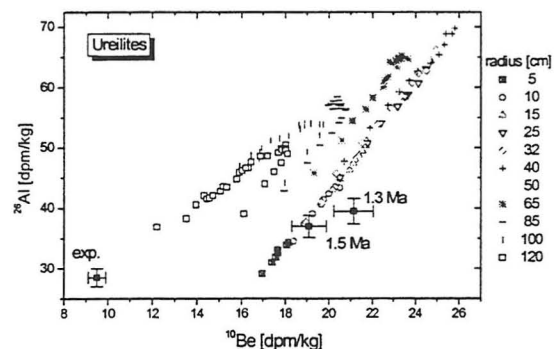


Fig. 5: Theoretical depth- and size-dependent production rates and experimental contents of ^{10}Be and ^{26}Al , uncorrected and corrected for an irradiation age of 1.3 Ma (t_{21}) and 1.5 Ma (t_3), respectively.

Conclusion:

As demonstrated, low activities of radionuclides do not necessarily reflect a short exposure time. In general, the more cosmogenic nuclides are analysed in a meteorite the more one can be sure to find the right interpretation. Complex or “unusual” histories, especially in the case of non-ordinary chondrites, can only be revealed reliably by measuring both sets of nuclides: stable and radioactive ones. Finally, only theoretical model calculations provide the tools for an adequate interpretation of the experimental cosmogenic nuclide data.

References:

- [1] Merchel S. (1998) *Ph.D. thesis, University of Cologne.*
- [2] Michel R. et al. (1996) *Nucl. Instr. Meth. Phys. Res., B113*, 434-444.
- [3] Altmaier M. (1996) *Diploma thesis, University of Cologne.*
- [4] Merchel S. and Herpers U. (1999) *Radiochim. Acta*, 84, 215-219.
- [5] Synal H.-A. et al. (1997) *Nucl. Instr. Meth. Phys. Res., B123*, 62-68.
- [6] Knie K. et al. (1997) *Nucl. Instr. Meth. Phys. Res., B123*, 128-131.
- [7] Patzer A.

(1999) *priv. com.*. [8] Scherer P. and Schultz L. *submitted to Meteoritics & Planet. Sci.*, [9] Scherer P. *et al.* (1998) *Meteoritics & Planet. Sci.*, 33, 259-265. [10] Pättsch M. (1999) *priv. com.*. [11] Wlotzka F. *et al.* (1995) *LPI Tech. Rpt. 95-02*, 72-73. [12] Schultz L. (1999) *priv. com.*.

Acknowledgment:

This study was partly supported by the Deutsche Forschungsgemeinschaft (DFG), ETH Zurich, and the Paul Scherrer Institut. Meteorite samples were kindly placed at our disposal by the Institut für Planetologie, Münster.

COSMOGENIC AND TRAPPED GAS COMPONENTS IN THE MARTIAN METEORITE DAR AL GANI 476 FROM HOT DESERT. S.V.S. Murty and R.K. Mohapatra, Physical Research Laboratory, Ahmedabad 380009, India.

Introduction: Dar al Gani 476 is the first Martian meteorite to be identified from the Libyan Sahara. It mostly consists of pyroxenes, feldspathic glass, olivine [1], and also about a few percent of carbonate of certain terrestrial weathering origin [2,3]. Based on the petrographic and chemical characteristics, it has recently been classified as a basaltic Shergottite [1]. The meteorite appears highly fractured and shows effects of metamorphism under a shock pressure in the range of 40 to 50 GPa [4]. A crystallization age of about 800 Ma [5], cosmic ray exposure age of 1.2 Ma [6] and terrestrial age of >32 Ka [7] are reported for DaG476. We received two subsamples, one from the surface (~110 mg) and another from the interior (~500 mg) from Dr. Zipfel (MPIC, Mainz) for the investigation of cosmogenic records and trapped gas composition.

Experimental: About 10 mg splits from the surface and interior samples were taken for nuclear track studies, while the rest of the samples without any further cleanup were packed in Al foils and used for the analysis of nitrogen and noble gases using standard

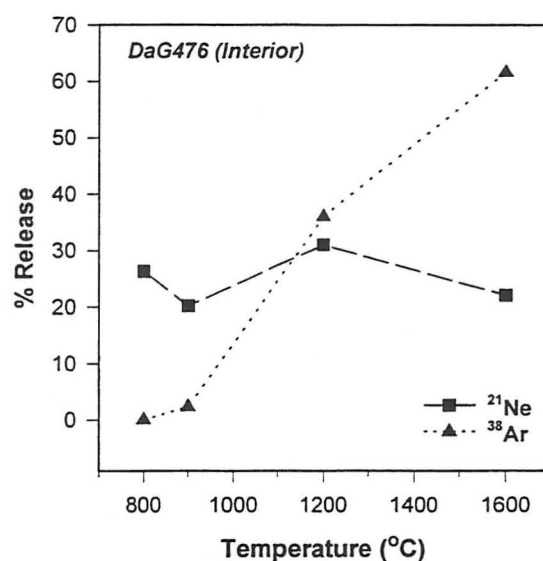


Fig.1. Release patterns of the cosmogenic neon and argon.

procedures [8]. Prior to analysis the samples were degassed with heat lamps (~150°C) for 48 hours. A combustion at 400°C in 2 torr O₂ was first carried out on these samples to get rid of the adsorbed gases and surficial contaminants, which yields negligible amounts of gases. Further gas extractions were carried out by stepwise pyrolysis by RF heating in a Mo crucible. An initial 800°C

Table 1. Neon and argon in DaG476.

| Samples | ^{22}Ne | ^{36}Ar | $^{20}\text{Ne}/^{22}\text{Ne}$ | $^{21}\text{Ne}/^{22}\text{Ne}$ | $^{38}\text{Ar}/^{36}\text{Ar}$ | $^{40}\text{Ar}/^{36}\text{Ar}$ |
|----------|------------------------------|------------------|---------------------------------|---------------------------------|---------------------------------|---------------------------------|
| | (10 ⁻¹⁰ cc STP/g) | | | | | |
| Surface | 70.9 | 12.3 | 5.069 ±.014 | 0.4887 .0035 | 0.9154 .0040 | 584 1 |
| Interior | 49.1 | 17.7 | 2.333 .018 | 0.6445 .0073 | 0.6453 .0013 | 801 5 |

Table 2. Cosmogenic gases (10^{-10} ccSTP/g) and exposure ages (Ma).

| Sample | ^{21}Ne | ^{38}Ar | T_{21} | T_{38} |
|----------|------------------|------------------|----------|----------|
| Surface | 33.7 | 9.8 | 1.16 | 1.07 |
| Interior | 31.2 | 8.5 | 1.07 | 0.92 |

step, intended to decrepitate the terrestrial carbonates was very successful, as monitored by the release of a huge amount of CO_2 accompanied by the Ar, Kr and Xe of near atmospheric (Earth's) composition. Gases were further extracted from the surface sample in one melting step at 1600°C , while for the interior sample we had additional steps of 900°C and 1200°C prior to the melting step, in an effort to resolve the different components more clearly.

The nitrogen and noble gas data for the two samples are presented in Tables 1 and 3. As can be seen, neither the concentrations nor the ratios for the noble gases match the earlier reported results [6]. This could be most likely due to the presence of variable amounts of terrestrial atmospheric component resulting from the desert-weathering. This contention is supported by the reasonable agreement in the cosmogenic contents (Table 2) which are

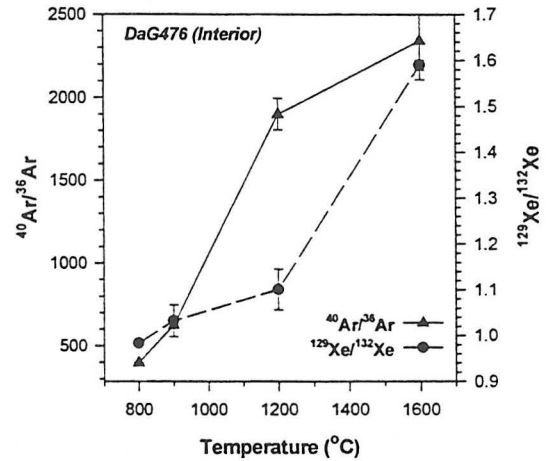


Fig. 2. Release patterns for the ratios $^{129}\text{Xe}/^{132}\text{Xe}$ and the cosmogenic corrected $^{40}\text{Ar}/^{36}\text{Ar}$.

unaffected by the addition of terrestrial component.

Neon and Argon: Variable amounts of trapped Ne and Ar are evident in these samples, a part of which is certainly of terrestrial origin (due to weathering in hot desert), while part is indigenous. The cosmogenic ^{21}Ne and ^{38}Ar evaluated for both these samples are given in Table 2. We use a trapped $^{36}\text{Ar}/^{38}\text{Ar} = 4.1 \pm 0.2$ and cosmogenic $^{36}\text{Ar}/^{38}\text{Ar} = 0.67$ in deriving $^{38}\text{Ar}_c$. Using the chemical composition of DaG476 [1] and the procedure of [9], the production rates are

Table 3. Nitrogen and trapped noble gases in DaG476.

| Sample | N (ppm) | $\delta^{15}\text{N}$ (‰) | $(10^{-10}$ cc STP/g) | | | | | $(^{40}\text{Ar}/^{36}\text{Ar})^*$ |
|----------|---------|---------------------------|-----------------------|------------------|-------------------|-----------------------------------|------------|-------------------------------------|
| | | | $^{36}\text{Ar}^*$ | ^{84}Kr | ^{132}Xe | $^{129}\text{Xe}/^{132}\text{Xe}$ | | |
| Surface | 9.89 | 7.94 ± 7.3 | 5.8 | 0.695 | 0.179 | 0.998 .004 | 1240 66 | |
| Interior | 4.89 | 7.17 1.10 | 12.1 | 0.527 | 0.055 | 1.125 .020 | 1177 38 | |

*corrected for cosmogenic contribution.

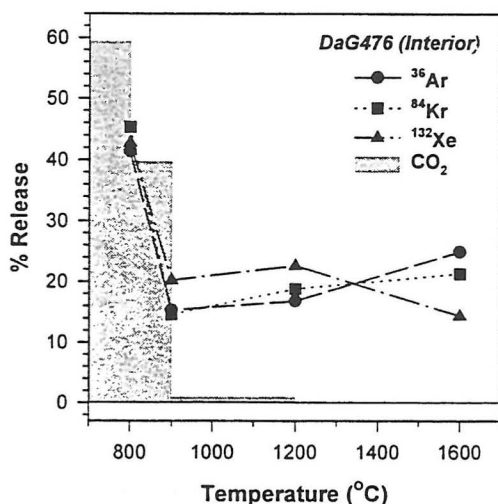


Fig. 3. Release patterns of the trapped noble gases and CO_2 (indicator for terrestrial carbonates).

derived. Due to large amounts of trapped Ne, it is not possible to derive the shielding parameter $(^{22}\text{Ne}/^{21}\text{Ne})_c$ very accurately and we use the production rates for an average shielding of $(^{22}\text{Ne}/^{21}\text{Ne})_c = 1.11$. The mean exposure age of 1.1 ± 0.1 is similar to the value reported earlier [6]. Since the cosmogenic component is not affected by addition of trapped gases from weathering, their release pattern (Fig. 1) will reflect those of indigenous sample gases. While ^{21}Ne is more or less uniformly released, ^{38}Ar had a peak release at 1600°C . The agreement between the exposure ages based on ^{21}Ne and ^{38}Ar points to the fact that no cosmogenic Ne or Ar loss occurred due to the terrestrial weathering. The cosmogenic corrected $^{40}\text{Ar}/^{36}\text{Ar}$ is ~ 1200 for both the samples. Considering the contribution of radiogenic ^{40}Ar from insitu decay of ^{40}K , the trapped ratio of $^{40}\text{Ar}/^{36}\text{Ar}$ in DaG476 should be much less than 1200. This lower value as

compared to the Martian atmospheric value of 2400 ± 200 [10] indicates the contribution of either the terrestrial atmospheric or Martian magmatic component. Considering the $^{40}\text{Ar}/^{36}\text{Ar}$ signatures of the temperature fractions, as the radiogenic component is expected to be released by 1200°C , the cosmogenic corrected $^{40}\text{Ar}/^{36}\text{Ar} \sim 2400$ in the 1600°C step (Fig. 2) clearly points to the presence of a Martian atmospheric component in DaG476.

Krypton and Xenon: Kr and Xe are almost entirely of trapped origin (either terrestrial or indigenous). In Fig. 3, the release patterns of trapped Ar, Kr and Xe are shown along with that of CO_2 [from the decrepitation

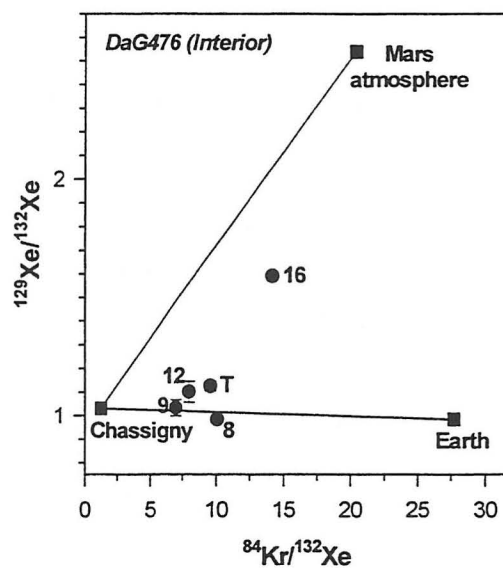


Fig. 4. Plot of $^{129}\text{Xe}/^{132}\text{Xe}$ vs. $^{84}\text{Kr}/^{132}\text{Xe}$. Most of the SNC data fall either along or above the Chassigny-Mars atmosphere mixing line. Numbers beside each point indicate the temperature in 100°C , T is for total.

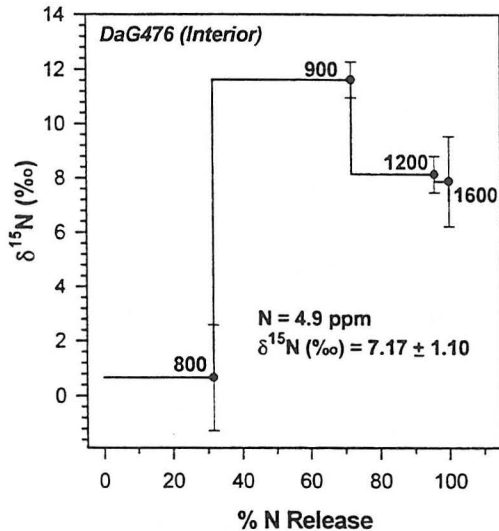


Fig.5. Release pattern of $\delta^{15}\text{N}$.

of the terrestrial carbonates (2,3)]. The peak release for all these gases at 800°C coincides with that of CO₂. This, together with the air-like isotopic ratios of the accompanying gases suggests that most of this fraction is of terrestrial origin. As the CO₂ amount decreases at higher temperature fractions, trapped gas of indigenous origin becomes clearly visible as indicated by the increase in the ratios ⁴⁰Ar/³⁶Ar and ¹²⁹Xe/¹³²Xe (Fig.2). The value of ¹²⁹Xe/¹³²Xe = 1.59 ± 0.01 in the 1600°C fraction, accompanied by ⁴⁰Ar/³⁶Ar ~2400, is a clear signature of the presence of a Martian atmospheric component in DaG476. The elemental ratio ⁸⁴Kr/¹³²Xe of ~10 in various temperature fractions is less than the value of 25 for Mars atmosphere [10]. In the case of chondritic meteorites a higher value of ⁸⁴Kr/¹³²Xe in 'desert finds' is a sure sign of the effect of terrestrial weathering [11], but for a Martian meteorite that is a 'desert find', such high ratio can also be due to the presence of a

Martian atmospheric component. In the plot of ¹²⁹Xe/¹³²Xe to ⁸⁴Kr/¹³²Xe (Fig.4) the high temperature data of DaG476 fall much above the Chassigny - Earth mixing line indicating the presence of a Martian atmospheric component.

Nitrogen: The differing N contents in both the samples are due to variable contributions from terrestrial weathering products. About 30% N released with δ¹⁵N ~0‰ in the 800°C fraction (Fig.5) clearly demonstrates this fact. There is no heavy N component characteristic of the Mars atmosphere even at higher temperatures, indicating the dominance of other indigenous N-components, and most likely the presence of magmatic N as inferred in the case of Shergotty, Chassigny and ALH84001 [7,12,13].

Acknowledgement: We thank Dr. J. Zipfel (MPIC, Mainz) for the DaG476 samples.

References: [1] Zipfel J. et al. (1999) LPSC 30 (CD ROM #1206); [2] Wright I.P. et al. (1999) LPSC 30 (CD ROM #1594); [3] MiKouchi T. (1999) LPSC 30 (CD ROM #1557); [4] Greshake A and Stoffler D. (1999) LPSC 30 (CD ROM #1377); [5] Jagoutz E. et al. (1999) LPSC 30 (CD ROM #1808); [6] Scherer P. and Schultz L. (1999) LPSC 30 (CD ROM #1144); [7] Nishiizumi K. et al. (1999) LPSC 30 (CD ROM #1966); [8] Murty S.V.S. and Mohapatra R. (1997) GCA 61 5417; [9] Eugster O. and Michel Th. (1995) GCA 59 177; [10] Pepin, R.O. (1991) Icarus 92, 2; [11] Scherer P. et al. (1994) In *Noble gas geochemistry and cosmochemistry* (ed. J. Matsuda) pp. 43; [12] Mohapatra R. K. et al. (1998) MAPS 33 A112; [13] Mathew K.J. et al. (1998) MAPS 33 655.

THERMAL EFFECTS ON MINERALOGY, NOBLE-GAS COMPOSITION, AND CARBONACEOUS MATERIAL IN CM CHONDRITES

Tomoki Nakamura, Fumio Kitajima, and Nobuo Takaoka

Department of Earth and Planetary Sciences, Graduate School of Science, Kyushu University 33, Hakozaki, Fukuoka 812-8581, Japan

Introduction

Many CM chondrites have been found among Antarctic meteorites that have experienced thermal metamorphism after aqueous alteration [e.g., 1-10]. They are samples of hydrous asteroids recording more advanced evolution processes than normal CM chondrites. In the present study, mineralogy, noble-gas composition, and carbonaceous material of five CM chondrites were characterized, in order to see progressive changes of CM chondrites with increasing degree of heating.

Samples and experimental procedure

Samples were categorized by the degree of heating based on the mineralogical data previously reported. Murray is unheated [11], A-881458 and Y-793321 are weakly heated [1, 12], and A-881334 and Y-86789 are strongly heated [9, 12]. A relatively large chip (~ 300 mg) from individual meteorites was cut to make thin slices. The slices are placed on a glass plate and exposed to X-ray to have powder diffraction of each meteorite. Observation of textures of the slices and of polished thin sections was made by an optical microscope and a scanning electron microscope (SEM). Two or three slices from each meteorite were analyzed for noble gases by stepped pyrolysis using a MM5400 mass spectrometer at Kyushu University equipped with a Ta furnace and a stainless steel purification line "Jack and the Beanstalk" [13]. For a characterization of carbonaceous macromolecular materials, instantaneous (not continuous heating) pyrolysis-GC analyses were performed. The pyrolysis was carried out at 740 °C for 3 sec. using Curie-point pyrolyzer. The GC column was Neutrabond-5 (30m x 0.25mm i.d.). The rate of GC oven temperature increase was programmed to be 4 °C/min. from 60 to 260 °C after holding the initial temperature for 10 minutes.

Results and Discussion

Texture

Most commonly observed texture in the five meteorites is that of primary accretionary rocks of CM chondrites defined by [14] where chondrules with typical diameter of 500 µm are thickly rimmed by fine-grained minerals of many

kinds and the rimmed chondrules are embedded in PCP-rich matrix. The textures of primary rocks change with the degree of heating increases. Comparison of textures between Murray and Y-86789 indicates that heating effects on textures include (1) an increase of pore spaces in both chondrules and matrix, probably due to shrinkage of phyllosilicates by dehydration, and (2) abundant presence of small grains of mainly troilite and minor amounts of kamacite in the matrix, instead of PCP. In contrast, Y-793321, and A-881458 contain portions showing a comminuted texture that appears to have formed by fragmentation and mechanical mixing of components of primary rocks. This indicates that the two meteorites experienced impacts on the meteorite parent bodies. Optical microscope observation of thin sections indicates that many olivines in Y-793321 show undulatory extinction, indicating that it has experienced impacts of S2 level [15].

Bulk mineralogy

X-ray diffraction of slices of individual samples indicates diverse mineralogy of the five meteorites. Murray contains abundant cronstedtite that is a major constituent of rims around chondrules and matrix and is characterized by strong 001 and 002 reflections at 7.1 and 3.6 Å, respectively [16]. Magnetite is more abundant than kamacite. Troilite is very minor. In the weakly heated samples, A-881458 contains abundant cronstedtite and shows very similar mineralogy to Murray, while Y-793321 contains very small amounts of cronstedtite whose 001 reflection is shifted towards the high diffraction angles, suggesting a slight reduction of interlayer spacing. It is known that complete decomposition of cronstedtite occurs at 470°C based on differential thermal analysis [17]. Therefore, the presence of little cronstedtite indicates that Y-793321 experienced heating at temperature close to 470°C.

The mineralogy of strongly heated samples A-881334 and Y-86789 differs from that of weakly heated samples. The strongly heated samples completely lack cronstedtite and contain kamacite greater than magnetite. This suggests that strong heating has caused dehydration and

subsequent reduction of oxygen fugacity. The complete lack of cronstedtite and magnetite and the abundant presence of anhydrous minerals such as olivine, low-Ca pyroxene, troilite, and pyrrhotite in Y-86789 indicate that it is a sample having experienced the highest degree of heating among the five samples investigated in this study. Observation of texture of Y-86789 showed that primary anhydrous silicates in both chondrules and matrix are replaced by fibrous phyllosilicate-like material. Thus, olivine and low-Ca pyroxene detected by X-ray diffraction are secondary in origin, produced by thermal decomposition of phyllosilicates. The presence of secondary low-Ca pyroxene suggests that this meteorite has been heated at temperature higher than 700°C based on the T-T-T diagram proposed by [3].

Noble gases

Elemental and Ne isotopic ratios indicate that Y-793321 and A-881458 are solar-gas rich samples, while Murray, A-881334, and Y-86789 are solar-gas poor samples. Solar-type noble gases in Y-793321 and A-881458 are expected to be in portions showing a comminuted texture that was located by SEM observation, since solar gases in CM chondrites are preferentially distributed in such portions [18, 19]. Concentrations of solar and primordial Ne in the two meteorites are determined by separating measured Ne into solar, Ne-A, and cosmogenic components (Fig. 1). Concentration of trapped ^{22}Ne (solar + Ne-A) is much higher in Y-793321 than that in A-881458, due to a large contribution of solar gases. Solar gases are usually released at low temperature because of shallow implantation depth into minerals. In fact, Ne in the low temperature steps of the two meteorites consists mostly of solar gases judging from isotopic ratios. But a release pattern of Y-793321 shows a reduction of solar-gas concentration extracted at low temperatures of 250 and 400 °C (Fig.1). The reduction can be ascribed to loss of solar gases by heating at approximately 400 °C which is consistent with the temperature estimated from the mineralogy of this meteorite.

Ne in the solar-gas poor samples consists mainly of primordial and cosmogenic gases. Concentrations of primordial Ne decrease in the order of Murray, A-881334, and Y-86789: those of Murray are higher than those of Y-86789 by one order of magnitude. Thus it is estimated that the degree of heating increases from Murray, A-881334, and to Y-86789. When the primordial Ne is partitioned into Ne-A2 and Ne-E, concentrations of the former decrease with the increasing degree of heating mainly due to

reduction of concentrations extracted in low temperature steps, whereas those of the latter are constant among the three meteorites (Fig. 2). This indicates that carrier phase of Ne-E is more resistant than that of Ne-A2 during the heating of CM chondrites [20].

Carbonaceous material

The observed quantities of pyrolyzates from strongly heated chondrite A-881334 were quite poor compared with the unheated chondrite Murray. The two weakly heated chondrites, A-881458 and Y-793321, gave intermediate amounts of pyrolyzates. The pyrolyzates are considered to be derived from edge defects with thermally weaker bonds compared with those in the condensed aromatic network. The amounts of pyrolyzates decrease when graphitization of chondritic carbonaceous materials proceeds at high temperature, because of the losses of such edge defects. Thus, amounts of pyrolyzates decrease when the chondrites have experienced higher degrees of heating. Y-86789, although it is a sample heated stronger than A-881334 based on the noble gas signature, yielded pyrolyzates greater than A-881334. The pyrogram of Y-86789 differs from that of Murray, A-881334, A-881458, and Y-793321, suggesting that the pyrolyzates in Y-86789 may be a trace of terrestrial weathering.

Acknowledgments: Comments on the paper by Dr. Ian. A. Franchi are much appreciated.

References:

- [1] Akai, J. (1988) *Geochim. Cosmochim. Acta*, **52**, 1593-1599.
- [2] Akai, J. (1990) *Proc. NIPR symp. Antarctic Met.*, **3**, 55-68.
- [3] Akai, J. (1992) *Proc. NIPR symp. Antarctic Met.*, **5**, 120-135.
- [4] Tomeoka, K., Kojima, H. and Yanai, K. (1989) *Proc. NIPR symp. Antarctic Met.*, **2**, 55-74.
- [5] Tomeoka, K. (1990) *Proc. NIPR symp. Antarctic Met.*, **3**, 40-54.
- [6] Paul, R. L. and Lipschutz, M. E. (1990) *Proc. NIPR symp. Antarctic Met.*, **3**, 80-95.
- [7] Kimura, M. and Ikeda, Y. (1992) *Proc. NIPR symp. Antarctic Met.*, **5**, 74-119.
- [8] Ikeda, Y., Noguchi, T. and Kimura, M. (1992) *Proc. NIPR Symp. Meteorites*, **5**, 136-154.
- [9] Matsuoka, K., Nakamura, T., Nakamura, Y. and Takaoka, N. (1996) *Proc. NIPR symp. Antarctic Met.*, **9**, 20-36.
- [10] Wang, M. S. and Lipschutz, M. E. (1998) *Meteoritics Planet. Sci.*, **33**, 1297-1302.

- [11] Tomeoka, K. and Buseck, P. R. (1985) *Geochim. Cosmochim. Acta*, **49**, 2143-2163.
- [12] Akai, J. and Tari, S. (1997) *LPI Technical Report 97-02 Part I*, 1-2.
- [13] Nakamura, T. and Takaoka, N. (1999) *Antarctic Met. Res.*, in press.
- [14] Metzler, K., Bischoff, A., and Stöffler, D. (1992) *Geochim. Cosmochim. Acta*, **56**, 2873-2897.
- [15] Stöffler, D., Keil, K., and Scott, E. R. D. (1991) *Geochim. Cosmochim. Acta*, **55**, 23845-3867.
- [16] Nakamura, T. and Nakamura, Y. (1996) *Proc. NIPR symp. Antarctic Met.*, **9**, 37-50.
- [17] Caillère, S. and Hénin, S. (1957) In *The differential thermal investigation of clays*. (eds by R. C. Mackenzie), pp. 207-230, Alden press, Oxford.
- [18] Nakamura, T., Nagao, K., and Takaoka, N. (1999a) *Geochim. Cosmochim. Acta*, **63**, 241-255.
- [19] Nakamura, T., Nagao, K., Metzler, K. and Takaoka, N. (1999b) *Geochim. Cosmochim. Acta*, **63**, 257-273.
- [20] Huss G. R. and Lewis R. S. (1995): *Geochim. Cosmochim. Acta*, **59**, 115-160.

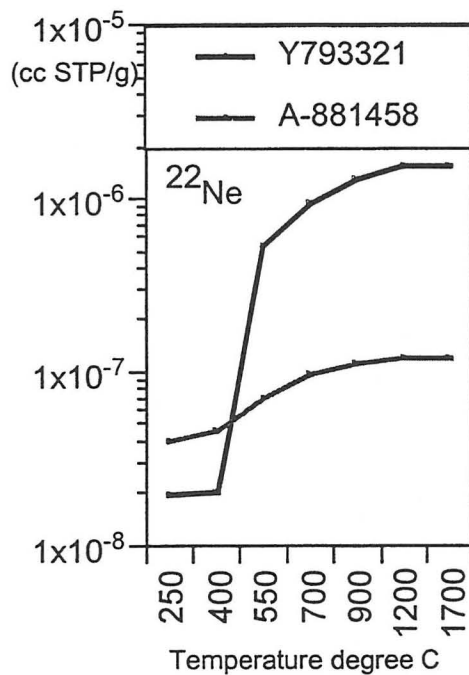


Fig.1. Release profiles of trapped ^{22}Ne (solar + Ne-A) in stepped pyrolysis.

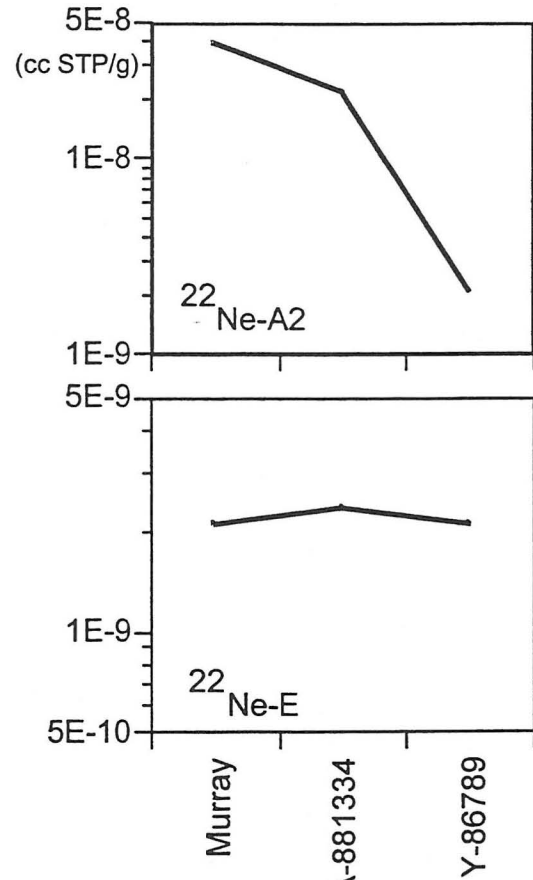


Fig.2. Total concentrations of Ne-A and Ne-E of the solar-gas poor samples. The degree of heating increases in the order of Murray, A-881334, and Y-86789.

TERRESTRIAL AGES OF ANTARCTIC METEORITES – UP DATE 1999

K. Nishiizumi¹ (kuni@ssl.berkeley.edu), M. W. Caffee², K. C. Welten¹, ¹Space Sciences Laboratory, University of California, Berkeley, CA 94720-7450, ²Geoscience and Environmental Technology, Lawrence Livermore National Laboratory, Livermore, CA 94550.

We are continuing our ongoing study of cosmogenic nuclides in Antarctic meteorites. In addition to the studies of exposure histories of meteorites, we study terrestrial ages and pairing of Antarctic meteorites and desert meteorites. Terrestrial ages of Antarctic meteorites provide information on meteorite accumulation mechanisms, mean weathering lifetimes, and influx rates. The determination of ³⁶Cl (half-life=3.01x10⁵ y) terrestrial ages is one of our long-term on-going projects, however, in many instances neither ³⁶Cl or ¹⁴C (5,730 y) yields an accurate terrestrial age. Using ⁴¹Ca (1.04x10⁵ y) for terrestrial age determinations solves this problem by filling the gap in half-life between ¹⁴C and ³⁶Cl ages. We are now applying the new ⁴¹Ca-³⁶Cl terrestrial age method as well as the ³⁶Cl-¹⁰Be method to Antarctic meteorites. Our measurements and ¹⁴C terrestrial age determinations by the University of Arizona group are always complementary.

We have measured ³⁶Cl in over 270 Antarctic meteorites since our previous compilation of terrestrial ages. Since a large number of meteorites have been recovered from many different icefields in Antarctica, we continue to survey the trends of terrestrial ages for different icefields. We have also measured detailed terrestrial ages vs. sample locations for Allan Hills, Elephant Moraine, and Lewis Cliff Icefields, where meteorites have been found with very long ages. Fig. 1 and 2 show the updated histograms of terrestrial ages of meteorites from the Allan Hills Main Icefield and Lewis Cliff Icefield. These figures include ¹⁴C ages obtained by the University of Arizona group. Pairs of meteorites are shown as one object for which the age is the average of all members of the same fall. The width of the bars represents 70,000 years, which was a typical uncertainty for ³⁶Cl ages. We reduced the uncertainty of terrestrial age determinations to ~40,000 years by using pairs of nuclides such as ⁴¹Ca-³⁶Cl or ³⁶Cl-¹⁰Be. Fig. 1 clearly indicates that meteorites found at the Allan Hills Icefields are much older than any other meteorites. The terrestrial ages cover a wide range and are as old as 2 My. Many of the Lewis Cliff meteorites are as old as the Allan Hills meteorites. So far, no clear correlation has been found between the terrestrial ages and the locations of the Lewis Cliff meteorites (see Fig. 2).

Acknowledgments: We thank A. J. T. Jull for providing unpublished ¹⁴C results. This work was supported by NASA and NSF grants.

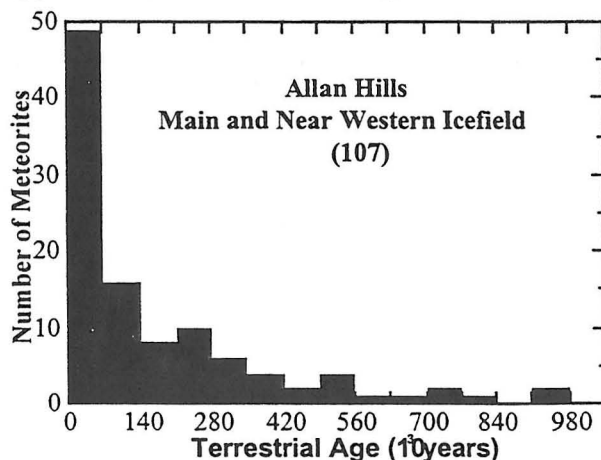


Figure 1. Terrestrial ages of Allan Hills.

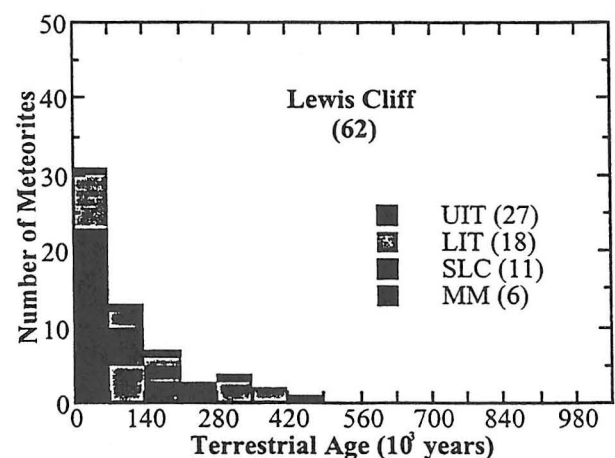


Figure 2. Terrestrial ages of Lewis Cliff.

TYPE I COSMIC SPHERULES: KEY TO A MAJOR, BUT POORLY SAMPLED, ASTEROID POPULATION? L. E. Nyquist, Mail Code SN2, NASA Johnson Space Center, Houston, TX 77058, l.nyquist@jsc.nasa.gov.

Introduction: Herzog *et al.* [1] have determined Fe, Ni, and Cr abundances in Type I cosmic spherules recovered from the deep sea, and also the isotopic fractionation of these elements during passage of the spherules through the terrestrial atmosphere. Isotopic fractionation for all three elements is typically large,

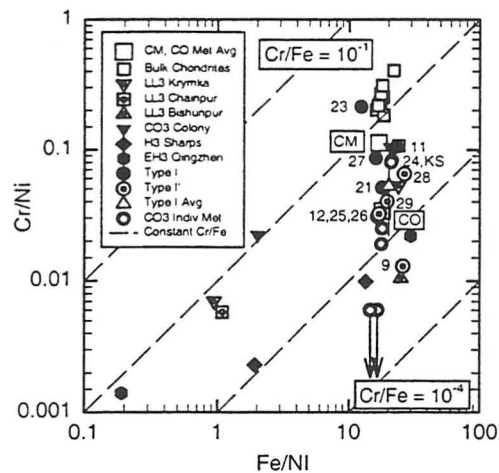


Figure 1. Pre-atmospheric Fe/Ni and Cr/Ni ratios for Type I spherules compared to those in bulk chondrites and chondritic metal [1]. Arabic numerals designate individual spherules. Type I' are spherules for which some parameters were determined by interpolation. Cr/Ni ratios for the majority of the spherules lie within the range for average metal from CM and CO chondrites. Metal from individual CO3 meteorites of high metamorphic grade can have lower Cr/Ni ratios as illustrated by downward-pointing arrows for metal from the CO3 meteorites Warren and Isna. Data sources are given in [6].

$\sim 16\%/amu$, corresponding to evaporative mass losses of $\sim 80-85\%$, assuming Rayleigh distillation from an open system. The corrected, pre-atmospheric, Cr/Ni and Fe/Ni ratios are shown in Figure 1, where they are compared to these ratios in bulk chondrites and chondritic metal. Although the calculated pre-atmospheric Fe/Ni ratio for the spherules is relatively constant at 19 ± 4 (σ_{mean}), the calculated pre-atmospheric Cr/Ni ratios vary by about two orders of magnitude. The Cr/Ni ratios are thus powerful discriminators for possible modes of origin of the spherules. For example, iron meteorites typically have low Cr contents and low Cr/Ni ratios, $\leq 3 \times 10^{-4}$. Thus, Type I spherules do not appear to be ablation products of iron meteorites, in contrast to an earlier suggestion [2].

Possible Origin of the Type I Spherules: The Type I spherules may stem from a variety of origins, but the one most obviously implied by the Fe, Ni, and Cr data is most interesting. Could the type I precursors be metal grains from carbonaceous chondrites? The most common asteroid spectral types resemble those of carbonaceous chondrites, but the orbits of the corresponding asteroids are not favorably situated to allow material from them to reach the earth [3]. Small particles, however, can be moved out of their dynamically determined orbits by Poynting-Robertson drag. The masses of the spherules analysed by [1] were $\sim 10^{-4}$ g. A 10^{-4} g stony micrometeoroid has a Poynting-Robertson lifetime at 1 AU of $\sim 3 \times 10^5$ yr [4]. The P-R lifetime scales proportionally to particle radius, density, and the square of the orbital radius [5], so a 10^{-4} g metallic particle initially in a circular orbit at 2.5 AU will have a P-R lifetime of $\sim 5 \times 10^6$ yr. Collisional lifetimes scale with the strength of the material, so that metallic particles should have much longer collisional lifetimes than stony ones of equivalent mass, at least an order of magnitude longer [3]. Grün *et al.* [4] calculate the collisional lifetime of a 10^{-4} g stony micrometeoroid as a few times 10^4 yr at 1 AU and a few times 10^2 yr at 0.1 AU. Thus, collisional lifetimes against destruction on the order of 10^6 yr for metallic particles at ~ 2.5 AU may not be unreasonable. If the collisional lifetime for an ~ 100 μg metallic particle is an appreciable fraction of the P-R lifetime; i.e., the time required for it to fall into the Sun from ~ 2.5 AU, there will be a significant probability for such a particle to reach a gravitational resonance where gravitational forces will place it more directly into an earth-crossing orbit. Thus, Type I spherules may be particularly hardy space travelers capable of routinely reaching Earth from places in the asteroid belt from which Earth is otherwise inaccessible.

A possible objection to origin of the Type I spherules from metallic grains from carbonaceous chondrite-like asteroidal parent bodies is the fine-grained nature of the metal in most carbonaceous chondrites. However, some CO chondrites are surprisingly metal-rich. Rubin *et al.* [6] estimated an original metallic (Fe,Ni) abundance of ~ 19 wt % for CO3 Colony, for example. Furthermore, metal in CO chondrites often occurs in "type-I chondrules" which are spongy-looking in thin section due to their high metal abundance [7].

Conclusions and Implications: The high Cr abundance of Type I cosmic spherules show that it is a

mistake to dismiss them as simply atmospheric ablation products of iron meteorites. On the contrary, they may contain among them our only samples of some carbonaceous asteroids which are poorly represented, if at all, among our larger meteorites. Particularly good candidates for such materials are the spherules with Cr/Ni ~0.02-0.1 (Figure 1). That such spherules are relatively abundant among the Type I's suggest that they represent a major main belt asteroid type.

Efforts to collect Type I spherules, especially from the Antarctic ice where a depositional stratigraphy might be preserved, should continue. Analysis of this material, altered as it is, may yield new insights into the nature of some primitive asteroids which have otherwise been poorly sampled. Analysts should bare in mind, however, that most Type I spherules have lost ~80-90% of their Fe, the major remaining component.

Thus, interelement fractionation is to be expected. Although such fractionation appears not to have significantly affected the relative proportions of Fe, Ni, and Cr in Type I's, this simple result should not be expected for elements which differ more in their volatility.

References: [1] Herzog G. F. *et al.*, (1999) *Geochim. Cosmochim. Acta*, 63, 1443-1457. [2] Blanchard M.B., *et al.*, (1980) *Earth and Planetary Sci. Lett.* 46, 178-190. [3] Chapman C. R. (1976) *Geochim. Cosmochim. Acta*, 40, 701-719. [4] Grün E., *et al.* (1985) *Icarus* 62, 244-272. [5] Wyatt S. P. and Whipple F. L. (1950) *Ap. J.*, 111, 558-565. [6] Rubin A. E., *et al.* (1985) *Meteoritics*, 20, 175-196. [7] McSween H. Y. (1977) *Geochim. Cosmochim. Acta* 41, 477-491.

DO WEATHERING EFFECTS INFLUENCE COSMIC RAY EXPOSURE AGES OF ENSTATITE CHONDRITES? Andrea Patzer & Ludolf Schultz, Max-Planck-Institute for Chemistry, Mainz, Germany (patzer@mpch-mainz.mpg.de)

Introduction. The cosmic ray record and exposure ages (CREA's) of 62 Enstatite chondrites have been reported recently [1]. As one of the main results, an age spectrum has been given ranging between 1 and 60 Ma. A similar spectrum is known for the ordinary chondrites. One surprising aspect, however, that has not been observed for ordinary chondrites, is a significant difference between CREA's calculated from cosmogenic ^{21}Ne and ^{38}Ar , respectively (Fig. 1). Since ^{21}Ne -exposure ages are believed to be the most reliable, not concordant Ar-ages need to be explained.

In some Enstatite chondrites (EC) with high concentrations of trapped Ar, high ^{38}Ar -ages compared to ^{21}Ne -ages are determined. This discrepancy is probably caused by insufficient correction for trapped ^{38}Ar as the trapped $^{36}\text{Ar}/^{38}\text{Ar}$ ratio is not well known. Other EC with lower abundances of trapped Ar show – again in comparison with the ^{21}Ne -ages – considerably lower ^{38}Ar -ages. In those cases we suggested that weathering effects may be responsible for the difference. Most notably Ca, one main target element of cosmogenic ^{38}Ar , partly resides in minerals readily affected by terrestrial alteration. The comparatively abundant metal phase (Kamazite) represents another target nuclide. The dissolution or decomposition of both metal and Ca-bearing minerals, like oldhamite (CaS) as well as plagioclase, presumably results in a loss of cosmogenic ^{38}Ar . As a consequence, the calculated ^{38}Ar -exposure ages are too small.

Several authors have investigated the influence of terrestrial weathering on the noble gases of meteorites. In 1978, for example, decreasing abundances of radiogenic and cosmogenic noble gases of the L6 chondrite Holbrook were found in three samples with increasing terrestrial ages [2]. Another paper summarizes the results of a study on the adsorption of atmospheric rare gases of chondrites from hot deserts [3]. Those authors also observed a terrestrial alteration effect on noble gas inventories. Especially heavily weathered samples reveal a loss of He and Ne. At the same time, atmospheric Kr and Xe are strongly enhanced. In another paper the influence of climate on weathering is reported [4]. It is suggested that the degree of weathering and the formation of secondary minerals in ordinary chondrites reflect ancient climatic conditions in a given area, e.g. yield a signature of that climate being present at the time the meteorite fell. The authors reconstruct the individual stages of weathering and differentiate between an initial, rather short alteration period and a second stage with less alteration pro-

cesses due to significant reduction of porosity and permeability.

In order to test the assumption that relatively low ^{38}Ar exposure ages of EC are caused by weathering reactions, we carried out an alteration experiment simulating the weathering of a meteorite in the field.

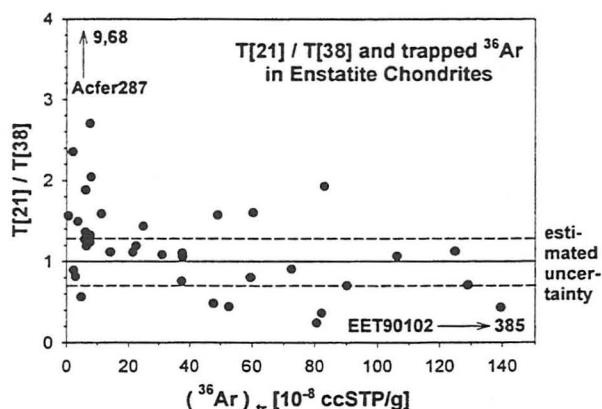


Fig. 1: Correlation of the trapped ^{36}Ar -content and the exposure age ratio $T[21]/T[38]$

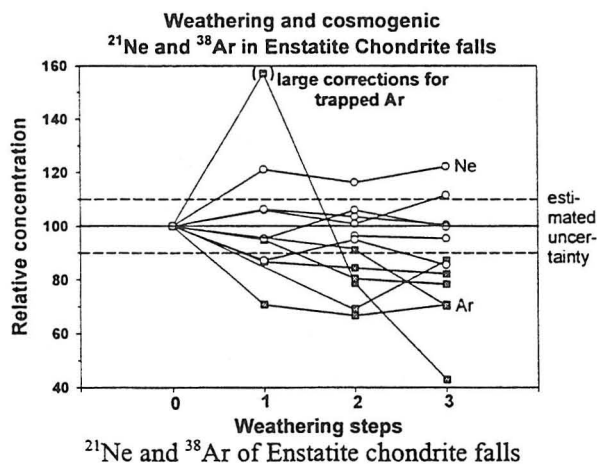
Procedure, results and discussion: The weathering treatment lasted 12 weeks and was divided into three steps each taking 4 weeks. We only chose between those samples that originally revealed concordant ^{21}Ne - and ^{38}Ar -exposure ages and selected 8 falls and finds from hot and cold deserts (names, types and sizes see Tab. 1). We then separated three small chunks of each meteorite in order to have material for noble gas measurements after each 4 week-period, respectively.

In the first step (week 1 – 4), the EC's were daily wetted with rain water and heated to 55° or 60°C during the day. This kind of treatment was also kept during the second phase (week 5 – 8). In the last interval (week 9 – 12), the samples were wetted and heated like before, but additionally frozen at -23°C for about 12 h each day. We intended to cause congelifraction which may lead to higher porosity of the chondritic material.

The cosmogenic ^3He - and ^{21}Ne -concentrations and calculated CREA's do not show any significant changes after the experimental treatment. Having a closer look to the amounts of cosmogenic ^{38}Ar , however, we observed an important difference: While the concentrations in EC-finds vary in an unpredictable manner, the abundances of EC-falls are generally lower than before (untreated). The gas amounts espe-

cially decreased after the first weathering step (Fig. 2). This kind of loss pattern, although the time interval was definitely shorter than real situations, seems to correlate with the initial rapid weathering described by [4] and explains the comparatively short ^{38}Ar -exposure ages in E-chondrites with low trapped Ar concentrations.

Fig. 2: The influence of weathering on cosmogenic



| Samples and weights [mg] | | | | |
|--------------------------|-----------|------------|-------------|--------------|
| sample | type | specimen I | specimen II | specimen III |
| Abee | EH4 m. b. | 11.87 | 28.06 | 38.60 |
| Grein002 | EH4/5 | 43.25 | 40.05 | 55.33 |
| Ilafegh009 | EL7 | 40.54 | 35.66 | 34.58 |
| LEW87223 | E3-an | 51.33 | 44.61 | 80.99 |
| LON94100 | EL6 | 32.19 | 42.83 | 44.20 |
| Pillistfer | EL6 | 33.03 | 14.82 | 27.73 |
| Qingzhen | EH3 | 40.63 | 41.47 | 75.19 |
| SAH97096 | EH3 | 33.57 | 29.50 | 41.00 |

Numbers I to III correspond to weathering steps 1 to 3
m. b. = melt breccia, an = anomalous

Tab. 1: List of samples, sample types and sample weights

In the literature, a decrease of the He and Ne content in meteorites with increasing terrestrial age and degree of weathering was also reported [2, 3]. This can be at least partly explained by a "dilution" effect. Weathering products which do not contain cosmogenic noble gases are added to the meteoritic sample and therefore lower the concentration of cosmogenic nuclides in the bulk sample. In this experiment, the time span was obviously too short to produce large quantities of secondary minerals.

However, we observed the $^{21}\text{Ne}/^{22}\text{Ne}$ -ratios tending to increase by a few percent during the weathering process for some samples (Fig. 3). Possibly, the change is due to the mobilisation of Na-bearing compounds [4, 5]. Na is one main target element of cos-

mogenic ^{22}Ne [e.g. 6] and hence, cosmogenic ^{22}Ne may be more influenced by weathering than ^{21}Ne . Besides this effect on cosmogenic gases, we found a trend of increasing $^{84}\text{Kr}/^{132}\text{Xe}$ -ratios as already described in [3] (Fig. 4). This kind of modification can be certainly attributed to an atmospheric contamination.

Fig. 3: Weathering effects on the cosmogenic $^{21}\text{Ne}/^{22}\text{Ne}$ -

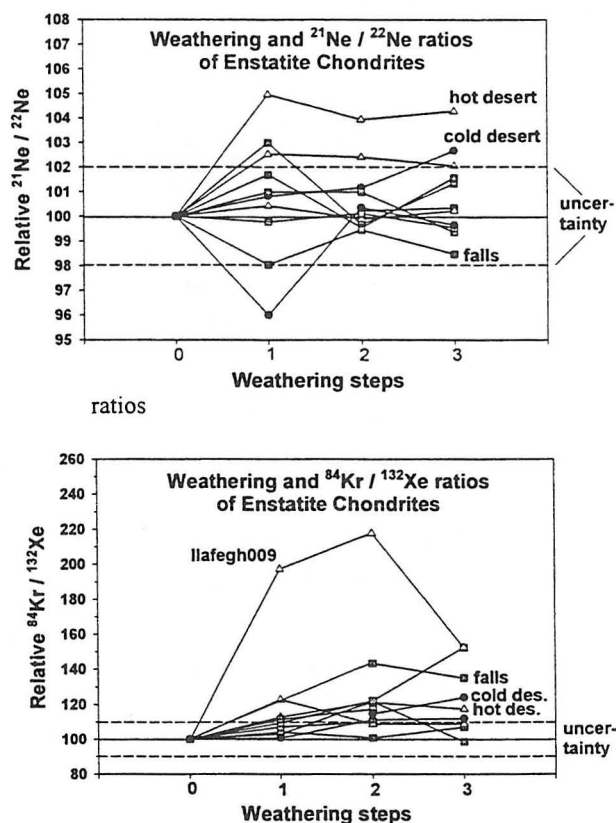


Fig. 4: Influence of weathering on the $^{84}\text{Kr}/^{132}\text{Xe}$ -ratios of Enstatite chondrites

References: [1] Patzer A. & Schultz L. (1998) *Met. Planet. Sci.* 33, A120 - A121. [2] Gibson E. K. & Bogard D. D. (1978) *Meteoritics* 13, 277-297. [3] Scherer P., Schultz L. & Loeken T. (1994) *Noble Gas Geochemistry and Cosmochemistry* (ed. J. Matsuda), 43-53. [4] Bland P. A. et al. (1998) *Geochim. Cosmochim. Acta* 62, 3169-3184. [5] Ozaki H. et al. (1999) *Ant. Met.* XXIV, NIPR Tokyo, 154-156. [6] Smith S. P. & Huneke J. C. (1975) *Earth Planet. Sci. Let.* 27, 191-199.

SOLAR-COSMIC-RAY-PRODUCED NUCLIDES IN EXTRATERRESTRIAL MATTER.

Robert C. Reedy¹, ¹Space and Remote Sensing Science Group (NIS-2), Mail Stop D436, Los Alamos National Laboratory, Los Alamos, NM 87545 USA (rreedy@lanl.gov).

Introduction: There are two main types of cosmic rays that have sufficient energy to induce nuclear reactions -- the galactic cosmic rays (GCR) and solar cosmic rays (also called solar energetic particles). Both types of particles can have production rates and production ratios in the small objects often found in cold and hot deserts that are different from those seen for most meteorites, which typically have radii of ~10-100 centimeters. GCR production rates are often lower than those for most meteorites [1]. GCR production ratios, such as $^{22}\text{Ne}/^{21}\text{Ne}$, are also often different in small objects.

Smaller meteoroids also are more likely to have nuclides made by solar-cosmic-ray (SCR) particles than typically-sized meteorites. The very small meteorite Salem had large amounts of SCR-produced radionuclides [2]. Meteorites recovered in Antarctica are more likely to contain SCR-produced nuclides than other meteorites [3]. Martian and lunar meteorites are also likely to have SCR-produced nuclides.

Production rates and profiles for SCR-produced nuclides in meteoroids have been calculated previously [e.g., 4]. However, the cross sections for the nuclear reactions making many SCR-produced nuclides, such as ^{10}Be , were not well measured then [cf., 5]. New rates and profiles are calculated here using good cross sections for the reactions making these nuclides.

Cross Sections for Making SCR-Produced Nuclides: Since about 1990, many cross sections have been measured for cosmogenic nuclides using protons [e.g., 6-8]. These cross sections have been used to unfold profiles of SCR-produced nuclides measured in several lunar samples [e.g., 8-10]. The average proton fluxes determined from these SCR-produced nuclides now show less scatter as a function of time in the past and suggest a trend of higher solar-proton fluxes for time periods less than a million years than for samples or nuclides that cover time periods of about 1 million year (~1 Ma) [11].

Cross sections have been compiled and evaluated for many SCR-produced nuclides. The nuclides studied here (and a reference to the cross sections used to study it) are 5730-year ^{14}C [8], 0.3-Ma ^{36}Cl [12], 0.7-Ma ^{26}Al and 1.5-Ma ^{10}Be [10], 3.7-Ma ^{53}Mn [Nishizumi, priv. comm.], and the stable noble-gas isotopes ^{21}Ne , ^{22}Ne , and ^{38}Ar [13]. These are the same nuclides that were used in the calculations for GCR-produced nuclides in small objects [1].

Fluxes of Incident Solar Protons: The average

flux of solar protons over the last few millions years as determined from ^{26}Al , ^{10}Be , ^{21}Ne , and ^{53}Mn was used. This average flux has an exponential-rigidity spectral shape with a shape parameter R_0 of 100 MV and an omnidirectional flux above 10 MeV at 1 AU, J_{10} , of 70 protons/cm²/s [11].

The fluxes of solar protons vary in the solar system, with the flux lower for greater distances D from the Sun [14]. The shape of this variation as a function of distance from the Sun is not well known, with various authors reporting variations ranging from D^{-1} (or even less) to D^{-3} . Thus most meteorites, which are exposed to SCR particles while at 2-3 AU for most of their orbit, will have been exposed to a smaller flux than used in these calculations. The average flux above for 1 AU will be used here, but it is probably much higher than the average flux seen by most meteoroids.

Calculations of SCR Production Rates: The calculations of the rates for producing these SCR-produced nuclides were done in the same way as my previous SCR calculations for meteorites [4]. The model is the solar-cosmic-ray one of Reedy and Arnold [15]. The irradiated objects were assumed to be spherical, and a range of radii R from zero to infinity was used, including several radii for smaller objects, such as 2 cm (or, using a density of 3.5 g/cm³, 7 g/cm²) as well as more typical sizes for meteorites (10, 20, and 50 cm).

The composition was an average for L-chondrites [16]. The more-common elements (and their abundances in g-element/g-meteorite) used in these calculations are O (0.377), Mg (0.149), Al (0.0122), Si (0.1850), K (0.000825), Ca (0.0131), Fe (0.215), and Ni (0.012). This composition was also used in calculating the rates that solar protons slowed and stopped in the irradiated object.

Calculated Rates and Profiles for SCR-Produced Nuclides: Results of these calculations are summarized below. Production rates are in units of atoms of nuclide per minute per kilogram of meteorite.

Approximate elemental production rates near the surface vary with the product nuclide. Oxygen makes most of the SCR-produced ^{10}Be (91%) and ^{14}C (97%), with the rest of the ^{10}Be being made from Mg (6%) and Si (2%). Magnesium is the main producer of ^{21}Ne (87%) and ^{22}Ne (83%), with Si the next most important target (11% and 14%, respectively). Silicon is the dominant source of ^{26}Al (72%), with the rest from Mg (11%) and Al (17%). Calcium is the main source of

^{36}Cl (78%) and ^{38}Ar (92%), with K (15% and 7%, respectively) and Fe (6% and 0.5%, respectively) making most of the rest. Iron makes about 98% of ^{53}Mn , with Ni making most of the remainder.

Table 1 gives the calculated production rates at the surface for L-chondrites with various radii.

| Nucl. | R=0 | R=2 | R=10 | R=50 |
|------------------|------|------|------|------|
| ^{10}Be | 4.4 | 3.3 | 2.4 | 2.2 |
| ^{14}C | 38. | 24. | 20. | 19. |
| ^{26}Al | 531. | 298. | 264. | 256. |
| ^{36}Cl | 2.6 | 1.8 | 1.4 | 1.3 |
| ^{53}Mn | 637. | 358. | 318. | 302. |
| ^{21}Ne | 541. | 300. | 268. | 255. |
| ^{22}Ne | 629. | 372. | 322. | 305. |
| ^{38}Ar | 81. | 47. | 42. | 40. |

The production rates at the very pre-atmospheric surface of an object in space are not very different except for very small objects. These very small objects have twice the surface production rates of a larger object.

Table 2 gives the calculated production rates at a depth of 1 cm from the surface for spherical L-chondrites with radii of 2, 10, and 50 cm and for a semi-infinite-slab geometry.

| Nucl. | R=2 | R=10 | R=50 | Slab |
|------------------|-----|------|------|------|
| ^{10}Be | 1.6 | 0.9 | 0.7 | 0.7 |
| ^{14}C | 8.4 | 4.4 | 3.6 | 3.4 |
| ^{26}Al | 59. | 30. | 25. | 23. |
| ^{36}Cl | 0.8 | 0.5 | 0.4 | 0.3 |
| ^{53}Mn | 68. | 35. | 28. | 27. |
| ^{21}Ne | 55. | 29. | 23. | 22. |
| ^{22}Ne | 98. | 51. | 41. | 39. |
| ^{38}Ar | 11. | 5.7 | 4.7 | 4.5. |

For a depth of 1 cm, the radii of the chondrite affects solar-proton production rates, with the higher rates in the smaller objects, where solar protons can

reach such a sample from more directions than for a larger object.

The production rates at the center of a 2-cm L-chondrite are about 0.8 of those at 1 cm because of the large fraction of solar protons that can pass through much of such a small object. Production rates in the center of a 10-cm spherical chondrite are lower by about an order of magnitude. The production-rate profiles in larger spheres decrease even more rapidly with depth than for a 10-cm object [4].

Conclusions: The production rates for solar-proton-produced nuclides calculated for spherical L-chondrites vary with the nuclide, the object's radius, and the sample's depth. Very small objects, such as cosmic dust, have very high solar-proton production rates. An object with a radius of ~2 cm has lower solar-proton production rates. However, such small meteoroids have solar-proton production rates that are higher than those in typical-sized (R~20-50 cm) meteoroids.

Objects recovered from cold or hot deserts that were small objects in space are much more likely to have preserved SCR-produced nuclides in them than would objects that were larger in space. These solar-proton production rates are uncertain because of the usually unknown orbit of the object and the uncertainties on how the fluxes of solar protons vary in the inner solar system. However, the presence of SCR-produced nuclides in an object is a good indication that the object was fairly small in space and that the sample was fairly close to the pre-atmospheric surface.

Acknowledgments: This work was supported by NASA and done under the auspices of the U.S. Department of Energy.

References: [1] Reedy R. C. (1995) *LPI-TR-95-02*, pp. 55-57. [2] Evans J. C. et al. (1987) *Lunar Planet. Sci. XVIII*, pp. 271-272. [3] Nishiizumi K. et al. (1995) *Lunar Planet. Sci. XXVI*, pp. 1053-1054. [4] Reedy R. C. (1987) *Lunar Planet. Sci. XVIII*, pp. 822-823. [5] Reedy R. C. and Marti K. (1991) in *The Sun in Time*, pp. 260-287. [6] Sisterson J. M. et al. (1997) *Nucl. Instrum. Methods, B123*, 324-329. [7] Michel R. et al. (1997) *Nucl. Instrum. Methods, B129*, 153-193. [8] Jull A. J. T. et al. (1998) *Geochim. Cosmochim. Acta*, 62, 3025-3036. [9] Rao M. N. et al. (1994) *Geochim. Cosmochim. Acta*, 58, 4231-4245. [10] Fink D. et al. (1998) *Geochim. Cosmochim. Acta*, 62, 2389-2402. [11] Reedy R. C. (1998) *Proc. Indian Acad. Sci. (Earth Planet. Sci.)*, 107, 433-440. [12] Sisterson et al. (1997) *Lunar Planet. Sci. XXVIII*, pp. 1329-1330. [13] Reedy R. C. (1992) *Lunar Planet. Sci. XXIII*, pp. 1133-1134. [14] Reedy R. C. et al. (1999) *Space Sci. Rev.*, in preparation. [15] Reedy R. C. and Arnold J. R. (1972) *J. Geophys. Res.*, 77,

537-555. [16] Wasson J. T. and Kallemeyn G. W.
(1988) *Phil. Trans. R. Soc. Lond. A*, 325, 535-544.

NOBLE GASES IN 15 METEORITES FROM THE SAHARA: EUCRITES, UREILITES, AND ORDINARY CHONDRITES. Peter Scherer, Matthias Pätsch and Ludolf Schultz, Max-Planck-Institut für Chemie, Postfach 3060, D-55020 Mainz, Germany (schultz@mpch-mainz.mpg.de).

Introduction: In recent years the Sahara has become an important source of new meteorite finds. Especially in Libya the two recovery areas Dar al Gani (DaG) and Hammadah al Hamra (HaH) have yielded between 1990 and 1999 more than 850 meteorites [1]. Several finds from hot deserts are heavily weathered and a meteoritic origin is not obvious from a first inspection. We report here noble gas analyses of 11 ordinary chondrites that are identified as meteorites by their noble gas record. These measurements have been carried out before other investigations took place and showed unambiguously that these rocks are meteorites. It should be mentioned that also several pseudometeorites with the appearance of meteorites were analyzed but their noble gas record did not indicate an extra-terrestrial origin; these results are not reported here. In addition, two eucrites and two ureilites from the Sahara were analyzed in connection with radionuclide measurements [2].

Results: Concentration and isotopic composition of He, Ne, Ar, Kr, and Xe have been determined in bulk samples (sample weights about 100 mgs). Apparatus and procedures of measurements were similar to those given in [3]. The results are presented in Tab.1. Uncertainties of gas concentrations are believed to be less than $\pm 5\%$, those of isotope ratios are generally less than $\pm 1\%$. Tab.1 also contains the cosmogenic isotope ratio ($^{22}\text{Ne}/^{21}\text{Ne}$)_c together with exposure ages, calculated from the cosmogenic nuclides ^3He , ^{21}Ne , and ^{38}Ar using methods given in [3,4,5]. For ureilites an average bulk chemistry was used to calculate production rates. Due to large variations of the chemical composition of this class, the calculated exposure age may have uncertainties of about 30%.

Discussion: Moderate to severely altered chondrites from hot deserts are characterized by a contribution of atmospheric gases [6]. This is seen best in an enhanced concentration of Kr. While trapped gases in chondrites have a $^{84}\text{Kr}/^{132}\text{Xe}$ ratio around 1, this ratio is 28 in the terrestrial atmosphere. Fig.1 compares measured ^{84}Kr and ^{132}Xe in the chondrites from Dar al Gani

measured here with those found in H chondrite falls [7]. Most of the values of chondrites from the hot desert are shifted to the right of the line defined by H-chondrite falls. This indicates severe weathering of these meteorite finds.

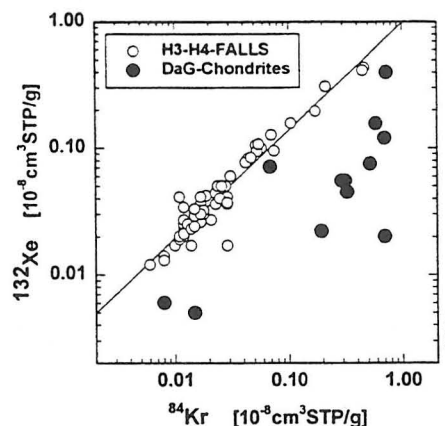


Fig.1: Plot of ^{84}Kr vs. ^{132}Xe in H-chondrite fall and chondrite finds from the Sahara.

The noble gases exclude pairing of the investigated chondrites. The H6 chondrite DaG 304 has a rather short exposure age of about 1 Ma. Implications concerning orbital parameters of such meteoroids are discussed in [8].

A short exposure age is also observed for the ureilite HaH 064 which is, however, not uncommon among ureilites. DaG 084 is not paired with two other ureilites from the Dar al Gani region (DaG 319 and DaG 340) [9].

References: [1] Weber D. *et al.* (this volume). [2] Merchel S. *et al.* (this volume). [3] Scherer P. *et al.* (1998) *Meteoritics Planet. Sci.* **33**, 259. [4] Eugster O. (1988) *Geochim. Cosmochim. Acta* **52**, 1649. [5] Eugster O and Michel Th. (1995) *Geochim. Cosmochim. Acta* **59**, 177. [6] Scherer P. and Schultz L. (1994) in: *Noble Gas Geochemistry and Cosmochemistry*, ed. J. Matsuda. [7] Schultz *et al.* (1990) *Meteoritics* **25**, 405. [8] Patzer A. *et al.* (1999) *LPSC XXX*. [9] Scherer P. *et al.* (1988) *LPSC XXIX*.

NOBLE GASES IN 15 METEORITES: P. Scherer et al.

| Class | ³ He | ⁴ He | ²⁰ Ne | ²¹ Ne | ²² Ne | ³⁶ Ar | ³⁸ Ar | ⁴⁰ Ar | ⁸⁴ Kr | ¹³² Xe | ²² Ne/ ²¹ Ne _c | Exposure Ages [Ma] | | | |
|--------------------------|-----------------|-----------------|------------------|------------------|------------------|------------------|------------------|------------------|------------------|-------------------|---|--------------------|-----------------|-----------------|------|
| | | | | | | | | | | | | T ₃ | T ₂₁ | T ₃₈ | |
| Dar al Gani | | | | | | | | | | | | | | | |
| Chondrites | | | | | | | | | | | | | | | |
| 298 | LL4 | 88.45 | 1968 | 16.60 | 17.97 | 19.83 | 1.82 | 2.15 | 6289 | 0.008 | 0.006 | 1.138 | 55.3 | 60.9 | 53.8 |
| 299 | H4 | 50.12 | 1527 | 10.70 | 8.87 | 10.43 | 11.06 | 2.91 | 7403 | 0.293 | 0.055 | 1.187 | 32.4 | 38.7 | 24.9 |
| 300 | H6 | 21.33 | 1167 | 3.66 | 3.54 | 4.30 | 6.64 | 1.86 | 4469 | 0.069 | 0.071 | 1.251 | 14.0 | 18.7 | 20.6 |
| 301 | L6 | 31.23 | 234 | 10.19 | 9.31 | 9.93 | 15.63 | 3.79 | 4246 | 0.587 | 0.156 | 1.077 | 19.2 | 23.8 | 23.1 |
| 302 | H5 | 46.34 | 1395 | 10.63 | 11.17 | 11.95 | 10.95 | 3.03 | 7613 | 0.015 | 0.005 | 1.097 | 29.2 | 34.0 | 25.1 |
| 304 | H6 | 1.14 | 810 | 2.56 | 0.33 | 0.54 | 14.39 | 2.78 | 8720 | 0.556 | 0.075 | 1.110 | 0.7 | 1.1 | 1.9 |
| 308 | H6 | 2.92 | 595 | 2.31 | 1.17 | 1.35 | 6.50 | 1.36 | 5093 | | | 1.073 | 1.8 | 3.2 | 3.3 |
| 309 | L6 | 13.62 | 763 | 3.61 | 2.22 | 2.84 | 6.69 | 1.55 | 7396 | 0.195 | 0.022 | 1.256 | 8.8 | 11.0 | 10.5 |
| 310 | H5/6 | 33.45 | 1578 | 7.92 | 7.97 | 8.55 | 8.37 | 2.24 | 6278 | 0.327 | 0.045 | 1.072 | 21.0 | 21.4 | 16.7 |
| 311 | H6 | 5.96 | 1150 | 2.61 | 1.63 | 1.82 | 7.33 | 1.54 | 6745 | 0.270 | 0.049 | 1.075 | 3.7 | 4.4 | 4.0 |
| 313 | L/LL4 | 15.06 | 1364 | 6.82 | 3.48 | 4.40 | 39.93 | 7.97 | 6249 | 0.728 | 0.397 | 1.200 | 9.6 | 14.7 | 15.3 |
| Eucrites | | | | | | | | | | | | | | | |
| 391 | EUC | 36.82 | 5837 | 5.82 | 5.93 | 6.78 | 4.04 | 4.71 | 2151 | | | 1.144 | 22.8 | 29.4 | 29.9 |
| 411 | EUC | 45.29 | 3228 | 6.99 | 7.34 | 8.27 | 3.24 | 3.46 | 1255 | | | 1.127 | 27.9 | 35.1 | 21.6 |
| Ureilites | | | | | | | | | | | | | | | |
| 084 | URE | 31.10 | 182 | 9.33 | 8.01 | 8.77 | 39.00 | 7.84 | 2709 | 0.499 | 0.200 | 1.100 | 18.7 | 18.6 | |
| Hammadah al Hamra | | | | | | | | | | | | | | | |
| 064 | URE | 2.40 | 108 | 1.988 | 0.35 | 0.59 | 499.10 | 94.65 | 1165 | 3.822 | 2.689 | 1.205 | 1.5 | 1.2 | |

Tab.1: Concentrations (in 10⁻⁸cm³STP/g) of He, Ne, Ar, ⁸⁴Kr and ¹³²Xe as well as the cosmogenic ²²Ne/²¹Ne ratio and calculated cosmic-ray exposure ages

DEFLATION AND METEORITE EXPOSURE ON PLAYA LAKES IN THE SOUTHWESTERN UNITED STATES: UNPAIRED METEORITES AT LUCERNE DRY LAKE, CALIFORNIA

Robert S. Verish,¹ Alan E. Rubin,² Carleton B. Moore,³ Ronald A. Oriti⁴; ¹P.O. Box 237, Sunland, CA 91040, USA; ²Institute of Geophysics and Planetary Physics, University of California, Los Angeles, CA 90095-1567, USA; ³Center for Meteorite Studies, Arizona State University, Tempe, AZ 85287-1604, USA; ⁴1610 Water Trough Rd., Sebastopol, CA 95472, USA.

Numerous dry lakes (playas) dot the Mojave Desert in Southern California and adjacent desert regions in Nevada and Arizona. Most have been significantly affected by deflation processes aided by the lack of protective vegetation and occurrence of fine-grained sediments.

Meteorites have been found on several playas including Lucerne Dry Lake, Rogers (formerly Muroc) Dry Lake, Rosamond Dry Lake, Roach Dry Lake, Alkali Lake, and an unnamed dry lake near the town of Bonnie Claire in Nye County, Nevada. Unpaired meteorites have been found near one another on the same playa.

Since 1963, 17 meteorite specimens (1.2-37.4 g), collectively called Lucerne Valley, have been found on Lucerne Dry Lake (Table 1). Most appear to be completely covered with fusion crust, suggesting that their small size is due to fragmentation in the atmosphere and not to terrestrial weathering. The collection of meteorites on Lucerne Dry Lake is aided by the paucity of terrestrial rocks coarser than small pebbles; this is unusual for dry lakes in the region. Sixteen of the meteorite specimens from Lucerne Dry Lake were available for analysis.

Out of the 16 analyzed stones, there are at least eight and probably nine separate meteorites (Table 2). The meteorites have retained the name Lucerne Valley (abbreviated LV) and are numbered in chronological order by the date on which they were found. The mean size of the nine distinct meteorites, taking pairing into account, is 17 g.

The large number of distinct meteorites from Lucerne Dry Lake implies that other dry lakes in the region should also be excellent candidates for high-yield meteorite-collecting areas.

Upon falling, small meteorites reach a terminal velocity of $\sim 300 \text{ m s}^{-1}$ and are unlikely to penetrate the lake bed surface when it is dry. When wet, the playas contain some suspended clay particles, but not enough to cause the meteorites to be deeply buried after the clay settles. Only rare catastrophic floods carrying large sediment loads would be able to bury the meteorites to depths $>1 \text{ m}$. However, there are two principal factors which render this scenario unlikely:

First, because discharge decreases downstream in arid channels, playa lakes are likely to receive only fine-grained sediments. Second, alluvial fans located between playa lakes and nearby mountains trap much of the total sediment load before it reaches the playas. It seems likely that the meteorites on Lucerne Dry Lake represent unburied remnants of strewn fields from small overlapping meteorite showers.

The ratio of separate meteorites to total number of specimens ($9/16 = \sim 0.6$) at Lucerne Dry Lake is among the highest in the world, comparable to that of well-characterized samples from Roosevelt County, New Mexico (~ 0.7). It results from two effects: First, no large meteorite showers such as that of the Holbrook fall, which produced ~ 14000 individual specimens, are represented at Lucerne Dry Lake. Second, lack of deep burial coupled with significant deflation have exposed remnants of distinct strewn fields.

Although all meteorites found to date at Lucerne Dry Lake are ordinary chondrites, these groups constitute only $\sim 80\%$ of falls and it is likely that less-common meteorite varieties will turn up. We are continuing to study meteorites recovered from other dry lakes in the Mojave desert.

Table 1. Meteorites recovered from Lucerne Dry Lake.

| sample | mass | sample | mass |
|--------|--------|--------|-------|
| LV001 | 15.8 g | LV010 | 6.4 g |
| LV002 | 5.8 | LV011 | 3.8 |
| LV003 | 7.5 | LV012 | 1.2 |
| LV004 | 37.4 | LV013 | 4.1 |
| LV005 | 3.1 | LV014 | 3.4 |
| LV006 | 26.9 | LV015 | 12.5 |
| LV007* | 4.8 | LV016 | 4.1 |
| LV008 | 2.0 | LV017 | 12.8 |
| LV009 | 3.0 | | |

*Specimen not analyzed.

Table 2. Classification and pairing of meteorites from Lucerne Dry Lake.

| | | | | Fa | pairs |
|-------|-----|----|----|----------|-----------------|
| LV001 | L6 | S2 | W3 | 24.3±0.3 | 004,005 |
| LV002 | LL4 | S2 | W3 | 27.5±0.6 | none |
| LV003 | H6 | S3 | W3 | 18.0±0.4 | none |
| LV006 | H4 | S2 | W3 | 18.4±0.4 | 008,009, 010 |
| LV011 | L6 | S4 | W3 | 24.5±0.2 | none |
| LV012 | H6 | S2 | W3 | 19.4±0.3 | none |
| LV013 | L5 | S2 | W3 | 25.3±0.3 | 014,016 |
| LV015 | LL6 | S3 | W2 | 30.9±0.1 | none |
| LV017 | L6 | S3 | W4 | 25.5±0.6 | none |

Iron meteorites from Antarctica: more specimens, still 40% ungrouped

J. T. Wasson. Institute of Geophysics and Planetary Physics, University of California, Los Angeles, CA 90095-1567 USA

Clarke (1986) was the first to recognize that ungrouped irons are more common in Antarctica than in the regions where most irons have been collected; his conclusion was based on the first 21 irons collected in Antarctica. Wasson et al. (1989) reported compositional data for 24 Antarctic irons and reported that 8 were ungrouped; the ungrouped fraction of 0.33 was found to be about twice that (0.153) observed in irons from the remainder of the world. Wasson (1990) reported data for 7 additional Antarctic irons, and reported that 12 of 31 were ungrouped, a fraction of 0.39.

In Table 1 I summarize the data obtained to date on independent Antarctic iron meteorites by our UCLA neutron-activation laboratory. With about 5 exceptions, the listed values are the means of duplicate determinations. We have now analyzed 40 independent iron meteorites; in Table 2 I list 8 other irons that proved to be paired with meteorites listed in Table 1. Because of the close relationship between pallasites and iron meteorites, in Table 3 I also list our data for two Ant-arctic pallasites that were studied at UCLA. Our new results confirm the previously reached conclusion about the abundance of ungrouped irons. In fact, the ungrouped fraction has increased slightly; of the 40 irons 16 are ungrouped, a fraction of 0.40. The two meteorites with pallasite structures are both small (≈ 50 g); one is ungrouped, the other a high-Ir anomalous member of the main-group pallasites (PMG).

The ultimate goal of a meteorite taxonomic system is to determine which meteorites formed in the same parent body. There is little doubt that the large magmatic groups IIAB, IIIAB and IVA are each from a single body, and no reason to believe that any other iron-meteorite groups could have formed in the same parent asteroids (even though IIIE is quite similar to IIIAB, it is compositionally resolvable).

Thus, one can hypothesize that we should expect irons from magmatic groups to have nearly constant Ga, Ge, Co and Cu, and inversely correlated Ir and Au; irons from nonmagmatic groups should have relatively small, correlated ranges of all siderophiles. To

search for possible related duos or trios among the ungrouped Antarctic irons I sorted the data in terms of Ga, Au and Co. The only possible relationship that suggested itself was between LEW88023 and ALH84233, but even here most of the expected compositional trends are not present. As a result, I tentatively conclude that these two ungrouped irons originated on separate parent bodies.

The chief caveat is that some of the ungrouped irons are so small that they could be slugs from impact altered chondrites or subchondritic regoliths such as Bencubbin, rather than fragments of large (>10 m diameter) metallic magmas. The three smallest (ALH84233, LEW85369, LEW88023) have recovered masses of 8, 10 and 14 g and are all ungrouped. The next smallest, with a mass of 15 g, is classified IIE, but group IIE (a) shows more scatter than most other groups, and (b) may consist of melts generated by impacts onto chondritic asteroids (Wasson and Wang, 1986; Ruzicka et al., 1999). If six small irons having masses ≤ 21 g are removed from the data set the fraction of ungrouped drops to $13/34 = 0.38$.

Wasson et al. (1989) and Wasson (1990) examined possible mechanisms that could cause irons from Antarctica to have been more efficient at sampling "minor" asteroids than those from the temperate and subtropical latitudes where most iron meteorites have been collected. As discussed in the latter work, the difference cannot be a latitudinal effect. Even though all Antarctic irons are collected at latitudes $>71^\circ$ whereas most other irons (630 of 660) were collected between 10 and 60° , primarily because of the 23.5° obliquity the Earth's spin axis, simulations show only minor latitudinal effects for a variety of meteoroid orbits (Halliday and Griffin, 1982).

Stochastic variations in meteoroid populations associated with differences in terrestrial ages are also implausible. There is no resolvable difference in terrestrial ages among the two sets of irons (Wasson, 1990).

The key difference seems to be the smaller size of many Antarctic irons. Wasson (1990)

Antarctic iron meteorites: Wasson J. T.

noted that the median mass of Antarctic irons of 300-400 g was 100X smaller than that of the nonAntarctic set. This median mass of Antarctic irons remains the same for this larger set if the smallest 1-3 irons are dropped from the list.

Probing further into the relationship between size and classification we discover that only 1 of the 6 Antarctic irons having masses >10 kg is ungrouped, and it (Lazarev) is the smallest of the set. Of the irons having masses in the range 30 g-10 kg, 12/28 (0.43) are ungrouped. Within this range there is no resolvable difference in the ungrouped fraction in sets based on logarithmic increments in mass.

Meteoroids travel from the Asteroid Belt to the Earth via two dominant escape routes: (a) the 3:1 period resonance with Jupiter, and (b) the ν_6 resonance of the variation of the orbital perihelion direction with that of Saturn. Meteoroids having orbits coincident with one or the other of these resonances are brought into Earth-crossing orbits within a short period of time. Recent work by Morbidelli and Gladman (1998) has shown that this transfer commonly occurs within ≈ 2 Ma, a factor of 5 shorter than had been indicated by earlier simulations.

Wasson (1990) pointed out that, compared to larger meteoroids, smaller objects are more efficiently transferred into orbits that are appreciably different from that of the parent asteroid. In other words, they tend to wander farther from home. It has long been understood that, during cratering events, the smaller the ejecta, the larger the mean ejection velocity. Thus, the probability that a small meteoroid can directly enter a resonance as a result of cratering ejection from the parent body increases as the size of the fragment decreases. Wasson (1990) also noted that the smaller the fragment, the larger the number of minor collisional events it will, on average, have experienced, and that these "jostling" events lead to a random walk of the orbital parameters away from those of the parent.

A suggested variant of this mechanism is that metallic meteoroids may be swept up by highly porous stony rubble piles. Thereafter the metal will be in an orbit similar to that

possessed by the stony material, which can also lead to a random walk away from the parental orbit. A key question is the fraction of metallic meteoroids that would survive such collisions. It seems plausible that the closer the match between the size of the meteoroids and the mean size of the rubble clasts, the larger the fraction that would survive as a single piece.

In summary, the fraction of ungrouped irons in the set of 40 independent irons from Antarctica is at least twice that of irons from the remainder of the world. The difference is attributed to the >100X smaller median size of the Antarctic irons. It is suggested that the parent-bodies of most ungrouped irons are in orbits far from orbital resonances that transfer meteoroids into Earth-crossing orbits within a few Ma. Independent of the parent-body orbit, the smaller the ejecta fragment, the higher the probability that it can reach a resonance. Thus the smaller the mean size of the collected meteorite, the larger the probability of sampling parent bodies in orbits far removed from the resonances.

Acknowledgements

I am indebted to several key colleagues for the reported INAA data, particularly F. Ulf-Møller, B.-G. Choi, E. A. Jerde and J. W. Richardson. I thank those who provided samples. The majority were provided by the U. S. Meteorite Working group, with most of the burden falling on R. S. Clarke. Important samples were also received from H. Kojima, K. Yanai, T. McCoy and L. Schultz. This research was supported in part by NASA grant NAG5-4568

References:

- Clarke R. S. (1990) *Lunar Planet. Inst. Tech. Rept.* **86-01**, 28-29.
- Halliday I. and Griffin A. A. (1982) *Meteoritics* **17**, 31-46.
- Morbidelli A. and Gladman B. (1998) *Meteoritics Plan. Sci.* **33**, 999-1016.
- Ruzicka A., Fowler G. W., Snyder G. A., Prinz M., Papike J. J. and Taylor L. A. (1999) *Geochim. Cosmochim. Acta* **63**, 2123-2143.
- Wasson J. T. (1990) *Science* **249**, 900-902.
- Wasson J. T. and Wang J. (1986) *Geochim. Cosmochim. Acta* **50**-725-732.
- Wasson J. T., Ouyang S., Wang J., Jerde E., *Geochim. Cosmochim. Acta* **53**-735-744.

Antarctic iron meteorites: Wasson J. T.

Appendix: The pairing of Lewis Cliff irons LEW87109 and LEW88631 with LEW85369.

Three tiny slugs of metal from the Lewis Cliff collection site were found to be closely related and should be paired. The total mass involved in these three specimens is only 10 g. The data for these three irons are listed in Tables 1 and 2. The range of compositions is larger than commonly observed within adjacent samples of the iron meteorite groups, but the trends are consistent with those expected for heterogeneous sampling of coexisting kamacite and taenite. Most elements have taenite/kamacite ratios in the range 2 to 5, but

Co and As have a greater affinity for kamacite than taenite. Thus, even though Ni, Ir and Au are higher by factors of 1.1 to 1.6 in LEW85369 than in LEW88631, we find it indicative of a close genetic relationship among these three that LEW87109 has an intermediate composition, and that Co and As are higher by factors of 1.05-1.08 in LEW88631 than in LEW85369. The Co in LEW87109 is again intermediate, the As is the same as that in LEW88631 to within experimental uncertainty.

The other paired irons listed in Table 2 have been discussed in earlier papers by our team.

Antarctic iron meteorites: Wasson J. T.

Table 1. Compositional data for 40 independent Antarctic iron meteorites.

| meteorite | mass kg | Cr μg/g | Co mg/g | Ni mg/g | Cu μg/g | Ga μg/g | Ge μg/g | As μg/g | Sb ng/g | W ng/g | Ir μg/g | Pt μg/g | Au μg/g | group |
|--------------------------------|------------|------------|------------|------------|------------|------------|------------|------------|------------|-----------|------------|------------|------------|---------|
| AllanHil ALH84165 | 0.095 | 118 | 5.03 | 80.6 | 178 | 20.1 | 40.0 | 4.21 | 20.0 | 1.09 | 3.49 | 12.9 | 0.646 | IIIAB |
| AllanHil ALH84233 | 0.014 | 12 | 5.39 | 64.6 | 168 | 14.0 | 63.0 | 14.4 | 273 | 0.99 | <0.003 | <0.7 | 1.040 | ungr |
| AllanHil ALHA76002 | 19.7 | 46 | 4.43 | 67.6 | 152 | 89.2 | 410 | 10.8 | 280 | 1.33 | 2.57 | | 1.515 | IAB |
| AllanHil ALHA77255 | 0.76 | 418 | 5.72 | 122.6 | 10 | 0.083 | 0.058 | 0.292 | <150 | 1.23 | 10.0 | | 0.071 | ungr |
| AllanHil ALHA77283 | 10.5 | 23 | 4.87 | 72.8 | 145 | 81.1 | 320 | 15.2 | 399 | 1.06 | 2.16 | 7.0 | 1.707 | IAB |
| AllanHil ALHA78100 | 17.8 | 43 | 4.38 | 55.0 | 136 | 60.0 | 182 | 4.08 | 52 | 4.03 | 27.0 | | 0.544 | IIAB |
| AllanHil ALHA78252 | 2.79 | 112 | 4.05 | 95.0 | 154 | 2.44 | 0.138 | 13.3 | 6.3 | 0.46 | 0.374 | | 2.536 | IVA |
| AllanHil ALHA80104 | 0.882 | 8 | 6.81 | 156.0 | 299 | 5.80 | 10.2 | 26.1 | 567 | 0.41 | 0.080 | | 2.660 | ungr |
| AllanHil ALHA81014 | 0.188 | 69 | 5.40 | 108.0 | 94 | 7.53 | 1.52 | 6.05 | 10 | 1.26 | 3.64 | | 1.110 | ungr |
| DerrPeak DRP78001 [^] | 251 | 35 | 4.64 | 63.0 | 117 | 56.1 | 135 | 9.55 | 101 | 0.66 | 0.014 | | 1.202 | IIAB |
| ElephMor EET83230 | 0.530 | 13 | 4.48 | 164.0 | 492 | 1.34 | 0.075 | 13.4 | 7 | 0.22 | 0.105 | | 2.660 | ungr |
| ElephMor EET83245 | 0.059 | 22 | 4.79 | 60.4 | 118 | 55.4 | 157 | 9.70 | 86 | 0.74 | 0.026 | | 1.070 | IIAB-an |
| ElephMor EET83333 | 0.189 | 19 | 4.88 | 80.6 | 184 | 74.8 | 226 | 15.7 | 459 | 0.80 | 2.88 | 6.8 | 1.750 | IAB |
| ElephMor EET83390 | 0.015 | 20 | 4.45 | 83.1 | 228 | 27.8 | 68.2 | 11.7 | 191 | 1.15 | 3.86 | 9.6 | 1.170 | IIIE |
| ElephMor EET84300 | 0.072 | 30 | 5.10 | 102.2 | 192 | 41.3 | 92.0 | 13.9 | 400 | 0.33 | 1.82 | 2.6 | 1.290 | ungr |
| ElephMor EET87504* | 0.041 | 46 | 5.29 | 208.6 | 1065 | 22.9 | 104 | 29.3 | 2752 | 0.39 | 3.01 | 8.0 | 1.957 | IAB-an |
| ElephMor EET87516 | 0.036 | 340 | 4.86 | 93.1 | 185 | 1.71 | 2.66 | 6.08 | 18 | 0.82 | 6.24 | 10.0 | 0.909 | ungr |
| ElephMor EET92029 | 2.43 | 18 | 5.06 | 82.2 | 123 | 23.8 | 82 | 10.1 | <100 | 0.34 | 0.087 | 4.4 | 1.176 | ungr |
| GrosvMtn GRO85201 | 1.40 | 67 | 5.15 | 84.7 | 146 | 20.0 | 42.3 | 7.41 | 68 | 0.57 | 0.359 | 6.2 | 1.010 | IIIAB |
| GrosvMtn GRO95511 | 0.064 | 19 | 4.87 | 81.8 | 197 | 72.8 | | 16.3 | 348 | 0.86 | 1.99 | 6.3 | 1.695 | IAB |
| GrosvMtn GRO95522 | 0.962 | 21 | 5.14 | 79.4 | 159 | 21.2 | | 7.42 | <100 | 0.74 | 0.650 | 8.9 | 0.871 | IIIAB |
| InlandForts ILD83500 | 2.52 | 29 | 9.46 | 174.5 | 338 | 19.3 | 47.9 | 11.4 | 122 | 0.71 | 7.15 | | 1.580 | ungr |
| Lazarev | 10.0 | 76 | 6.93 | 96.4 | 226 | 15.2 | 24.0 | 8.94 | 81 | 0.90 | 3.94 | 10.5 | 1.020 | ungr |
| LewisClif LEW85369 | 0.010 | 50 | 3.33 | 74.2 | 318 | 46.8 | 100 | 13.4 | 519 | 0.69 | 3.49 | 6.3 | 1.490 | ungr |
| LewisClif LEW86211 | 0.163 | 796 | 5.41 | 87.7 | 463 | 34.6 | 280 | 14.3 | 350 | 2.50 | 31.6 | 33.9 | 1.418 | ungr |
| LewisClif LEW86540 | 0.021 | 12 | 5.99 | 182.9 | 479 | 4.30 | 2.8 | 28.8 | 845 | <60 | 0.04 | <2.0 | 1.813 | III CD |
| LewisClif LEW88023 | 0.008 | 12 | 5.52 | 69.0 | 163 | 11.8 | 58.9 | 16.2 | 337 | 1.08 | 0.007 | 1.1 | 1.163 | ungr |
| Mt. Wegener | 3.48 | 125 | 4.99 | 75.9 | 158 | 19.3 | 38.1 | 4.27 | 34 | 1.01 | 3.64 | 11.2 | 0.614 | IIIAB |
| MtHowe HOW88403 | 2.48 | 812 | 4.34 | 86.1 | 382 | 22.1 | 53.2 | 11.9 | 360 | 0.96 | 4.70 | 7.9 | 1.249 | ungr |
| NeptuneMountains | 1.07 | 23 | 4.72 | 72.0 | 148 | 78.2 | 269 | 14.4 | 315 | 0.91 | 2.20 | | 1.620 | IAB |
| PecoraEscr PCA91003 | 0.117 | 29 | 4.62 | 70.8 | 148 | 82.6 | 327 | 13.0 | 338 | 1.11 | 3.61 | 5.9 | 1.504 | IAB |
| PurgPeak PGPA77006 | 19.1 | 25 | 4.69 | 71.6 | 148 | 79.4 | 284 | 14.5 | 426 | 0.96 | 2.16 | | 1.579 | IAB |
| RecklPeak RKPA80226 | 0.160 | 23 | 4.88 | 82.6 | 173 | 67.6 | 255 | 17.0 | 450 | 0.90 | 2.06 | | 1.740 | IAB |
| ThielMtn TIL91725 | 0.091 | 209 | 4.70 | 79.3 | 98 | 73.6 | 234 | 12.7 | 429 | 1.02 | 3.67 | 6.2 | 1.529 | IAB |
| WiscRng WIS91614 | 0.299 | 122 | 4.98 | 75.7 | 172 | 18.6 | | 3.71 | <100 | 1.19 | 7.910 | 14.6 | 0.580 | IIIAB |
| Yamato Y75031 | 0.392 | 40 | 5.93 | 141.0 | 452 | 30.3 | 232 | 20.2 | 990 | 0.96 | 0.401 | 5.7 | 2.070 | ungr |
| Yamato Y75105 | 0.020 | 46 | 4.87 | 59.1 | 132 | 58.2 | 170 | 4.30 | | 2.11 | 2.50 | | 0.700 | IIAB |
| Yamato Y790517 | 0.190 | 36 | 5.44 | 70.7 | 118 | 19.8 | 47.0 | 8.03 | 55 | 0.69 | 0.523 | | 0.924 | ungr |
| Yamato Y790724 | 2.17 | 124 | 4.97 | 79.8 | 192 | 20.4 | 35.9 | 3.66 | 31 | 1.31 | 9.25 | | 0.556 | IIIAB |
| Yamato Y791694 | 0.071 | <84 | 4.69 | 71.6 | 148 | 79.4 | 255 | 34.2 | 3980 | <0.3 | 0.24 | | 1.860 | IAB |

Analyzed specimens: *EET87506; [^]DRPA78009.

Antarctic iron meteorites: Wasson J. T.

Table 2. Compositional data for specimens of 8 Antarctic irons paired with meteorites listed in Table 1.

| meteorite | specimen | group | Cr | Co | Ni | Cu | Ga | Ge | As | Sb | W | Ir | Pt | Au |
|------------|-----------|-------|-----------------|---------------|---------------|-----------------|-----------------|-----------------|-----------------|---------------|-----------------|-----------------|-----------------|-----------------|
| | | | $\mu\text{g/g}$ | mg/g | mg/g | $\mu\text{g/g}$ | $\mu\text{g/g}$ | $\mu\text{g/g}$ | $\mu\text{g/g}$ | ng/g | $\mu\text{g/g}$ | $\mu\text{g/g}$ | $\mu\text{g/g}$ | $\mu\text{g/g}$ |
| ALHA76002p | ALHA77250 | IAB | 31 | 4.50 | 69.4 | 158 | 92.7 | 411 | 11.3 | 310 | 1.82 | 2.50 | | 1.450 |
| ALHA76002p | ALHA77290 | IAB | 123 | 4.45 | 69.7 | 165 | 91.9 | 423 | 11.3 | 320 | 1.55 | 2.49 | | 1.460 |
| ALHA76002p | ALHA77263 | IAB | 29 | 4.47 | 66.5 | 143 | 97.9 | | 11.9 | 360 | 1.51 | 2.53 | | 1.565 |
| ALHA76002p | ALHA77289 | IAB | 32 | 4.57 | 66.6 | 145 | 96.8 | 408 | 12.2 | 242 | 1.55 | 2.72 | | 1.510 |
| ALHA78100p | ALHA81013 | IIAB | 85 | 4.45 | 54.8 | 147 | 58.3 | 192 | 3.86 | 39 | 3.74 | 30.8 | | 0.532 |
| LEW85369p | LEW87109 | ungr | 34 | 3.56 | 64.3 | 152 | 53.3 | | 14.3 | | 0.82 | 2.99 | 7.4 | 1.339 |
| LEW85369p | LEW88631 | ungr | 59 | 3.61 | 60.2 | 165 | 47.4 | 135 | 14.1 | 290 | 0.73 | 2.18 | 5.2 | 1.316 |
| Y75031p | Y791076 | ungr | 15 | 5.94 | 139.0 | 402 | 32.0 | 264 | 24.5 | 1200 | 1.17 | 0.393 | | 2.280 |

Table 3. Compositional data on two Antarctic meteorites having pallasitic structures. The PCA specimen is an anomalous main group pallasite, the Yamato specimen is an ungrouped pallasite.

| meteorite | group | mass | Cr | Co | Ni | Cu | Ga | Ge | As | Sb | W | Ir | Pt | Au |
|---------------------|--------|-------|-----------------|---------------|---------------|-----------------|-----------------|-----------------|-----------------|---------------|-----------------|-----------------|-----------------|-----------------|
| | | kg | $\mu\text{g/g}$ | mg/g | mg/g | $\mu\text{g/g}$ | $\mu\text{g/g}$ | $\mu\text{g/g}$ | $\mu\text{g/g}$ | ng/g | $\mu\text{g/g}$ | $\mu\text{g/g}$ | $\mu\text{g/g}$ | $\mu\text{g/g}$ |
| PecoraEscr PCA91004 | PMG-ai | 0.050 | 32 | 5.12 | 95.7 | 128 | 23.7 | 57.4 | 15.8 | 170 | 0.33 | 0.764 | 3.0 | 2.006 |
| Yamato Y8451 | Pungr | 0.055 | 90 | 7.98 | 145.4 | 522 | 19.6 | 59.1 | 19.4 | 1169 | 1.49 | 6.87 | 16.6 | 2.102 |

THE LIBYAN METEORITE POPULATION D. Weber¹, J. Zipfel² & A. Bischoff¹

¹Institut für Planetologie, Wilhelm-Klemm-Str. 10, 48149 Münster, Germany, bischoa@nwz.uni-muenster.de; ²Max-Planck-Institut für Chemie, Postfach 3060, 55020 Mainz, Germany, zipfel@mpch-mainz.mpg.de

Introduction: During the last decade more than 2000 meteorites were found in the Sahara. Two extraordinary recovery areas are the Hammadah al Hamra (HH) and the Dar al Gani (DG) regions in Libya, where more than 850 meteorites were collected from 1990 to 1999 (>800 meteorites from 1994-1999). At present, more than 750 meteorites are classified (Meteoritical Bulletins No. 71, 80-83 [1-5]) by detailed mineralogical and chemical studies. The classifications include the meteorite class and usually the degrees of shock metamorphism and weathering, the chemical composition of major phases (e.g., olivine and pyroxene) and striking petrographic features such as brecciation or the occurrence of shock veins or impact melts. The mentioned find sites are large, flat and almost featureless desert areas (the so-called "Regs"), covered with light-coloured sediments. The erosion rate is low as indicated by terrestrial ages of the meteorites up to 30000 years or even more [6]. In these areas, the meteorite search is done by car. From the field of view, the average driving distance and find rate per day, a meteorite abundance of around 1.2 meteorites per square kilometer can be calculated. However, the single mass of a meteorite from the Sahara (and especially from DG and HH) is usually larger than 150g, which is, on average, higher than the typical masses of meteorites from Antarctica, Roosevelt County and Nullarbor, which range between 10 and 100g. It can be concluded that most small samples in the Sahara were overlooked and that, therefore, the meteorite abundance should be higher than the estimated value of 1.2/km².

Results: In order to perform a statistical analysis of the Libyan meteorite population, paired samples must be recognized. Theoretically, the number of paired samples can be estimated by comparing find locations and petrologic features of the meteorites, but also by the degree of shock metamorphism and weathering, and, if the data are present, the oxygen isotopic composition, and abundances of noble gases and cosmogenic nuclides. For rare meteorite classes, which are of scientific interest, pairing can easily be recognized because of their particular petrological and chemical features and the detailed study of them (e.g. oxygen isotopes, noble gases). In this work, we make a detailed statistical analyses of the DG and HH meteorites classified in Münster and Mainz. This study includes 630 meteorites (HH: 235, DG: 395), divided into 565 ordinary chondrites (H: 295, L: 216, LL: 54), 44 carbonaceous chondrites, 3 Rumuruti chondrites, 16 achondrites, and 2 iron meteorites. Detailed petrographical and chemical studies allowed a solution to the pairing problem of the more rare meteorite classes. The achondrites comprise 6 unpaired ureilites, three unpaired eucrites and two unpaired Lunar meteorites, one winonaite, and one Martian meteorite. The three Rumurutites and both iron meteorites are not paired, whereas the 44 carbonaceous chondrites represent only seven distinct meteorites (2 COs, 2CKs, 1 Coolidge-type, one unusual C3 meteorite, and one CH) [compare 7]. Pairing among ordinary chondrites is not easy to estimate, as there are too many rocks from the same find site showing very similar mineral compositions and degrees of shock metamorphism and weathering. This is especially the case for the most common meteorite types, such as H5 or L6.

Discussion: The classification of a large number of meteorites from one region gives the opportunity to characterize the meteorite population and to compare it with other populations or with the world falls. In the case of the Libyan meteorite population it is first necessary to solve the pairing problem of the ordinary chondrites before a comparison with other populations can be done. Table 1 shows the Libyan meteorite population in comparison to the Nullarbor and Antarctic finds and the world falls. Assuming a value of e.g., 60% unpaired ordinary chondrites as suggested in other works [8], the Libyan meteorite population would have a low abundance of carbonaceous chondrites, iron meteorites, and achondrites, and a very high abundance of ordinary chondrites. As mentioned before, pairing of ordinary chondrites is difficult to solve, and the possibility that more than 40% of the ordinary chondrites are actually paired must be considered. As pairing among carbonaceous chondrites is easy to obtain (due to detailed studies), we normalized our data to the percentage of carbonaceous chondrites among the world falls (Table 1). By doing this, the Libyan meteorite population is quite similar to other populations or the world falls. The

THE LIBYAN METEORITE POPULATION D. Weber¹, J. Zipfel² & A. Bischoff¹

only significant difference is the low abundance of iron meteorites. Furthermore, the percentage of paired ordinary chondrites from Libya can be calculated. From the 565 identified ordinary chondrites only 127 samples appear to be unpaired, which results in a percentage of about 77% paired samples.

Table 1. The Libyan meteorite population (assuming 40% paired ordinary chondrites or normalized to abundance of carbonaceous chondrites among world falls) in comparison to other populations and world falls [9, 10].

| Meteorite class | Nullarbor finds n=107 | Antarctica finds n=1100 | World falls n=835 | Libya finds 40% paired OC n=364 | | Libya finds Norm. to CC n=152 | |
|-----------------|--------------------------|----------------------------|----------------------|---------------------------------------|-------|-------------------------------------|-------|
| Chondrites | 93.4% | 91.3% | 86.2% | 348 | 95.6% | 137 | 90.2% |
| Ordinary | 87.9% | 87.9% | 80.0% | 339 | 93.1% | 127 | 83.6% |
| Carbonaceous | 4.6% | 2.7% | 4.6% | 7 | 1.9% | 7 | 4.6% |
| Enstatite | 0.9% | 0.7% | 1.6% | - | - | - | - |
| Rumuruti | ? | ? | ~0.1% | 3 | 0.8% | 3 | 2.0% |
| Achondrites | 2.9% | 5.8% | 7.9% | 13 | 3.6% | 13 | 8.5% |
| Mesosiderites | 0.9% | 0.7% | 1.1% | - | - | - | - |
| Irons | 2.8% | 2.2% | 4.8% | 2 | 0.6% | 2 | 1.3% |

Conclusions: The classification of a large number of Libyan meteorites does not only result in the recognition of scientifically important samples (such as Lunar or Martian meteorites), but helps also to improve the characterization of the Libyan meteorite population. This population is very similar to other populations and the world falls, but has a low abundance of iron meteorites. Iron meteorites, dark in appearance and with large masses, could have been collected in the past and used as tools or other objects by the local people. An exact characterization of the Libyan meteorite population, however, is limited by the pairing problem of ordinary chondrites.

References: [1] Wlotzka F. (1991) *Meteoritics*, 26, 255-262; [2] Grossmann J. N. (1996) *Meteoritics & Planet. Sci.*, 31, A175-A180; [3] Grossmann J. N. (1997) *Meteoritics & Planet. Sci.*, 32, A159-A166; [4] Grossmann J. N. (1998) *Meteoritics & Planet. Sci.*, 33, A221-A240; [5] Grossmann J. N. (1999) *Meteoritics & Planet. Sci.*, 34, in press; [6] Wlotzka F., Jull A. J. T. and Donahue D. J. (1995) In *Workshop on Meteorites from Cold and Hot Deserts*. [7] Weber D. and Bischoff A. (1998) *Meteoritics & Planet. Sci.*, 34, A164; [8] Bischoff A. and Geiger T. (1995) *Meteoritics*, 30, 113-122; [9] Bevan A. W. R. (1992) *Records of the Australian Museum*; [10] Koeberl C., Delisle G. and Bevan A. W. R. (1992) *Die Geowissenschaften*, 8, 220-225.

DEGREE OF WEATHERING OF H-CHONDRITES FROM FRONTIER MOUNTAIN, ANTARCTICA.
K.C. Welten and K. Nishiizumi, Space Sciences Laboratory, University of California, Berkeley, CA 94720-7450, USA.

Introduction: One of the factors that determines the survival time of meteorites on the Earth's surface is the rate of weathering. For meteorites from hot deserts, a clear correlation is found between the degree of weathering and the terrestrial age [1], but for Antarctic meteorites this correlation is weak or even lacking [2-5]. The lack of a clear correlation can partly be attributed to the two-stage history of many Antarctic meteorites, which spend part of their terrestrial residence time in the ice before they are exposed on the ice. Recently, it was found that for Lewis Cliff (LEW) meteorites local conditions on the ice play an important role in the weathering process [5,6]. This work focuses on weathering effects in ordinary chondrites from Frontier Mountain (FRO), North Victoria Land. Although most FRO meteorites were classified as weathering category A or B [7,8], many are contaminated with terrestrial uranium, deposited from meltwater [7]. This suggests that weathering plays a more significant role than the qualitative A-B-C weathering index indicates. We therefore determined the degree of weathering more quantitatively, by deriving the amount of oxidized metal from the concentrations of Fe and Ni in the non-magnetic fraction of 23 H-chondrites and 1 L-chondrite [5]. The results will be compared with those of LEW meteorites and will be discussed in terms of terrestrial age and location of find on the ice.

Experimental: Meteorite samples of 1-2 g were gently crushed in an agate mortar and the metallic phase was separated with a hand magnet. The metallic phase was used for cosmogenic radionuclide measurements to determine the terrestrial age of the meteorites [9]. After homogenizing the non-magnetic (stone) fraction, we dissolved 100 mg samples in a mixture of HF/HNO₃. Ali-

quots of the dissolved samples were measured with atomic absorption spectroscopy (AAS) to determine the concentrations of Fe and Ni in the non-magnetic fraction. The AAS results are listed in Table 1.

Results. Concentrations of Fe in the stone fractions of FRO H-chondrites range from 141 to 188 mg/g, compared to an average of 135 ± 3 mg/g for the non-magnetic fraction of H-chondrite falls [5,10]. The Ni concentrations range from 3.6 to 11.3 mg/g, compared to an average value of 2.7 ± 1.0 mg/g for fresh H-chondrite silicates [5]. Figures 1 and 2 show that the concentrations of Fe and Ni in the stony phase are negatively correlated to the amount of metal separated from the bulk meteorite and roughly follow the expected trends corresponding to the oxidation of metal to hydrous Fe-Ni-oxides. We thus used the equations given in [5] to derive the amount of oxidized metal (M_{ox}) from the measured Fe and Ni concentrations.

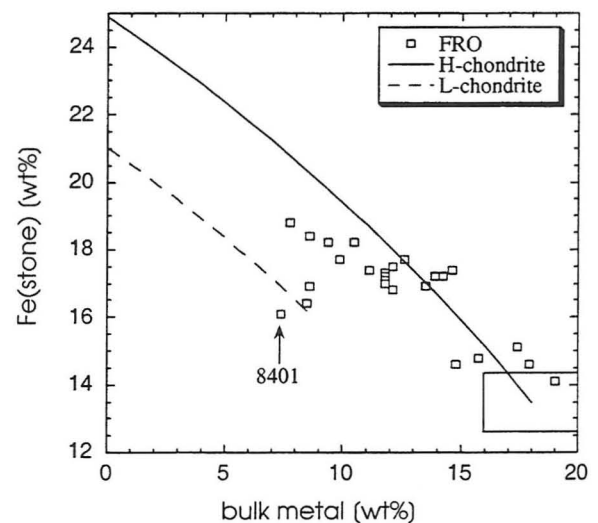


Fig. 1. Concentration of Fe in stony fraction vs. bulk metal content of FRO meteorites, compared to expected trends due to oxidation of metal in average H- and L-chondrites. The box represent the observed values for H-chondrite falls [10].

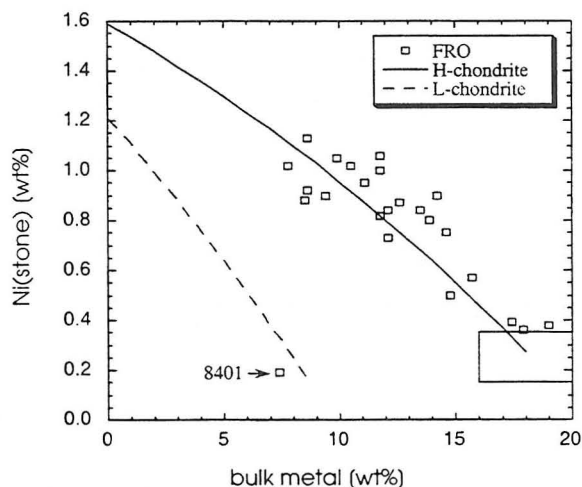


Fig. 2. Concentration of Ni in stony fraction vs. bulk metal content of FRO meteorites, compared to expected trends due to oxidation of metal in H- and L-chondrites. The box represents values for H-chondrite falls, assuming that the non-magnetic phase still contains ~ 0.6 wt% taenite, as explained in [5].

The amount of oxidized metal in FRO H-chondrites ranges from 1-9 wt%, whereas the L6 chondrite FRO 8401 contains no detectable amount of oxidized metal. The low degree of weathering for FRO 8401 is consistent with the low concentration of U in this meteorite [7]. Fig. 1 as well as Fig. 3 suggest that some of the more weathered H-chondrites seem to have lost significant amounts of Fe. We therefore use the value of $M_{ox}(Ni)$ as the indication of degree of weathering

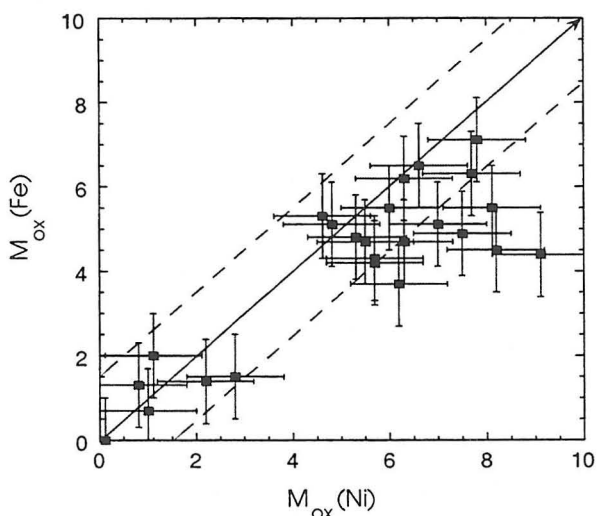


Fig. 3. Amount of oxidized metal derived from Fe and Ni concentration in non-magnetic fraction. The solid line represents a 1:1 relation, the dashed lines combined error bars of 1.0 wt% in $M_{ox}(Fe)$ and $M_{ox}(Ni)$.

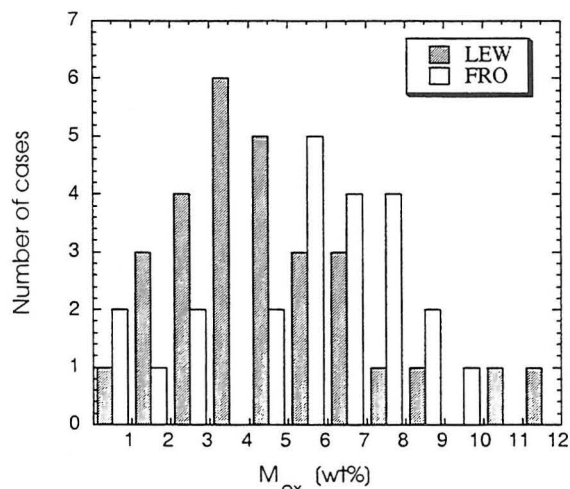


Fig. 4. Comparison of amount of oxidized metal in 23 H-chondrites from the FRO stranding area with values obtained for 29 H-chondrites from the LEW stranding area.

Discussion: The distribution of M_{ox} values shows a similar range as for LEW meteorites, but the FRO meteorites peak at higher M_{ox} values (5-8 wt%) than the LEW meteorites (3-5 wt%). This can not be attributed to differences in terrestrial age, since FRO meteorites are generally younger than LEW meteorites [9]. A possible explanation for the higher weathering rates at FRO is that meltwater is present more frequently or more abundantly than at LEW. Again, no clear correlation is found between weathering and terrestrial age, although the four least weathered meteorites are all younger than 100 ky (Fig. 5).

A speculative interpretation of Fig. 5 is that it shows two populations with different weathering rates: (i) samples that plot along the solid line represent meteorites which spent most of their terrestrial residence in the ice (where weathering presumably proceeds slowly) and only recently emerged from the ice, and (ii) samples which plot near the dashed curve represent meteorites which spent a significant part of their terrestrial residence time on the ice and experienced higher weathering rates, possibly as a result of the repeated interaction with meltwater. On the basis of the presence of meltwater streams and lakes during at least one of the field seasons, it has been suggested that meltwater occurs at least a few days per

year [11]. The initial stage of rapid weathering indicates it takes less than 50 ky on the ice to induce a moderate degree of weathering, i.e. 4-8 wt% of oxidized metal. This suggests that even meteorites with terrestrial ages of 100-250 ky showing moderate degrees of weathering may have spent only 50 ky or less on the ice.

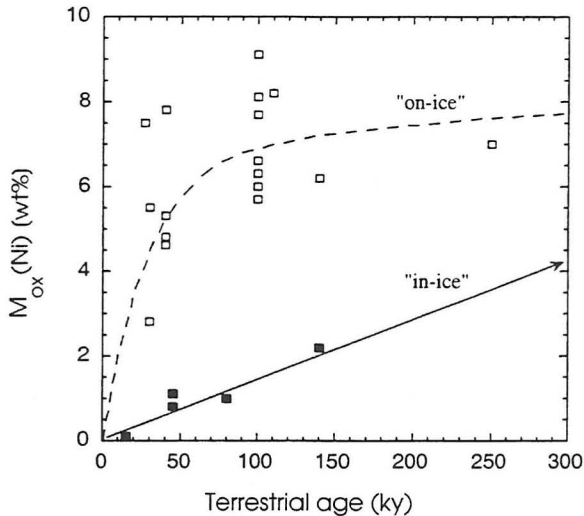


Fig. 5. Amount of oxidized metal in FRO chondrites as a function of terrestrial age. The dashed curve represent a rough correlation through the open symbols assuming a relatively rapid period of initial weathering followed by a more gradual overall increase [4]. The line through the solid symbols represents a linear increase of the degree of weathering with terrestrial age.

More interesting are the meteorites which show low degrees of weathering, since they probably emerged from the ice fairly recently: according to Fig. 5 less than a few thousand years ago. If the location of find represents the position where these meteorites emerged from the ice, then the terrestrial age is also the formation age of the ice - within a few ky. This condition is only fulfilled for meteorites >170 g for which no significant wind movement was observed over a two-year period, whereas stones with masses between 25-100 g were moved over distances up to 20 m/y [11].

The very low degree of weathering of FRO 8401, combined with its weight of 942 g, lead us to conclude that the formation age of the ice at its location of find (Fig. 6) is

similar to the terrestrial age of FRO 8401, i.e. • 15 ky. For the other four meteorites with low degrees of weathering (FRO 90002, 90043, 90059 and 90151), we can not directly link their location of find with the ice they emerged from, since these smaller specimens were probably moved by strong winds, which predominantly blow from the South-Southeast. However, it must be noted that all four meteorites have higher terrestrial ages (up to ~140 ky) and were found downstream from FRO 8401, as would be expected on the basis of simple ice-flow models. It therefore seems plausible that all four meteorites emerged from the ice downstream from FRO 8401 and were probably not windblown over large distances. We are currently investigating a larger meteorite (1.67 kg) with minor signs of weathering to confirm the general trend.

If the above interpretation is correct, then the age of the ice increases from ~15 ky to ~140 ky over a distance of only ~2.5 km. This age gradient seems rather high compared to measured ice-flow rates of 40-80 cm/y near the location of find of FRO 8401 [11], but may not be totally unrealistic if one considers that the ice becomes stagnant in the depression near the firn-ice edge, where most meteorites were found.

Conclusions. Although H-chondrites from Frontier Mountain have on the average lower terrestrial ages than those at the Lewis Cliff stranding area, they are more weathered. The higher weathering rate at FRO can possibly be explained by the higher abundance of meltwater, which is consistent with the U-contamination reported by [7] and would also explain the observation that the most weathered FRO samples seem to have lost some of their Fe.

Most FRO meteorites show moderate degrees of weathering, corresponding to 25-50% of their metal being oxidized. The terrestrial ages of these meteorites show that moderate degrees of weathering can be reached within less than 50 ky of rapid weathering, probably due to exposure on the ice surface. A few meteorites which were

found on the blue ice seem to have escaped this rapid weathering, which suggests they emerged from the ice fairly recently. Although the effect of wind-movement makes the link between terrestrial age and ice age rather speculative for small specimens, the general trend seems consistent with simple ice-flow models. We therefore conclude that the combined studies of terrestrial age, weathering effects and ice-flow may provide valuable new information on the age of the ice and the meteorite accumulation mechanism.

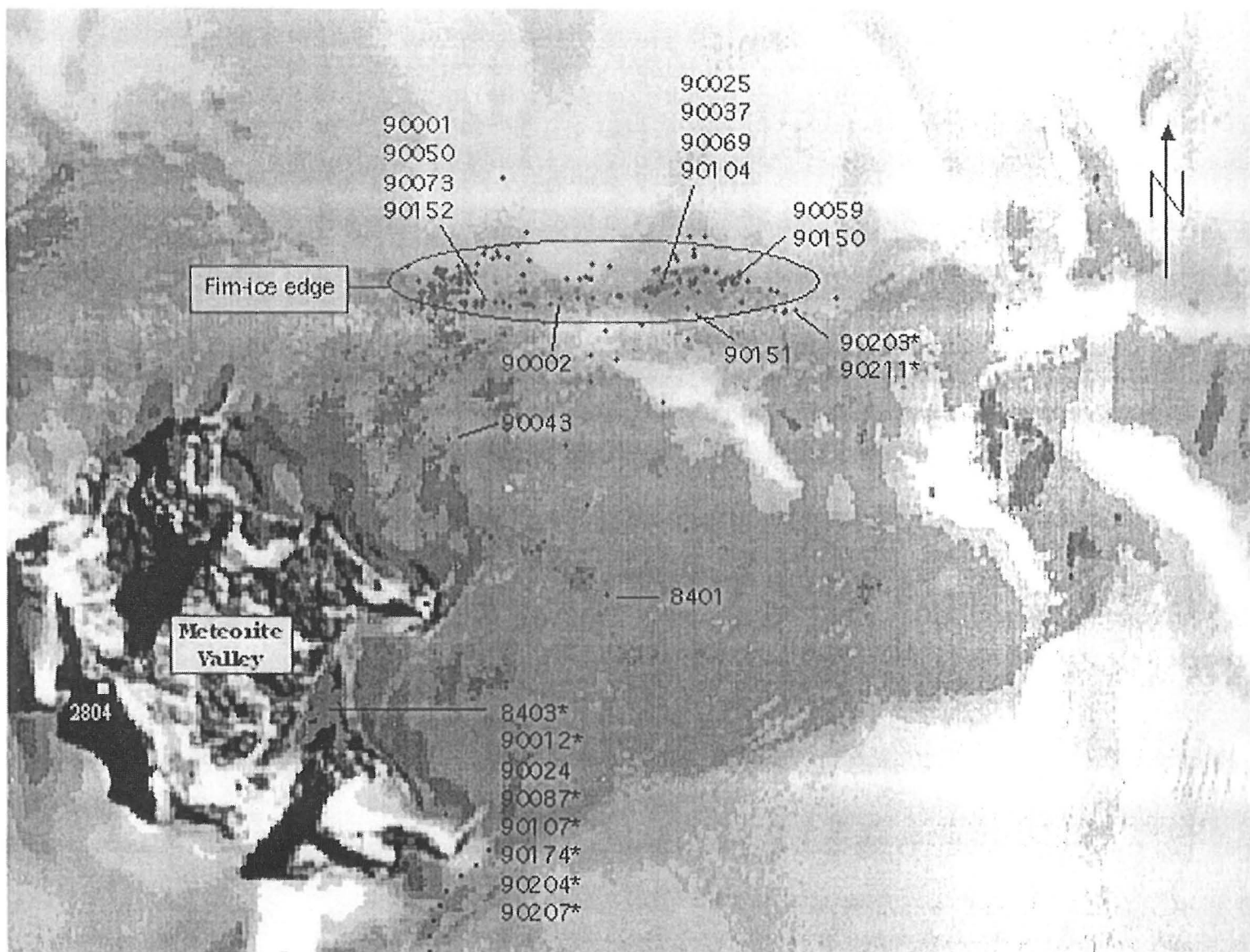
Acknowledgments. We thank EU-ROMET for the meteorite samples. This work was supported by NASA grant NAG-5-4992.

References: [1] Bland P. A. et al. (1996) *GCA* 60, 2053-2059. [2] Nishiizumi K. et al. (1989) *EPSL* 93, 299-313. [3] Burns R. G. et al. (1995) *Meteoritics* 30, 1-9. [4] Bland P. A. et al. (1998) *Geological Soc., London, Spec. Publ.* 140, 43-58. [5] Welten K. C. (1999) *MAPS* 34, 259-270. [6] Welten K. C. et al. (1999), *MAPS* 34 (supplement) [7] Delisle G. et al. (1989) *Geol. Jb.* E38, 488-513. [8] Delisle G. et al. (1993) *Meteoritics* 28, 126-129. [9] Welten K. C. et al. (1999) *Antarct. Meteorite Res.* 12, 94-107. [10] Jarosewich E. (1990) *Meteoritics* 25, 323-337. [11] Folco L. (1997) Ph.D thesis, The Open University, UK, pp. 188.

Table 1. Absolute amount (M_{ox}) and relative fraction ($\%M_{ox}$) of oxidized metal in FRO meteorites, derived from concentrations of Fe and Ni in non-magnetic fraction and bulk metal content.

| FRO | pair | Mass [g] | T(terr) [ky] | Metal [wt%] | Fe [mg/g] | Ni [mg/g] | M_{ox} (Fe) | M_{ox} (Ni) | M_{tot} [wt%] | $\%M_{ox}$ |
|-------|------|-------------|-----------------|----------------|--------------|--------------|------------------|------------------|--------------------|------------|
| 90001 | a | 76.1 | 40±10 | 13.9 | 172 | 8.0 | 4.8 | 5.3 | 19.2 | 27 |
| 90050 | a | 15.8 | 40±10 | 7.8 | 188 | 10.2 | 7.1 | 7.8 | 15.6 | 50 |
| 90073 | a | 20.6 | 40±10 | 12.1 | 175 | 7.3 | 5.3 | 4.6 | 16.7 | 28 |
| 90152 | a | 18.3 | 40±10 | 14.6 | 174 | 7.5 | 5.1 | 4.8 | 19.4 | 25 |
| 90002 | b | 22.1 | 45±15 | 17.4 | 151 | 3.9 | 2.0 | 1.1 | 18.5 | 6 |
| 90043 | b | 38.4 | 45±15 | 17.9 | 146 | 3.6 | 1.3 | 0.8 | 18.7 | 4 |
| 90069 | c | 17.7 | 30±5 | 15.7 | 148 | 5.7 | 1.5 | 2.8 | 18.5 | 15 |
| 90150 | c | 16.7 | 30±5 | 11.8 | 172 | 8.2 | 4.7 | 5.5 | 17.3 | 32 |
| 8403 | d | 19.4 | 100±30 | 12.6 | 177 | 8.7 | 5.5 | 6.0 | 18.6 | 32 |
| 90012 | d | 6.9 | 100±30 | 10.5 | 182 | 10.2 | 6.3 | 7.7 | 18.2 | 42 |
| 90087 | d | 8.3 | 100±30 | 9.9 | 177 | 10.5 | 5.5 | 8.1 | 18.0 | 45 |
| 90107 | d | 10.3 | 100±30 | 8.6 | 169 | 11.3 | 4.4 | 9.1 | 17.7 | 51 |
| 90174 | d | 12.7 | 100±30 | 12.1 | 168 | 8.4 | 4.2 | 5.7 | 17.8 | 32 |
| 90203 | d | 11.3 | 100±30 | 9.4 | 182 | 9.0 | 6.2 | 6.3 | 15.7 | 40 |
| 90204 | d | 12.6 | 100±30 | 8.6 | 184 | 9.2 | 6.5 | 6.6 | 15.2 | 43 |
| 90207 | d | 4.0 | 100±30 | 13.5 | 169 | 8.4 | 4.3 | 5.7 | 19.2 | 30 |
| 90211 | d | 11.9 | 100±30 | 14.2 | 172 | 9.0 | 4.7 | 6.3 | 20.5 | 31 |
| 90025 | e | 11.8 | 140±30 | 8.5 | 164 | 8.8 | 3.7 | 6.2 | 14.7 | 42 |
| 90151 | e | 33.6 | 140±30 | 14.8 | 146 | 5.0 | 1.4 | 2.2 | 17.0 | 13 |
| 90024 | - | 16.5 | 250±30 | 11.1 | 174 | 9.5 | 5.1 | 7.0 | 18.1 | 39 |
| 90037 | - | 13.1 | 110±30 | 11.8 | 170 | 10.6 | 4.5 | 8.2 | 20.0 | 41 |
| 90059 | - | 30.4 | 80±30 | 19.0 | 141 | 3.8 | 0.7 | 1.0 | 20.0 | 5 |
| 90104 | - | 10.9 | 27±5 | 11.8 | 173 | 10.0 | 4.9 | 7.5 | 19.3 | 39 |
| 8401 | - | 942.3 | 15±5 | 7.4 | 161 | 1.9 | 0.0 | 0.1 | 7.5 | 1 |

Fig. 6. Location of find of meteorites (red dots) on Frontier Mountain stranding area (courtesy of L. Folco). Numbers with asteriks(*) represent fragments of the FRO 90174 H5/6 chondrite shower. The map covers an area of 11x8 km².



COSMOGENIC RADIONUCLIDES IN HOT DESERT CHONDRITES WITH LOW ^{14}C ACTIVITIES: A PROGRESS REPORT. K. C. Welten¹, K. Nishiizumi¹ and M. W. Caffee², ¹Space Sciences Laboratory, University of California, Berkeley, CA 94720-7450, USA, ²CAMS, Lawrence Livermore National Laboratory, Livermore, CA 94550, USA.

INTRODUCTION. Terrestrial ages of meteorites from hot deserts provide an important tool to estimate meteorite fluxes to the Earth. Most desert meteorites have terrestrial ages less than 40 ky [1,2], but a few achondrites from the Sahara region were recently shown to have significantly higher ages, up to ~100 ky [3,4]. In general, ^{14}C (half-life = 5730 y) is the most suited radionuclide to determine terrestrial ages for desert meteorites. However for meteorites with ages >35 ky, the concentration of cosmogenic ^{14}C has decreased to a level at which it becomes difficult to distinguish between cosmogenic ^{14}C and terrestrial contamination. These meteorites may therefore be much older than 35 ky. We selected chondrites with low ^{14}C activities (≤ 2 dpm/kg) [5,6] for measurements of the concentrations of cosmogenic ^{36}Cl (half-life = 3.01×10^5 y) and ^{41}Ca (half-life = 1.04×10^5 y) in the metal phase. Since the ratio of $^{41}\text{Ca}/^{36}\text{Cl}$ in the metal phase of chondrites is relatively constant and well known, the measured ratio is a direct measure of the terrestrial age [7]. A major problem is that most or sometimes all of the metal in these old "hot desert" meteorites has been oxidized to hydrated Fe-Ni-oxides. Therefore, we also measured the concentrations of ^{10}Be , ^{26}Al and ^{36}Cl in the stony phase in order to constrain the terrestrial age as much as possible.

SAMPLES. We selected seven ordinary chondrites, three from Algeria (Acfer 290, 298, 307) and four from Roosevelt County, New Mexico (RC 044, 048, 049, 059). Except for RC 049, which is an LL4 chondrite, all samples are L-chondrites, and were previously studied by Bland and coworkers [2]. The three Acfer samples show about 35% oxidation (the percentage of total Fe existing as Fe^{3+}), whereas the RC samples show higher degrees of weathering, ranging from 40-83% oxidation. We noticed that especially RC 044 and 049, the

two most weathered samples, were extremely friable.

EXPERIMENTAL. After crushing 1-2 g of bulk samples, we separated the magnetic fraction from the non-magnetic fraction. The magnetic fraction was first purified with 0.2N HCl and then with concentrated HF to remove attached troilite and silicates, respectively. Unfortunately, this procedure dissolved most of the magnetic fraction, which contained very little unaltered metal to begin with [2]. For only three samples (Acfer 290, 307 and RC 059), relatively clean metal could be separated, although it still contained more silicates (1-5 wt%) than is usual for the purified metal fraction of fresh falls or Antarctic chondrite samples (<0.1-0.2 wt%). Both the metal fraction – if available – and the non-magnetic silicate fraction were dissolved for ^{10}Be , ^{26}Al , ^{36}Cl and ^{41}Ca analyses. Here we discuss some preliminary results.

RESULTS AND DISCUSSION. The ^{36}Cl concentrations in the metal phase of Acfer 290 and 307 indicate terrestrial ages less than 100 and 180 ky, respectively, whereas a third metal sample (RC 059) was lost. The concentrations of ^{10}Be and ^{26}Al in the metal phase indicate considerable contamination with silicates and are therefore not useful.

The concentrations of ^{10}Be and ^{26}Al in the stony phase of the three Acfer samples and of RC 048 and 059 are relatively constant at 18-22 and 48-72 dpm/kg, respectively. Also ^{36}Cl in these samples is relatively constant at 4.9-5.7 dpm/kg, except for the somewhat lower value of 3.5 dpm/kg in RC 048. However, RC 044 and 049 show very low ^{36}Cl concentrations (1.1-2.2 dpm/kg) and extremely high ^{10}Be (~40 dpm/kg) and ^{26}Al concentrations (~100-110 dpm/kg). The low ^{36}Cl concentrations can be explained by leaching of cosmogenic ^{36}Cl during weathering processes, especially since these two RC samples are the most weathered desert

meteorites investigated by Bland et al. [2]. However, the high ^{10}Be and ^{26}Al concentrations must have another cause. A possible explanation is that almost 50% of the original meteorite's mass was leached from the sample, whereas the associated ^{10}Be and ^{26}Al was incorporated into the weathering products. Several observations support this scenario: (1) RC 044 and 049 are the most weathered desert samples reported, showing the highest ratio of $\text{Fe}^{3+}/\text{Fe}(\text{total})$, (2) the density of the two samples seems about a factor of two lower than for other desert meteorites, suggesting that the original minerals have been replaced by low-density weathering products and (3) chemical analysis of RC 049 by XRF show significant (20-40%) losses of Mg, Si and Ca [2]. Further measurements and leaching experiments are in progress to study the distribution of cosmogenic radionuclides within weathered desert meteorites and to develop a method that leads to reliable ages.

CONCLUSIONS. For highly weathered desert meteorites it is difficult to determine terrestrial ages using the $^{41}\text{Ca}/^{36}\text{Cl}$ method due to the lack of unaltered metal. The measurement of ^{36}Cl and ^{41}Ca in the silicate fraction can provide useful age information, especially in combination with ^{10}Be and ^{26}Al , as was shown

for several achondrites [3,4]. However, our ^{10}Be and ^{36}Cl results have shown that extreme care has to be taken with the interpretation of cosmogenic nuclides in weathered meteorites, since these samples can not be considered as "closed systems". It was shown that ^{36}Cl is easily leached out of weathered silicates, whereas ^{10}Be and ^{26}Al are preferentially concentrated in weathering products, leading to extremely high ^{10}Be and ^{26}Al concentrations in the most weathered samples..

ACKNOWLEDGMENTS. We thank Tim Jull at the University of Arizona, Tucson, for selecting suitable samples and Jutta Zipfel at the MPI in Mainz for providing the meteorites samples. This work was supported by NASA grant NAG5-4992, and was partially performed under the auspices of the U.S. DOE by LLNL under contract W-7405-ENG-48.

REFERENCES. [1] Jull A. J. T. et al. (1990) GCA 54, 2895-2898, [2] Bland P. A. et al. (1998) GCA 62, 3169-3184 [3] Nishiizumi K. et al. (1998) Lunar Planet Sci. XXIX, CD-ROM, #1957. [4] Nishiizumi K. et al. (1999) Lunar Planet Sci. XXX, CD-ROM, #1966. [5] Wlotzka F. et al. (1995) LPI Tech. Rpt. 95-02, 72-73. [6] Jull A. J. T. et al. (1991) Lunar Planet. Sci. XXII, 667-668. [7] Nishiizumi K. and Caffee M. W. (1998) MAPS 33, A117.

Table 1. Concentrations of cosmogenic ^{10}Be , ^{26}Al and ^{36}Cl in desert meteorites with low ^{14}C activities.

| Sample | Class | ^{14}C age ⁵ (ky) | Oxidation(%) | ^{10}Be (dpm/kg) | ^{26}Al (dpm/kg) | ^{36}Cl (dpm/kg) | |
|-----------|-------|--|--------------|---------------------------|---------------------------|---------------------------|---------|
| | | | | Stone | Stone | Metal [#] | Stone |
| Acfer 290 | L6 | 29 | 34.3 | 18.7±0.2 | 51±3 | 19.7±0.3 | 4.9±0.1 |
| Acfer 298 | L6 | >42 | 35.1 | 19.4±0.3 | 57±3 | - | 5.2±0.1 |
| Acfer 307 | L5 | 32 | 33.6 | 20.1±0.3 | 72±4 | 16.4±0.3 | 5.5±0.1 |
| RC 044 | L6 | 31 | 56.2 | 38.7±0.6 | 109±5 | - | 2.2±0.1 |
| RC 048 | L6 | >44 | 45.0 | 17.8±0.3 | 48±3 | - | 3.5±0.1 |
| RC 049 | LL4 | 38 | 82.5 | 41.2±0.5 | 99±5 | - | 1.1±0.1 |
| RC 059 | L6 | 26 | 40.4 | 21.7±0.3 | 56±3 | - | 5.7±0.1 |

⁵Ages for Acfer samples from [5], those for RC samples from [6] [#]Not yet corrected for silicate contribution

NOBLE GASES IN DESERT METEORITES: HOWARDITES, UNEQUILIBRATED CHONDRITES, REGOLITH BRECCIAS AND AN LL7. R. Wieler, H. Baur, H. Busemann, V. S. Heber, and I. Leya, ETH Zürich, Isotope Geology and Mineral Resources, NO C61, CH-8092 Zürich, Switzerland; wieler@erdw.ethz.ch

We present He, Ne, and Ar data of 39 samples from 17 meteorites of various types. For three CV3 and two unequilibrated ordinary chondrites Kr and Xe data are also reported. The analyses served various purposes, e. g. to check for presence of solar noble gases, to determine concentrations of primordial noble gases, to study cosmic ray exposure ages including possible parent body exposures, and to recognize paired meteorites.

The data are shown in Tables 1 and 2. ^{21}Ne exposure ages are calculated with the cosmogenic nuclide production model by Leya et al. [1], assuming average chemical composition of the respective meteorite class and taking the $(^{22}\text{Ne}/^{21}\text{Ne})_{\text{COS}}$ ratio as shielding parameter. In some cases we had to assume additionally a meteoroid radius ≤ 32 cm. We report an age range ($T_{\text{min}}^{21} - T_{\text{max}}^{21}$) rather than a single age to indicate that even when $(^{22}\text{Ne}/^{21}\text{Ne})_{\text{COS}}$ is available, meteoroid size and sample depth are not unambiguously known, hence the ^{21}Ne production rate is only constrained to within certain limits. The mean production rates used here compare well with those given by Eugster [2] and Eugster and Michel [3] for $(^{22}\text{Ne}/^{21}\text{Ne})_{\text{COS}}$ values between 1.08 - 1.12 (chondrites) and 1.10 - 1.15 (howardites), respectively. On the other hand, our values are up to 30% lower for high $(^{22}\text{Ne}/^{21}\text{Ne})_{\text{COS}}$ values, i. e. small meteorites and low shielding (see ref. [1] for details).

Howardites

QUE97001 and *QUE97002* are two relatively large Antarctic howardites (2.4 and 1.4 kg, resp.). A preliminary description is given in [4]. Several samples from matrix portions and inclusions were analysed for each meteorite, primarily to search for regolith noble gas signatures, i. e. solar-wind implanted noble gases and possible differences in cosmic-ray exposure ages that would indicate an exposure near the parent body surface, similar to e. g. Kapoeta [5, 6]. None of the *QUE97001* samples contains even traces of solar Ne, since all show $^{20}\text{Ne}/^{21}\text{Ne} < 0.97$. *QUE97002* might contain very minor amounts of solar Ne, since in 4 out of 5 samples $^{20}\text{Ne}/^{21}\text{Ne}$ falls between 1.02-1.24. However, the trapped noble gases in the dark inclusion *QUE97002,17/cc* - presumably one of several millimeter-sized carbonaceous chondrite xenoliths - are very probably primordial meteoritic gases and not solar noble gases. Therefore, the traces of trapped gases in the other *QUE97002* samples may well also be from tiny carbonaceous chondrite xenoliths. *QUE97002* is thus an example that xenoliths can be abundant in howardites whose noble gas signature does not reveal an extensive regolith history.

Five out of six *QUE97001* samples have within $\pm 6.5\%$ the same $^{21}\text{Ne}_{\text{COS}}$ concentration of $(8.55 \pm 0.55) \cdot 10^{-8} \text{ cc/g}$, whereas *QUE97001,17/dark* contains 43% less $^{21}\text{Ne}_{\text{COS}}$. This does not indicate a substantial regolith exposure of the first four samples, however, since *QUE97002,17/dark* was less shielded than the other samples, shown by its higher

$^{22}\text{Ne}/^{21}\text{Ne}_{\text{COS}}$, such that its nominal exposure age range is less than 20% lower than the mean range of the other 5 samples. Furthermore, this sample presumably was rich in plagioclase, i. e. Ca, as indicated by its very high concentration of $^{38}\text{Ar}_{\text{COS}}$. Plagioclase is leaky for cosmogenic He and Ne [7], which explains also the low $^3\text{He}_{\text{COS}}$ of this sample. We calculate a "best" meteoroid exposure age for *QUE97001* of 35 Ma as the mean of all mean ^{21}Ne ages. Unfortunately, this long meteoroid exposure age makes this meteorite not well suited for the initial purpose of this study, namely to search for cosmogenic noble gas excesses resulting from a parent body exposure.

Such parent body effects are probably neither observable in *QUE97002*, although both $^{21}\text{Ne}_{\text{COS}}$ and $^3\text{He}_{\text{COS}}$ are about 20% higher in *QUE97002,16* than in the other three howarditic samples of this meteorite. This difference is well within the scatter to be expected due to different target element abundances in ~ 30 mg sized howardite samples. The carbonaceous chondrite xenolith *QUE97002,17/cc* contains two times less ^3He than the other samples of this meteorite, which is probably due to diffusive He loss. The ^{21}Ne age (and also the ^{38}Ar age) of the xenolith are not significantly different from the respective values of the other samples, the more so since uncertainties in target element abundances in a 3.6 mg sample are substantial. *QUE97002* does therefore not allow to substantiate the observation made by Pedroni [5], who observed that a carbonaceous chondrite inclusion had the lowest nominal exposure age of any Kapoeta sample, and interpreted this to reflect the true meteoroid (4π) age of this meteorite. The "best" exposure age of *QUE97002* is 18 Ma. *QUE97001* and *QUE97001* are therefore not paired.

Hughes 005 is a 284 g howardite from the Nullarbor Plain [8]. We analyzed two different ~ 4 mm sized dark inclusions and two matrix samples. Probably none of the samples contains solar Ne (the highest upper limit for $^{20}\text{Ne}_{\text{sol}}$ is $\sim 0.4 \cdot 10^{-8} \text{ cc/g}$ in matrix sample 2). Hence, all ^4He of $(4040-11150) \cdot 10^{-8} \text{ cc/g}$ is essentially radiogenic. Matrix sample 1 shows thus the highest clearly radiogenic ^4He concentration of any howardite reported so far, and with the exception of one sample of the eucrite Stannern ($^4\text{He}_{\text{rad}} = 12700 \cdot 10^{-8} \text{ cc/g}$) also the highest radiogenic ^4He concentration reported for any HED meteorite [9]. As for the two *QUE* meteorites, the variable concentrations of cosmogenic ^{21}Ne and ^{38}Ar are mostly, if not entirely, due to inhomogeneous target element abundances such that different parent body exposure durations are not discernible. Variations in $^3\text{He}_{\text{COS}}$ are probably at least partly caused by He loss from plagioclase.

Carbonaceous chondrites (CV3)

The main purpose of these (and further) analyses on CV3 chondrites was to check whether oxidized and reduced subgroups might show similar clusters of exposure ages, suggesting a common parent body (E. R. D. Scott, pers. comm. 1994). Hints for a cluster in the 9 Ma range

NOBLE GASES IN DESERT METEORITES: R. Wieler et al.

have recently been noted [10]. This cluster would mostly be defined by oxidized CV3s, but also two of four members of the reduced subgroup with known exposure ages (Efremovka & Leoville, ref. [10]) have nominal ages of 9.4 and 10.8 Ma, respectively. Arch measured here has a rather ill-defined exposure age of ~20-40 Ma. The large uncertainty is caused by the missing shielding information, since the large amounts of solar Ne (next paragraph) do not allow us to deduce the $(^{22}\text{Ne}/^{21}\text{Ne})_{\text{COS}}$ ratio. Note that exposure ages of CV chondrites are often imprecise due to a lack of shielding information caused by the presence of solar or primordial Ne [e. g. 10]. Despite this uncertainty, it is clear that the exposure age of Arch is higher than the presumed cluster age. Furthermore, neither of the two oxidized CV3s measured here fall near this 9 Ma value.

The Ne isotopic data clearly show that the trapped Ne in Arch is solar. This is confirmed by the $(^4\text{He}/^{20}\text{Ne})_{\text{T}}$ ratio of 390. The $^{20}\text{Ne}/^{22}\text{Ne}$ ratio of the solar gases of ~12.1 is relatively low, which is common for desert meteorites (Arch is from Roosevelt County, NM). Such low $^{20}\text{Ne}/^{22}\text{Ne}$ ratios relatively close to the SEP-Ne value of 11.2 [11] indicate partial removal by weathering of the outermost grain layers containing the SW component. In fact, some desert meteorites contain pure trapped SEP-Ne (e. g. 12, 13). Despite this loss, Arch is the CV3 chondrite with the highest reported concentration of solar He and Ne [9]. Note that the Arch sample analysed by Scherer and Schultz [10] even contained almost twice as much solar Ne as ours.

All three CV meteorites contain primordial Kr and Xe in amounts typical for CVs [10], whereby part of the Kr in Arch probably is atmospheric contamination, as is common for desert finds [14]. ALH81003 has a high $^{129}\text{Xe}/^{132}\text{Xe}$ ratio of ~4.2, in line with its rather low $^{132}\text{Xe}_{\text{prim}}$.

Unequilibrated enstatite and ordinary chondrites

The main purpose of these analyses was to determine the concentrations of primordial noble gases and in some cases to check for the presence of solar noble gases.

LEW87223: This meteorite is an anomalous E3 (or EL3) chondrite [e. g. 15]. It is brecciated [15] but contains no or hardly any solar Ne (an upper limit for $^{20}\text{Ne}_{\text{sol}}$ is $\sim 0.3 \cdot 10^{-8}$ cc/g, but this may also be primordial Ne). The most remarkable fact about this meteorite from the noble gas perspective is its primordial ^{36}Ar concentration of only $\sim 1.5 \cdot 10^{-8}$ cc/g, which is very low for a type 3 chondrite and the lowest of any enstatite chondrite reported except for Bethune and Happy Canyon [9]. An explanation for this may be noble gas loss upon shock, since there is other evidence that this meteorite was altered by brecciation and heating [15]. On the other hand, in enstatite chondrites primordial noble gas concentrations generally correlate considerably less well with petrographic type than in other meteorite classes [e. g. 16, 15]. Probably in line with this observation, Zhang et al. [15] note that the Van Schmus and Wood petrologic classification scheme is less well suited for enstatite chondrites than for ordinary chondrites.

As noted by [15], the exposure age of ~6-9 Ma of the anomalous E chondrite LEW87223 is in the center of the age range for EL chondrites of 4-18 Ma.

UOCs: As expected, the concentrations of primordial ^{36}Ar in the unequilibrated ordinary chondrites roughly correlate inversely with their petrographic subtype. LL3.2 ALH78170 has the highest concentration of primordial ^{36}Ar measured here of $\sim 86.3 \cdot 10^{-8}$ cc/g. The low exposure age of this meteorite also allows for a precise determination of the concentration of primordial $^{20}\text{Ne}_{\text{prim}}$ of $1.94 \cdot 10^{-8}$ cc/g, yielding $(^{20}\text{Ne}/^{36}\text{Ar})_{\text{prim}} = 0.022$. Some of the other UOCs here also allow us to determine a (somewhat less precise) $(^{20}\text{Ne}/^{36}\text{Ar})_{\text{prim}}$ ratio, assuming $(^{20}\text{Ne}/^{21}\text{Ne})_{\text{COS}} = 0.88 \pm 0.02$ [1]. All values $(^{20}\text{Ne}/^{36}\text{Ar})_{\text{prim}}$ are between 0.024-0.065, similar to those of the Q-component [17]. Possibly, all these meteorites have lost a much larger part of their primordial Ne-A compared to the loss fraction of Ne-Q.

LL7 chondrite ALH84027

As expected from its petrographic type, this meteorite contains extremely low amounts of trapped noble gases. The concentration of $^{36}\text{Ar}_{\text{prim}}$ is $\sim 0.046 \cdot 10^{-8}$ cc/g, and the fact that $^{20}\text{Ne}/^{21}\text{Ne} > 1$ is therefore probably rather due to a somewhat imprecise blank correction for this small and gas-poor sample than to discernible amounts of trapped Ne. Only very few noble gas analyses of type 7 chondrites have been reported, and ALH84027 shows the lowest $^{36}\text{Ar}_{\text{prim}}$ concentration of any of these [9]. Moreover, this meteorite shows among the lowest - if not the lowest - $^{36}\text{Ar}_{\text{prim}}$ values of any reliable chondrite analysis reported in the Schultz compilation.

The exposure age of ALH84027 is 3.0-3.5 Ma. Only one other LL chondrite with a similar age has been reported [18], namely Meru (LL6), for which Graf and Marti [19] report a ^{21}Ne age of 3.7 Ma.

Regolith breccias Zag and Hughes 021

Zag is a large solar-gas-rich H3-6 chondritic breccia (recovered mass 175 kg) that fell in August 1998 in Western Sahara or Morocco [20]. We analysed two "dark" matrix samples, two samples from what appeared to be light inclusions, and one sample from an inclusion darker than the matrix. All samples were chipped from raw surfaces of a single ~150 g piece. Except for the dark inclusion, they all contained solar noble gases, which means that we did not succeed to sample a light clast uncontaminated by solar-wind rich matrix. The most gas-rich sample m2 has a relatively high concentration of solar Ne, similar to well-known gas-rich meteorites as Khor Temiki, Pantar, and Weston and still within a factor of about 5-10 of the record-holders Acfer111, Fayetteville, Kapoeta, and Noblesville [9]. However, the $^4\text{He}/^{20}\text{Ne}$ ratio in all solar-gas rich samples is only around 100-150, lower than for most of the meteorites mentioned above and also e. g. Arch, which show values around 300-600. Solar He and Ne in Zag, like those in Kapoeta & Noblesville, are therefore relatively strongly elementally fractionated relative to the $^4\text{He}/^{20}\text{Ne}$ value in the solar wind of 650 as measured in chondritic metal [21]. $(^{20}\text{Ne}/^{22}\text{Ne})_{\text{sol}}$ ratios of the four gas-rich Zag samples are between 12.2-12.5, slightly higher than e. g. in Arch, as expected for a fresh fall.

Sample Zag d has $^{22}\text{Ne}/^{21}\text{Ne}_{\text{COS}} = 1.11$ and $^3\text{He}/^{21}\text{Ne} = 4.6$, indicating that the analysed specimen comes from an

"average" shielding depth. The exposure age of 5.5 - 6.1 Ma puts Zag near the lower end of the prominent 7 Ma peak in the exposure age histogram of H-chondrites [e. g. 22]. No parent body exposure episode can be discerned for any Zag sample.

Hughes 021, classified as L3, also contains large amounts of solar noble gases and is thus a regolith breccia.

Summary

For several meteorites here an entry in the Guinness Book of Records might be appropriate: Hughes 005 is very high in radiogenic ^4He , Arch is the CV3 chondrite with the highest concentration of solar noble gases, LEW87223 is the enstatite chondrite with the lowest reported primordial ^{36}Ar concentration, and the LL7 chondrite 84027 shows possibly the lowest $^{36}\text{Ar}_{\text{prim}}$ concentration of all chondrites measured so far. Other interesting observations are that Zag, a large recent chondrite fall, contains substantial amounts of solar noble gases and that the howardites QUE97001 and QUE97002 are not paired. Neither these two meteorites nor the anomalous E chondrite LEW87223 show evidence in their noble gas signatures for an exposure in the parent body regolith.

Acknowledgements

Samples were generously provided by UCLA, JNMC, and mainly by NASA's Meteorite Working Group, partly with the help of Ed Scott and Derek Sears. Work supported by the Swiss National Science Foundation.

References

- 1: Leya I. et al. (1999) *Meteoritics Planet. Sci.*, submitted.
- 2: Eugster O. (1988) *Geochim. Cosmochim. Acta* 52, 1649.
- 3: Eugster O. and Michel T. (1995) *Geochim. Cosmochim. Acta* 59, 177.
- 4: Antarctic Meteorite Newsletter (1998) 21(2), NASA, Houston, TX.
- 5: Pedroni A. (1989) Diss. ETH Zürich #8880, 224pp.
- 6: Pun A. et al. (1998) *Meteoritics Planet. Sci.* 33, 835.
- 7: Bogard D. D. and Cressy P. J. (1973) *Geochim. Cosmochim. Acta* 37, 527.
- 8: *Met. Bull.* 73 (1992) *Meteoritics* 27, 481.
- 9: Schultz L. and Franke L. (1998) Noble gas data compilation, pers. comm. on diskette.
- 10: Scherer P. and Schultz L. (1999), *Meteoritics Planet. Sci.*, submitted.
- 11: Benkert J.-P. et al. (1993) *J. Geophys. Res.* 98(E7), 13147.
- 12: Scherer P. et al. (1998) *Meteoritics Planet. Sci.* 33suppl., A135.
- 13: Padia J. T. and Rao M. N. (1986) LPI Tech. Rpt. 86-01, 74., Houston TX.
- 14: Scherer P. et al. (1994) in: *Noble Gas Geochem. and Cosmochem.* (ed. J. Matsuda), Terrapub. Tokyo, 43.
- 15: Zhang Y. H. et al. (1995) *J. Geophys. Res.* 100(E5), 9417.
- 16: Crabb J. and Anders E. (1981) *Geochim. Cosmochim. Acta* 45, 2443.
- 17: Busemann H. (1998) Diss. ETH Zürich #12988, 182pp.
- 18: Kirsten T. et al. (1963) *Geochim. Cosmochim. Acta* 27, 13.
- 19: Graf T. and Marti K. (1994) *Meteoritics* 29, 643.
- 20: *Met. Bull.* 83 (1999) *Meteoritics Planet. Sci.* 34, in press.
- 21: Murer C. A. et al. (1997) *Geochim. Cosmochim. Acta* 61, 1303.
- 22: Graf T. and Marti K. (1995) *J. Geophys. Res.* 100(E10), 21247.

Table 2: Kr and Xe in desert meteorites

| Sample | ^{84}Kr | 78/84 | 80/84 | 82/84 | 83/84 | 86/84 | | | | |
|---------------|-------------------|---------|---------|---------|---------|---------|---------|---------|---------|--|
| Arch (206mg) | 0.623 | 0.0158 | 0.0398 | 0.2015 | 0.2015 | 0.3075 | | | | |
| ALH81003 | 0.084 | 0.0164 | 0.0648 | 0.2106 | 0.2021 | 0.3083 | | | | |
| ALH85006 | 0.2501 | 0.0511 | 0.0418 | 0.2006 | 0.2013 | 0.3097 | | | | |
| GRO95505,7 | 0.297 | | 0.0406 | 0.2036 | 0.2043 | 0.3117 | | | | |
| GRO95505,10 | 0.284 | | 0.0411 | 0.2039 | 0.2019 | 0.309 | | | | |
| GRO95505,11 | 0.1505 | | 0.0410 | 0.2043 | 0.2045 | 0.311 | | | | |
| WSG95300,9 | 0.326 | 0.00677 | 0.0401 | 0.2008 | 0.201 | 0.309 | | | | |
| WSG95300,11 | 0.334 | | 0.0404 | 0.2016 | 0.2026 | 0.311 | | | | |
| | ^{132}Xe | 124/132 | 126/132 | 128/132 | 129/132 | 130/132 | 131/132 | 134/132 | 136/132 | |
| Arch (206 mg) | 0.269 | 0.00443 | 0.00397 | 0.0794 | 1.066 | 0.1584 | 0.8119 | 0.3915 | 0.3363 | |
| ALH81003 | 0.0905 | 0.00465 | 0.0043 | 0.0854 | 4.244 | 0.1612 | 0.8179 | 0.388 | 0.3289 | |
| ALH85006 | 0.3198 | 0.00449 | 0.00399 | 0.0806 | 1.241 | 0.1604 | 0.8143 | 0.3937 | 0.3367 | |
| GRO95505,7 | 0.356 | 0.00445 | 0.00410 | 0.0806 | 1.068 | 0.1598 | 0.812 | 0.380 | 0.320 | |
| GRO95505,10 | 0.353 | 0.00457 | 0.00400 | 0.0802 | 1.072 | 0.1590 | 0.813 | 0.379 | 0.321 | |
| GRO95505,11 | 0.170 | 0.00453 | 0.00416 | 0.0810 | 1.101 | 0.1610 | 0.818 | 0.378 | 0.3229 | |
| WSG95300,9 | 0.403 | 0.00449 | 0.00407 | 0.0797 | 1.057 | 0.1592 | 0.815 | 0.377 | 0.316 | |
| WSG95300,11 | 0.341 | 0.00448 | 0.00399 | 0.0811 | 1.071 | 0.1621 | 0.824 | 0.385 | 0.3228 | |

^{84}Kr and ^{132}Xe concentrations in [$10^{-8} \text{ cm}^3 \text{STP/g}$].

Uncertainties of gas concentrations ~6%; uncertainties of isotopic ratios: ~2% for $^{124,126}\text{Xe}/^{132}\text{Xe}$ and $^{78}\text{Kr}/^{84}\text{Kr}$, ~5-7% for all other ratios.

Table 1: He, Ne, and Ar in desert meteorites

| Sample | mass | ³ He | ⁴ He | ²⁰ Ne | ²¹ Ne | ²² Ne | ³⁶ Ar | ³⁸ Ar | ⁴⁰ Ar | ²¹ Ne _{cos} | (22/21) _{cos} | T ²¹ _{min} | T ²¹ _{max} | ³⁸ Ar _{cos} | |
|-----------------------|----------------|-----------------|-----------------|------------------|------------------|------------------|------------------|------------------|------------------|---------------------------------|------------------------|--------------------------------|--------------------------------|---------------------------------|------|
| Howardites | | | | | | | | | | | | | | | |
| QUE97001,12 | light | 57 | 44.6 | 3680 | 7.90 | 8.27 | 9.48 | 3.36 | 2.621 | 693 | 8.27 | 1.14 | 30 | 38 | 2.27 |
| QUE97001,21 | dark | 40 | 49.9 | 1928 | 9.09 | 9.48 | 10.89 | 1.635 | 1.768 | 838 | 9.48 | 1.14 | 34 | 44 | 1.66 |
| QUE97001,20 | light | 25 | 43.5 | 2868 | 7.85 | 8.18 | 9.50 | 3.08 | 2.594 | 625 | 8.18 | 1.16 | 31 | 41 | 2.30 |
| QUE97001,17 | light | 20 | 45.7 | 4200 | 8.08 | 8.52 | 9.78 | 3.07 | 2.381 | 583 | 8.52 | 1.14 | 30 | 39 | 2.05 |
| QUE97001,17 | dark | 23 | 32.4 | 5310 | 4.70 | 4.87 | 5.80 | 2.814 | 4.10 | 1218 | 4.87 | 1.19 | 27 | 30 | 4.07 |
| QUE97001,13 | light+dark | 27 | 47.4 | 3980 | 7.97 | 8.32 | 9.64 | 3.31 | 2.415 | 592 | 8.32 | 1.16 | 32 | 42 | 2.04 |
| | | | | | | | | | | | | | <i>mean age:</i> | 31 | 39 |
| QUE97002,16 | dark | 26 | 23.04 | 3910 | 4.14 | 3.32 | 4.07 | 3.19 | 2.612 | 1165 | 3.32 | 1.19 | 18 | 22 | 2.29 |
| QUE97002,14 | light+dark | 37 | 19.71 | 4960 | 2.969 | 2.696 | 3.28 | 2.207 | 2.517 | 1984 | 2.695 | 1.20 | 16 | 19 | 2.40 |
| QUE97002,15 | light+dark | 33 | 18.78 | 4280 | 2.848 | 2.786 | 3.37 | 2.026 | 2.588 | 1518 | 2.785 | 1.20 | 16 | 20 | 2.51 |
| QUE97002,17 | dark | 28 | 19.38 | 3150 | 3.20 | 2.650 | 3.23 | 2.250 | 2.547 | 1175 | 2.648 | 1.19 | 15 | 18 | 2.42 |
| QUE97002,17 | dark incl., cc | 3.6 | 10.68 | 3770 | 11.01 | 2.522 | 4.10 | 21.90 | 5.07 | 831 | 2.49 | 1.25 | 17 | 21 | 1.08 |
| | | | | | | | | | | | | | <i>mean age:</i> | 16 | 20 |
| Hughes 005 | dark incl. | 178 | 33.8 | 4800 | 4.87 | 4.75 | 5.85 | 0.922 | 1.041 | 867 | 4.75 | 1.23 | 32 | 37 | 0.99 |
| Hughes 005 | matrix | 100 | 21.49 | 11150 | 2.522 | 2.404 | 3.03 | | | | 2.403 | 1.25 | 16 | 18 | |
| Hughes 005 | matrix | 141 | 21.01 | 10490 | 2.593 | 2.457 | 3.09 | 1.829 | 2.004 | 2249 | 2.457 | 1.25 | 16 | 19 | 1.89 |
| Hughes 005 | dark incl. | 75 | 12.49 | 4040 | 3.62 | 3.60 | 4.46 | 1.374 | 2.068 | 1838 | 3.60 | 1.24 | 24 | 28 | 2.06 |
| | | | | | | | | | | | | | <i>mean age:</i> | 22 | 25 |
| CV3 chondrites | | | | | | | | | | | | | | | |
| Arch | | 206 | 98.5 | 216400 | 564 | 8.00 | 53.5 | 65.6 | 13.29 | 507 | 6.59 | | 20 | 41 | |
| Arch | | 217 | 90.3 | 187400 | 483 | 8.05 | 46.9 | | | | 6.84 | | 21 | 43 | |
| ALH81003 | | 122 | 26.69 | 2269 | 5.05 | 4.13 | 4.88 | 8.07 | 1.955 | 2701 | 4.13 | 1.15 | 19 | 22 | 0.50 |
| ALH85006 | | 116 | 5.95 | 3160 | 9.00 | 1.449 | 2.424 | 24.01 | 4.68 | 1047 | 1.42 | 1.06 | 3.9 | 4.6 | 0.2 |

Table 1 (cont.): He, Ne, and Ar in desert meteorites

| Sample | mass | ³ He | ⁴ He | ²⁰ Ne | ²¹ Ne | ²² Ne | ³⁶ Ar | ³⁸ Ar | ⁴⁰ Ar | ²¹ Ne _{cos} | (²² / ²¹) _{cos} | T ²¹ _{min} | T ²¹ _{max} | ³⁸ Ar _{cos} | |
|----------------------------------|-------------|-----------------|-----------------|------------------|------------------|------------------|------------------|------------------|------------------|---------------------------------|--|--------------------------------|--------------------------------|---------------------------------|-----|
| unequilibrated chondrites | | | | | | | | | | | | | | | |
| LEW87223 | E3anom | 89 | 10.66 | 896 | 1.665 | 1.556 | 1.803 | 1.703 | 0.557 | 2820 | 1.555 | 1.14 | 6.2 | 7.1 0.27 | |
| LEW87223 | E3anom | 53 | 12.60 | 1017 | 2.080 | 1.984 | 2.273 | 1.649 | 0.516 | 2870 | 1.983 | 1.13 | 7.9 | 9.0 0.23 | |
| ALH78046 | L3 | 91 | 8.47 | 838 | 3.10 | 3.06 | 3.40 | 5.17 | 1.259 | 3750 | 3.060 | 1.10 | 8.5 | 10 0.33 | |
| ALH78170 | L3.2 | 198 | 3.13 | 1006 | 2.484 | 0.621 | 0.906 | 86.4 | 16.24 | 3570 | 0.614 | 1.10 | 1.7 | 2.0 | |
| ALH83010 | L3.3 | 82 | 22.75 | 170.3 | 6.01 | 5.88 | 6.58 | 21.98 | 4.67 | 469 | 5.880 | 1.10 | 16 | 19 0.62 | |
| ALH83010 | L3.3 | 230 | 22.42 | 163.3 | 5.91 | 5.89 | 6.58 | 17.74 | 3.86 | 353 | 5.880 | 1.10 | 16 | 19 0.60 | |
| ALH78138 | LL3 | 247 | 31.9 | 1288 | 7.10 | 6.31 | 7.45 | 64.2 | 12.72 | 5490 | 6.300 | 1.16 | 26 | 30 0.75 | |
| EET83213 | LL3.7 | 143 | 45.6 | 1450 | 10.87 | 10.59 | 11.85 | 16.79 | 4.12 | 5830 | 10.580 | 1.10 | 29 | 39 1.10 | |
| GRO95505,7 | L3.6 | 100 | 42.8 | 1689 | 8.20 | 6.75 | 8.22 | 46.5 | 9.30 | 5260 | 6.75 | 1.19 | 36 | 40 0.64 | |
| GRO95505,10 | L3.6 | 63 | 45.2 | 1719 | 8.83 | 7.19 | 8.76 | 47.2 | 9.85 | 4990 | 7.19 | 1.19 | 38 | 42 1.12 | |
| GRO95505,11 | L3.6 | 70 | 45.2 | 2062 | 8.51 | 7.69 | 9.20 | 26.90 | 5.59 | 5970 | 7.69 | 1.18 | 38 | 43 0.61 | |
| WSG95300,9 | H3.4 | 60 | 47.1 | 1755 | 10.67 | 8.68 | 10.17 | 61.1 | 12.34 | 3430 | 8.67 | 1.14 | 35 | 39 0.98 | |
| WSG95300,11 | H3.4 | 77 | 46.0 | 1701 | 10.73 | 8.92 | 10.29 | 59.4 | 12.07 | 2450 | 8.91 | 1.12 | 31 | 36 1.03 | |
| Hughes 021 | L3 | 98 | 83.9 | 208500 | 1658 | 11.65 | 147.8 | 56.1 | 11.54 | 2280 | 7.4 | --- | 20 | 53 --- | |
| type 7 chondrite | | | | | | | | | | | | | | | |
| ALH84027 | LL7 | 29 | 4.06 | 1069 | 0.639 | 0.598 | 0.719 | 0.1062 | 0.0911 | 5830 | 0.598 | 1.19 | 3.0 | 3.5 0.081 | |
| H3-6 regolith breccia | | | | | | | | | | | | | | | |
| Zag l1 | light clast | 62 | 11.66 | 15150 | 100.6 | 1.991 | 10.04 | 5.66 | 1.266 | 9250 | 1.74 | | 5.8 | 6.4 0.23 | |
| Zag l2 | light clast | 74 | 8.52 | 6820 | 44.0 | 1.680 | 5.21 | 3.26 | 0.824 | 8170 | 1.57 | | 5.2 | 5.8 0.24 | |
| Zag d | dark clast | 21 | 7.47 | 1192 | 1.677 | 1.616 | 1.811 | 1.183 | 0.406 | 6550 | 1.616 | 1.11 | 5.4 | 6.0 0.21 | |
| Zag m1 | matrix | 46 | 10.21 | 11700 | 76.5 | 1.737 | 7.74 | 6.45 | 1.391 | 5740 | 1.55 | | 5.2 | 5.7 0.20 | |
| Zag m2 | matrix | 37 | 35.61 | 44200 | 432 | 2.825 | 36.9 | 27.91 | 5.43 | 5440 | 1.74 | | 5.8 | 6.4 | |
| | | | | | | | | | | | | <i>mean age:</i> | | 5.5 | 6.1 |

Sample mass in [mg], gas concentrations in [10^{-8} cm³STP/g], ²¹Ne exposure age, T²¹, in [Ma]. Cosmogenic ²¹Ne, ²¹Ne_{cos}, calculated assuming trapped Ne to be a mixture of solar Ne (SW-Ne and SEP-Ne) for Arch, and Zag, and primordial meteoritic Ne for the other meteorites. Exposure age range, T²¹_{min} - T²¹_{max}, calculated as explained in text. For all Zag samples, the (²²Ne/²¹Ne)_{cos} ratio of sample m1 is thereby assumed.

Uncertainties: ~5% for gas concentrations, ~0.5-1% for Ne isotopic ratios and ³⁶Ar/³⁸Ar.

Identical Origin for Halide And Sulfate Efflorescences On Meteorite Finds and Sulfate Veins In Orgueil

M.E. Zolensky, SN2, NASA, Johnson Space Center, Houston, TX 77058 USA.

Introduction: Halide and sulfate efflorescences are common on meteorite finds, especially those from cold deserts [1]. Meanwhile, the late-stage sulfate veins in Orgueil are universally accepted as having originated by the action of late-stage high fO_2 aqueous alteration on an asteroid [2]. I suggest here that these phenomena have essentially the same origin.

Indigenous Halides in Meteorites.

In a report that is generally ignored today, Berkley et al. [3] described finding the halides halite (NaCl) and sylvite (KCl) in seven ureilites. Although contamination can almost never be completely excluded from such reports, they did describe finding these minerals on freshly broken surfaces of ureilite falls. Similarly, Barber [4] reported finding halite and sylvite associated with waxy hydrocarbons on a freshly exposed surface of Murchison. In the past year we have found halite and sylvite within two freshly-fallen H chondrites, Monahans (1998) and Zag [5]. It is now clear that these halides are indigenous, and common to both chondrites and achondrites.

Previous studies have indicated that Cl is inhomogeneously distributed in meteorites [6], with the result that the solar abundance is not well known. Halite was noticed in Monahans (1998) because of its attractive purple color and large grain size, and this permitted special sampling and thin-sectioning procedures to be employed which preserved the halides. Similarly, the report of halite in Monahans (1998) led to its recognition in Zag. It is possible that halite is commonly present in chondrites, but has been overlooked, resulting in considerable errors in bulk Cl determinations for chondrites. Further, I suggest that a considerable fraction of the ubiquitous sulfate/halide efflorescence noted on Antarctic meteorites [1] is derived from dissolution and reprecipitation of indigenous halite (and sulfides), rather than from components introduced from the ice as is commonly assumed.

Terrestrial Origin for Sulfate Veins in Orgueil: Consolmagno and Britt [7] have recently reported

bulk porosities for chondrites measured at the centimeter scale. In particular, they found a bulk porosity for Orgueil (~20%) far in excess of that reported by Corrigan et al. [8]. However, I have previously noted a problem with this important meteorite. Inspection of old polished mounts of Orgueil often reveal that they are cracked, and considerably exfoliated due to the hydration, remobilization and precipitation of hydrous magnesium sulfates (e.g. epsomite) in cracks *after polishing*. This recrystallization of the sulfates causes cracks to expand dramatically, resulting in greatly increased porosity. There is therefore considerable danger in measuring porosities in meteorites containing atmospherically unstable phases, since they will alter and cause dramatic changes in the meteorite physical properties. In any case, I suggest that some or all of the late stage sulfate veining in Orgueil has resulted from dissolution of indigenous Orgueil sulfate and sulfide minerals *on Earth*, and subsequent reprecipitation of sulfates from the fluids. This process would have happened each time the meteorite experienced changes in local humidity, resulting in many terrestrial generations of sulfate veining. However, I still maintain that the carbonate veins are indeed asteroidal in origin.

References: [1] Langenauer and Krähenbühl (1998), *Earth Planet. Sci. Letts.* **120**, 431; [2] Zolensky and McSween (1988) In *Meteorites and the Early Solar System* (J. Kerridge and M. Matthews, Eds., U. A. Press, pp.114-143; [3] Berkley et al. (1979) *Geophys. Res. Letts.* **5**, 1075; [4] Barber (1981) *Geochim. Cosmochim. Acta* **45**, 945; [5] Zolensky et al., (1999) *Meteoritics*, Meteoritical Society Meeting Abstract; [6] Tarter (1981) *The Abundance and Distribution of Chlorine in Meteorites* (PhD Thesis, Arizona State Univ.), 170pp; [7] Consolmagno and Britt (1998) *Meteoritics & Planet. Sci.* **33**, 1231-1241; [8] Corrigan et al. (1997) *Meteoritics & Planet. Sci.* **32**, 509-515.

LIST OF WORKSHOP PARTICIPANTS

Conel Alexander
 Dept. of Terrestrial Magnetism
 Carnegie Institution
 5241 Broad Branch Rd NW
 Washington DC 20015
 USA
 alexande@clrs1.ciw.edu

Alex Bevan
 Dept. Earth & Planet. Sci.
 Western Australian Museum
 of Natural Science
 Perth WA 6000
 AUSTRALIA
 bevana@museum.wa.gov.au

Phil Bland
 Natural History Museum
 Department of Mineralogy
 Cromwell Road
 London SW7 5BD
 UNITED KINGDOM
 phib@nhm.ac.uk

Paul Buchanan
 NASA Johnson Space Center
 Mail Code SN2
 Planetary Science Branch
 Houston TX 77058
 USA
 pbuchana@ems.jsc.nasa.gov

Marc Caffee
 Inst. Geophys. & Planet. Phys.
 Livermore Natl. Lab.
 Livermore CA 94550
 USA
 caffee@llnl.gov

Ghislaine Crozaz
 Washington University
 Earth and Planetary Sciences Dept
 One Brookings Drive, Box 1169
 St. Louis MO 63130
 USA
 gcw@howdy.wustl.edu

Gillian Drennan
 Dept. of Geology
 Univ. of the Witwatersrand
 PO WITS 2050
 Johannesburg
 SOUTH AFRICA
 065.ruth@cosmos.wits.ac.za

Ahmed El Goresy
 Max-Planck-Inst. für Chemie
 Abteilung Kosmochemie
 Joachim-Becker-Weg 27
 D-55128 Mainz
 GERMANY
 goresy@mpich-mainz.mpg.de

George Flynn
 State University of New York
 Hudson Hall, Room 223
 101 Broad Street
 Plattsburgh NY 12901
 USA
 flynnj@splava.cc.plattsburgh.edu

Ian Franchi
 The Open University
 Planetary Sciences Research Inst.
 Waldon Hall
 Milton Keynes MK7 6AA
 UNITED KINGDOM
 i.a.franchi@open.ac.uk

Monica Grady
 Natural History Museum
 Department of Mineralogy
 Cromwell Road
 London SW7 5BD
 UNITED KINGDOM
 mmg@nhm.ac.uk

Ulrich Herpers
 Abt. Nuclearchemie
 Univ. Köln
 Otto-Fischer-Str. 12-14
 D-50674 Köln
 GERMANY
 ulrich.herpers@uni-koeln.de

Huber, Heinz
Baumgasse 25-27/2P
1030 Wien
AUSTRIA
a8825407@unet.univie.ac.at

Timothy Jull
University of Arizona
Department of Physics
1118 East 4th Street
Tucson AZ 85721-0081
USA
jull@u.arizona.edu

Candace Kohl
294 Torrey Pines Terrace
Del Mar CA 92014
USA
ckohl@ucsd.edu

Tomoko Kojima
Dept. of Earth & Planet. Sci.
Kobe University, Nada
Kobe 657-8501
JAPAN
kojima@shidahara1.planet.sci.kobe-u.ac.jp

David Kring
University of Arizona
Lunar and Planetary Laboratory
1629 E. University Blvd.
Tucson AZ 85721-0092
USA
kring@lpl.arizona.edu

Michael Lipschutz
Purdue University
Department of Chemistry
BRWN/WTHR Chemistry Building
West Lafayette IN 47907-1393
USA
rnaapuml@vm.cc.purdue.edu

Ursula Marvin
Harvard-Smithsonian Ctr. Astrophysics
Mail Stop 52
60 Garden Street
Cambridge MA 02138-1516
USA
umarvin@cfa.harvard.edu

Gordon McKay
NASA Johnson Space Center
Mail Code SN2
Planetary Science Branch
Houston TX 77058
USA
gordon.mckay@jsc.nasa.gov

Silke Merchel
Max-Planck-Institut für Chemie
Abteilung Kosmochemie
J.-J. Becker-Weg. 27
D-55128 Mainz
GERMANY
merchel@mpch-mainz.mpg.de

Takashi Mikouchi
NASA Johnson Space Center
Mail Code SN2
Planetary Science Branch
Houston TX 77058
USA
tmikouchi@ems.jsc.nasa.gov

Sripada Murty
Physical Research Laboratory
Navrangpura
Ahmedabad-380 009
INDIA
murty@prl.ernet.in

Tomoki Nakamura
Kyushu University
Earth and Planetary Sciences
Faculty of Science
Hakazaki Fukuoka 812-8581
JAPAN
tomoki@planet.geo.kyushu-u.ac.jp

Kunihiko Nishizumi
Space Sci. Lab.
Univ. of California
Berkeley CA 94720-7450
USA
kuni@ssl.berkeley.edu

Larry Nyquist
NASA Johnson Space Center
Mail Code SN2
Planetary Science Branch
Houston TX 77058
USA
l.nyquist@jsc.nasa.gov

Matthias Pätsch
 Max-Planck-Institut für Chemie
 J.J. Becherweg 27
 D-55128 Mainz GERMANY
 paetsch@mpch-mainz.mpg.de

Andrea Patzer
 Max-Planck-Institut für Chemie
 J. J. Becher-Weg 27
 D-55128 Mainz
 GERMANY
 patzer@mpch-mainz.mpg.de

Richard Pugh
 4617 NE 26th Av
 Portland OR 97211
 USA

Robert Reedy
 Los Alamos National Laboratory
 Group NIS-2
 Mail Stop D436
 Los Alamos NM 87545
 USA
 rreedy@lanl.gov

Sara Russell
 Natural History Museum
 Department of Mineralogy
 Cromwell Road
 London SW7 5BD
 UNITED KINGDOM
 sarr@nhm.ac.uk

Ludolf Schultz
 Max-Planck-Institut für Chemie
 Abteilung Kosmochemie
 Jos. J.-Becher-Weg 27
 D-55128 Mainz
 GERMANY
 schultz@mpch-mainz.mpg.de

Derek Sears
 Dept. Chem. & Biochem.
 Univ. of Arkansas
 Fayetteville AR 72201
 USA
 meteor@comp.uark.edu

Robert Walker
 Washington University
 McDonnell Center for Space Sciences
 Box 1105/One Brookings Drive
 St. Louis MO 63130-4899
 USA
 rmw@howdy.wustl.edu

David Wallis
 Unit for Space Sci. & Astrophys.
 School of Phys. Sci.
 University of Kent
 Canterbury CT2 7NR
 UK
 dw22@ukc.ac.uk

Dietmar Weber
 Westfälische Wilhelms Universität
 Institut für Planetologie
 Wilhelm-Klemm-Str 10
 D-48149 Münster
 GERMANY
 weberd@uni-muenster.de

John Wasson
 Inst. Geophys. & Planet. Phys.
 Univ. of California
 Los Angeles CA 90095-1596
 USA
 jtwasson@ucla.edu

Kees Welten
 University of California
 Space Sciences Laboratory
 Berkeley CA 94720-7450
 USA
 kcwelten@uclinky.berkeley.edu

Rainer Wieler
 ETH-Zurich
 Isotope Geology C61
 CH-8092 Zürich
 SWITZERLAND
 wieler@erdw.ethz.ch

Jutta Zipfel
 Max-Planck-Institut für Chemie
 Abteilung Kosmochemie
 Joh.-J.-Becher-Weg 27
 D-55128 Mainz
 GERMANY
 zipfel@mpch-mainz.mpg.de

Michael Zolensky
 NASA Johnson Space Center
 Mail Code SN2
 Planetary Science Branch
 Houston TX 77058
 USA
 Michael.e.zolensky1@jsc.nasa.gov